



COMMERCIAL ASSET RECOMMENDER TOOL (CART): DRAFT ALGORITHM DESCRIPTION DOCUMENT

11/30/2020

TABLE OF CONTENTS

1.0 INTRODUCTION.....	4
1.1 Purpose and Objective of this Document.....	4
1.2 Scope / Limitations	4
1.3 Framework and Layout of Document.....	4
2.0 CART ARCHITECTURE INTRODUCTION AND USE CASE.....	5
3.0 OVERVIEW OF THE ALGORITHMS AND DOCUMENTATION APPROACH	6
3.1 Overview of CART Analytical Flow	6
3.2 Algorithm Documentation Approach	9
3.3 Common Algorithms or Preconditions	9
4.0 COVERAGE AND THROUGHPUT	10
4.1 Introduction.....	10
4.2 RF Coverage	11
4.3 RF Coverage Gaps	14
4.4 Effective Communication Time.....	17
4.5 Throughput.....	19
5.0 USER BURDEN ALGORITHMS	21
5.1 Communications Payload: Antenna Size and Weight calculation based on the mission parameters.....	22
5.2 Communications Payload: Antenna Pointing Impacts / Burden	29
6.0 OTHER ALGORITHMS	32
6.1 Navigation Needs: Navigation Capability and GNSS Options.....	32
6.2 Commercial Network Status and Mission Adoption	34
6.3 Spectrum Regulatory	36
6.4 Ranking Algorithm	37
7.0 REFERENCES	40
APPENDIX A: RF COVERAGE ANALYSIS AND MODELING.....	42
APPENDIX B: SIGNAL ACQUISITION ANALYSIS AND MODELING.....	54
APPENDIX C: NETWORK MODELING.....	75
APPENDIX D: REGRESSION MODELS DESCRIPTION	83
APPENDIX E: LIST OF ACRONYMS.....	87

LIST OF FIGURES

Figure 1. CART Overview and Use Case Perspective	6
--	---

Figure 2. CART Analytical Flow.....	8
Figure 3. The two common algorithm templates: regression-model-based and logic-based	9
Figure 4. Modeling and Relationships between Communications Service Performance Evaluation Components	11
Figure 5. RF Coverage – Impacts of Orbital Geometry.....	12
Figure 6. Illustration of RF Coverage Results and Regression Fit for IridiumNext – User Inclination 30-deg, Varying Altitude (km)	12
Figure 7. Logic Flow: RF Coverage	14
Figure 8. RF Coverage Gaps.....	15
Figure 9. Logic Flow: RF Coverage Gap.....	16
Figure 10. Sample Comparison – Effective Communications Time (right) Prediction of 34% vs. RF Coverage (left) at 39% -- for Iridium Next (User at 30-deg Inclination)	17
Figure 11. Logic Flow: Effective Communication Time.....	19
Figure 12. Logic Flow: Throughput.....	21
Figure 13 Logic flow: calculation of the required EIRP for any system and for any given altitude	24
Figure 14 The geometry of the beam steerable antenna structure for the EIRP calculation	25
Figure 15Algorithm description to determine the antenna gain	26
Figure 16 Logic Flow: Reference Antenna Size and Mass.....	29
Figure 17. Logic Flow: Pointing Burden	32
Figure 18. Logic Flow: Navigation Needs.....	34
Figure 19. Logic Flow: Network Status & Mission Adoption Feasibility.....	35
Figure 20. Logic Flow: Spectrum Regulatory Status.....	37
Figure 21. Logic Flow: Analyze / System Comparison Ranking	39

LIST OF TABLES

Table 1. Data Volume / Throughput: Qualitative Descriptors and Assumptions for Quantitative Values	20
Table 2. Sample Antenna Pointing Mechanisms from Moog Inc.....	31

1.0 INTRODUCTION

1.1 Purpose and Objective of this Document

The Space Communications and Navigation (SCaN) Program at NASA is moving toward further commercialization of communications and navigation services for NASA user missions in near-Earth space. The Commercial Asset Recommender Tool (CART) is intended to assist in this transition by providing a user-friendly means of evaluating how well a specific commercial system will support a given NASA user's communication needs.

CART is a data analytics dashboard which estimates the performance and applicability of commercial communication systems by leveraging stored model data and a combination of analytical methods to estimate non-modeled points, as well as logic functions. This Algorithm Description Document (ADD) details the associated algorithms supporting the performance evaluation, spanning RF coverage, network throughput, user burden, and other factors. The ADD will be updated as CART evolves.

1.2 Scope / Limitations

This version of CART development assesses commercial '*space-based relay*' options and not the '*Direct to Earth (DTE)*' commercial services that are being considered. This focus is justified given that this latter effort is already well underway and is somewhat simpler than the more complex task of assessing viability of commercial satellite relay systems. CART is designed to accommodate for future integration and evaluation of information regarding relevant commercial DTE networks if desired.

In addition, CART currently supports the evaluation of the commercial space-based relay options for Earth-orbiting users in circular (or near-circular) orbits. Elliptical and highly elliptical orbits will be addressed at later time through modeling and associated updates to the associated regression models.

1.3 Framework and Layout of Document

The CART data analytics dashboard provides users with information corresponding to an underlying evaluation framework that was developed in the first phase of the commercial systems study in FY19 [1] and evolved to reflect the improvements in model fidelity. The scope of CART includes the following major analyses components and associated algorithms:

- **Coverage and Throughput Algorithms:** The evaluation begins with Radio Frequency (RF) coverage assessment, followed by subsequent impacts to RF coverage through incorporation of signal acquisition estimates and network acquisition and handoffs to create a resultant "effective communications time." Gaps in RF coverage are also evaluated, and throughput estimates (data volume per day) is provided.
- **User Burden Algorithms:** User burden addresses estimates of the communications payload such as antenna size and mass for various antenna options. Many of the commercial constellations are in LEO or MEO, introducing challenging dynamics. Part of the user burden evaluation includes assessment of pointing rate and potential impacts on the user to accommodate those pointing rates through body or mechanical steering (such as with a parabolic antenna).

- **Other Algorithms:** CART addresses a variety of other considerations spanning navigation, availability of the service relative to user launch date, the RF spectrum used by a commercial system relative to current regulatory efforts to allow for space-to-space use, and overarching algorithms used to rank order results for multiple systems.

After providing additional context for CART and a description of the CART architecture in Section 2, and introductory information on the overarching analytical flow algorithm documentation approach in Section 3, the remainder of the document builds on the major analyses components as introduced.

- Section 4: Coverage and Throughput Algorithms
- Section 5: User Burden Algorithms
- Section 6: Other Algorithms

The appendices provide additional detail and supporting material as follows:

- Appendix A: RF Coverage Analysis and Modeling
- Appendix B: Signal Acquisition Analysis and Modeling
- Appendix C: Network Modeling
- Appendix D: Regression Models
- Appendix E: Acronyms

2.0 CART ARCHITECTURE INTRODUCTION AND USE CASE

The high-level CART architecture is shown in Figure 1. The user interacts with CART via the user interface (UI), providing information about the mission and its communication and navigation needs/expectations, and receiving results indicating which commercial systems are potentially suitable for the mission. To provide these results to the user, CART uses logic functions which access analytics functions (such as regression models) and supporting data on the commercial systems and additional reference information. Analytics use the results of modeling and simulation (i.e. RF coverage) for sets of parametric reference users, providing the basis for predicted performance in support of the end user's mission.

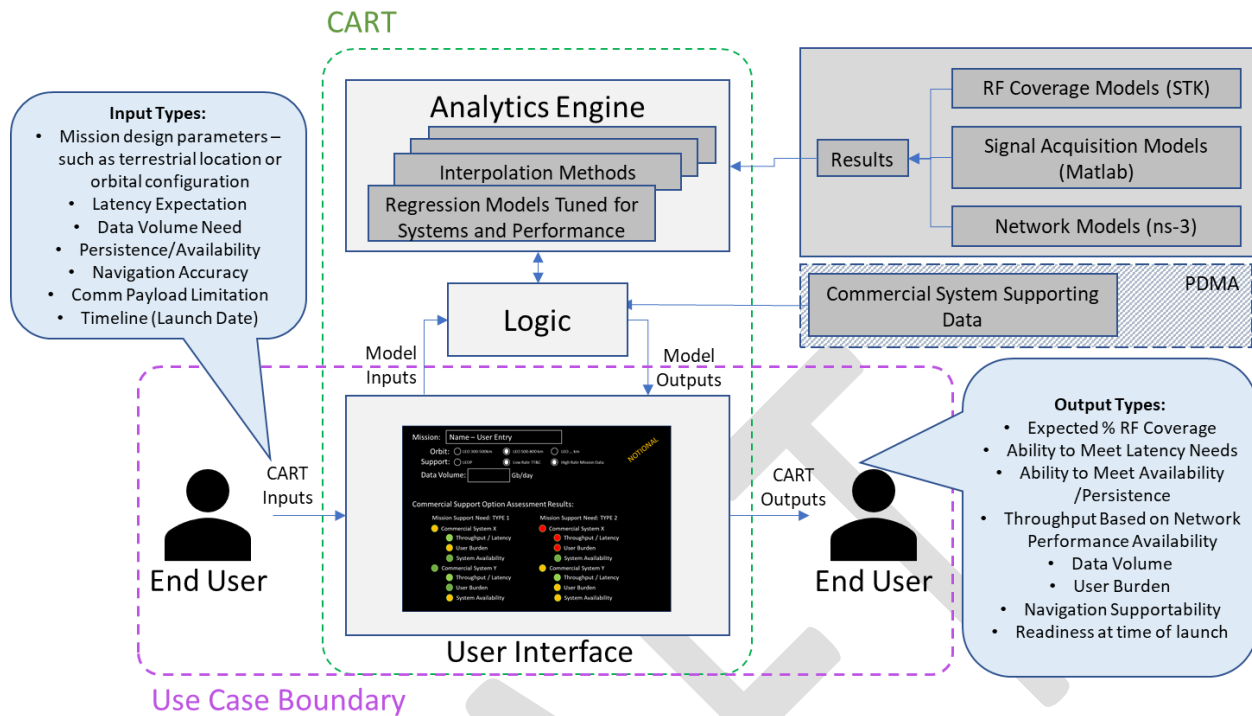


Figure 1. CART Overview and Use Case Perspective

Multiple use cases were initially developed [2] to guide the long-term planning for CART. As the development of CART has progressed the representation of the primary use case can be synthesized into two key functions:

- The user may “explore” the commercial systems, reviewing their characteristics, or accessing underlying model repositories.
- Alternatively, the user may “analyze” the commercial systems by investigating their performance and capabilities through interactive visuals and data displays, or through comparisons across systems driven by user input regarding a mission definition and communications needs.

The objective is to provide the user with an understanding of the system capabilities and a first-level assessment of how well various commercial relay solutions could support a mission needs. In this use case scenario, the end user of the CART is a SCaN Systems Engineer or Mission Designer.

3.0 OVERVIEW OF THE ALGORITHMS AND DOCUMENTATION APPROACH

3.1 Overview of CART Analytical Flow

An overview of the CART analytical flow is depicted in Figure 2. The diagram depicts the three components of the CART architecture as vertical slices; UI, Logic, and Analytics; and the three major components of evaluation as horizontal slices; Coverage and Throughput, User Burden, Other Factors. Source model data and supporting or reference information stored in the database and used by CART is shown at the far right of the figure. Source model data is inclusive of RF and

signal acquisition models and simulation results (STK and Matlab) and network simulation results (NS3). Commercial system reference information includes communication system parameters, relay orbital positions, and when the constellation is expected to be operational, as examples. Other reference information includes information on spectrum regulatory changes, examples of COTS products for mass and size reference (e.g. antennas), etc.

The flows within the figure highlight the relationships between the supporting data, analytics, logic functions and user inputs and outputs. Each horizontal flow, with user input and output, and a logic node (pink) and/or analytics node (purple), is represented in the document by a unique algorithm description and detailed flow diagram.

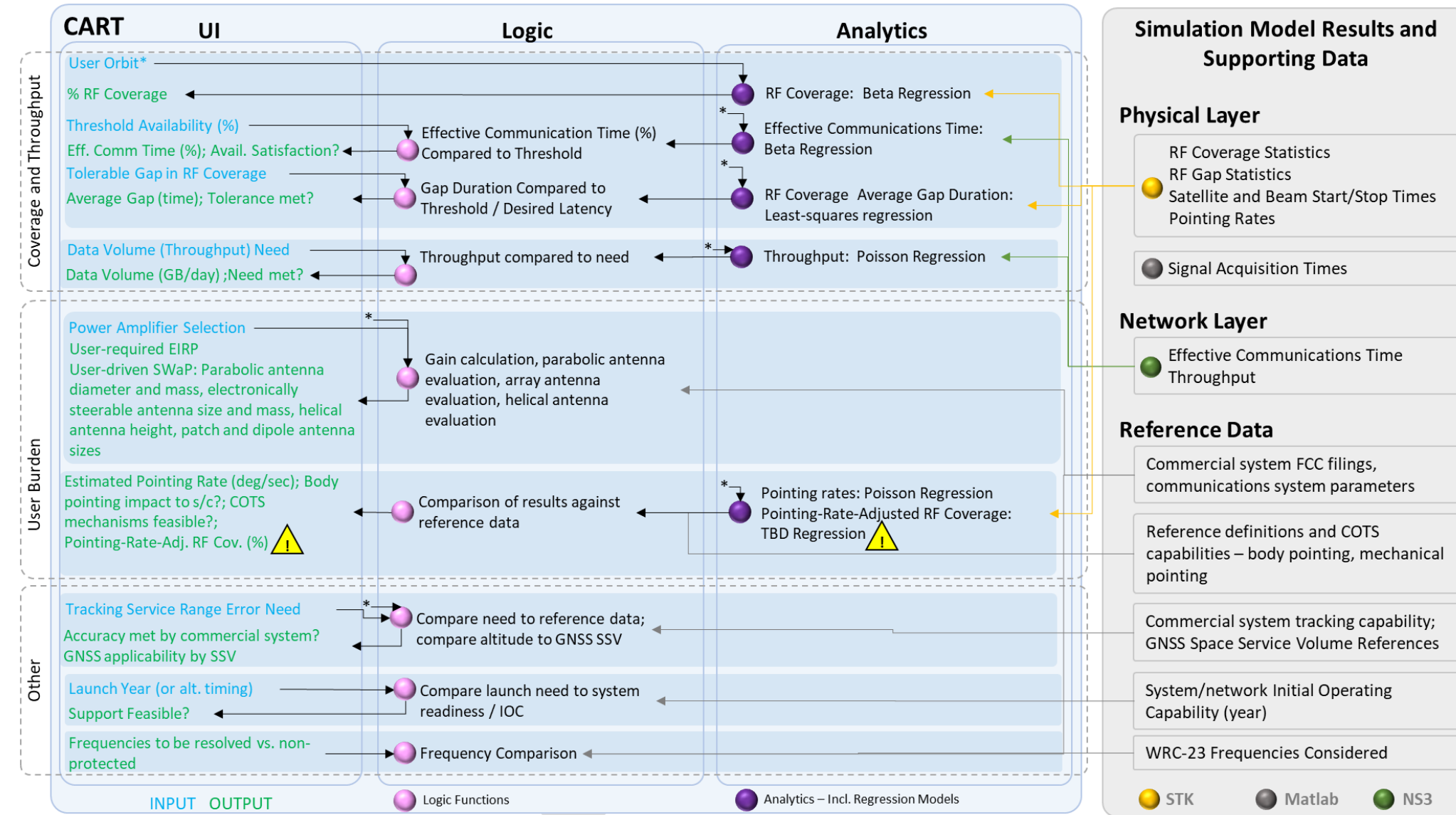


Figure 2. CART Analytical Flow

3.2 Algorithm Documentation Approach

For each element in the framework and the associated logic in CART, the following will be provided:

- Objective of the algorithm.
- Inputs and outputs.
- Algorithm description (narrative, flow diagram, or equations as appropriate).
- Assumptions or limitations. Assumptions or limitations already denoted in the scope discussion, Section 1.2, will not be noted in individual algorithm descriptions.

Most of the algorithms in the document are illustrated by flow diagrams. Although the algorithms for each evaluation element have unique aspects, they generally follow one of two templates: regression-model-based, or logic-based flows, as shown in Figure 3.

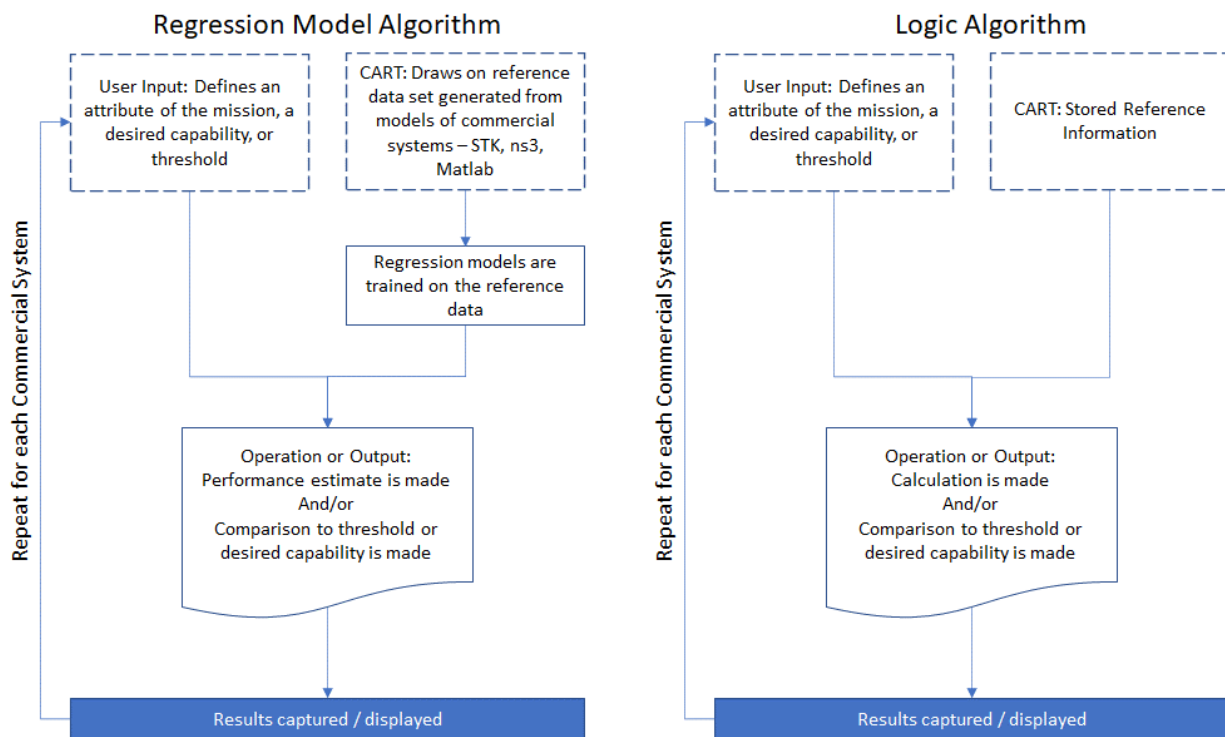


Figure 3. The two common algorithm templates: regression-model-based and logic-based

3.3 Common Algorithms or Preconditions

Upon review of the complete set of algorithms, processing steps that are common across multiple evaluation processes have been identified and described here separately. In follow-on algorithm descriptions, these common steps are referred to as appropriate.

3.3.1 Altitude Compatibility

Assessing or projecting the commercial system performance for user-specified mission input is predicated on some basic compatibility between the user/mission and the commercial system. An example is the precondition that a user orbit operates below the altitude of the commercial relay system.

3.3.1.1 Objective

This algorithm completes this basic altitude compatibility evaluation, and the results are a gateway or starting point for other algorithms described in the remainder of the document.

3.3.1.2 Inputs/Outputs

CART database references:

- Commercial relay system identification (name)
 - Maximum shell* altitude (km)

CART user input:

- User altitude or perigee altitude, expressed in (km)

CART output:

- Altitude viability status: Yes/No

3.3.1.3 Algorithm Description

Logic flow for this algorithm is as follows:

- If user mission altitude < Maximum of Altitude {Shell1, ..., ShellN} then
 - Commercial Relay altitude viability status = Yes
- Else,
 - Commercial Relay altitude viability status = No

The evaluation flow is repeated for each representative commercial system against the user input parameters.

*The term “shell” is used to differentiate relay satellites at different altitudes if a constellation is composed of satellites not all at a single altitude.

3.3.1.4 Assumptions/Limitations

Commercial communications satellite services are directed terrestrially – e.g. no “upward-looking” services. This is in keeping with the principle of the primary study that a NASA mission user is taking advantage of an existing or planned system in which other terrestrial/mobile etc. users are stakeholders and, as such, the service volume is directed in the nadir direction relative to the relay satellites vs. zenith.

4.0 COVERAGE AND THROUGHPUT

4.1 Introduction

Section 4 provides the first assessment of commercial communications system suitability, beginning with RF Coverage and determining Effective Communication Time, by accounting for signal acquisition impacts and network layer functions. The relationship between these evaluations and the source models is depicted in Figure 4. The foundational calculation is RF coverage, which is described in the next subsection, and the subsequent evaluation factors follow.

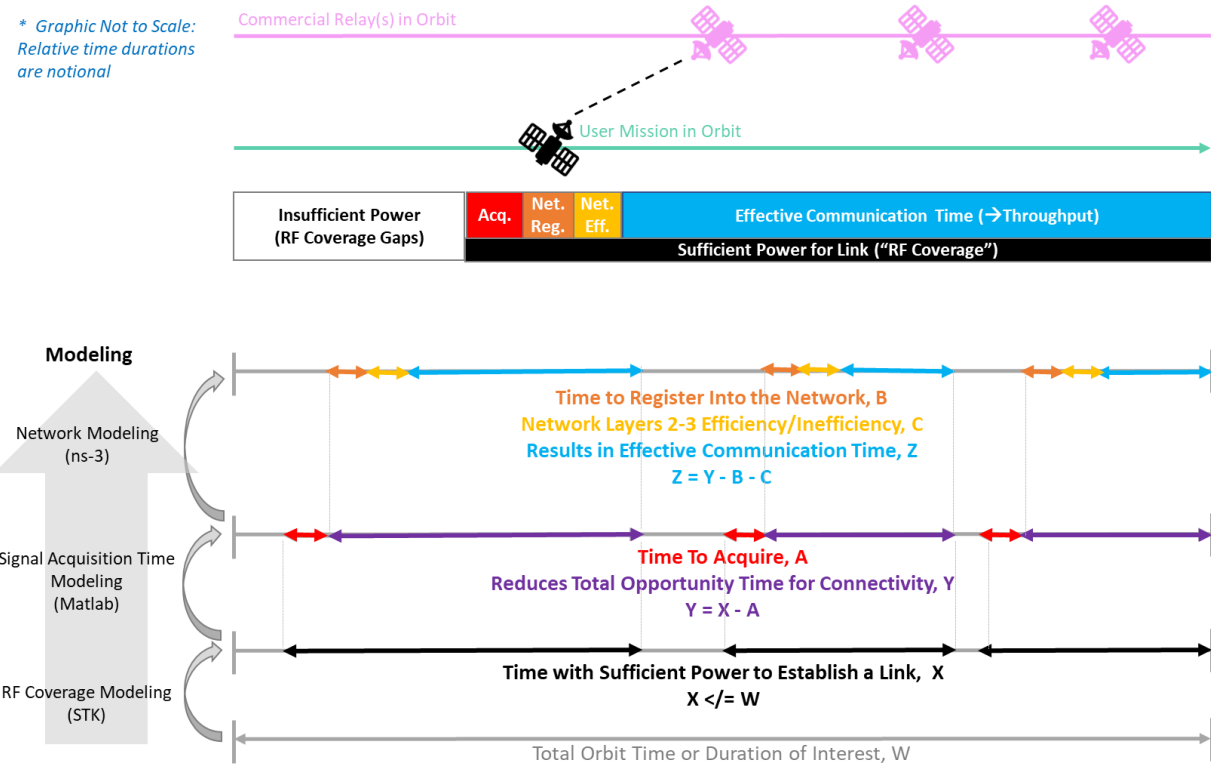


Figure 4. Modeling and Relationships between Communications Service Performance Evaluation Components

4.2 RF Coverage

RF Coverage is captured as a percentage, representing the duration that the user satellite has enough signal power to close the communications link with the commercial communications system, over a defined period. The model in STK defines the relative position of the user based on altitude and inclination, and the relay system orbit and communications parameters. Based on available data, either the system's beam patterns are modeled explicitly, or a simplified geometric model is employed. The STK model captures the losses associated with both the off-boresight position between the user and the relay (θ , Θ) and the range over time as shown in Figure 5. At each time step, if the power received at the relay is equal or better than the required threshold, and the margin on the link is sufficient, the user satellite at that time step has RF coverage. The resultant RF coverage statistics the accumulated performance over the scenario interval. The modeling is repeated for a parametric set of users, varying altitude, and inclination incrementally. Regression curves are employed to allow a prediction of performance based on the sample set. An example illustration is provided in Figure 6, wherein the CART user sees that RF coverage for an example user at 30deg inclination and 300km altitude (red point) receives 35% coverage; modeled points for other altitudes are depicted in blue, and the regression curve is in gold.

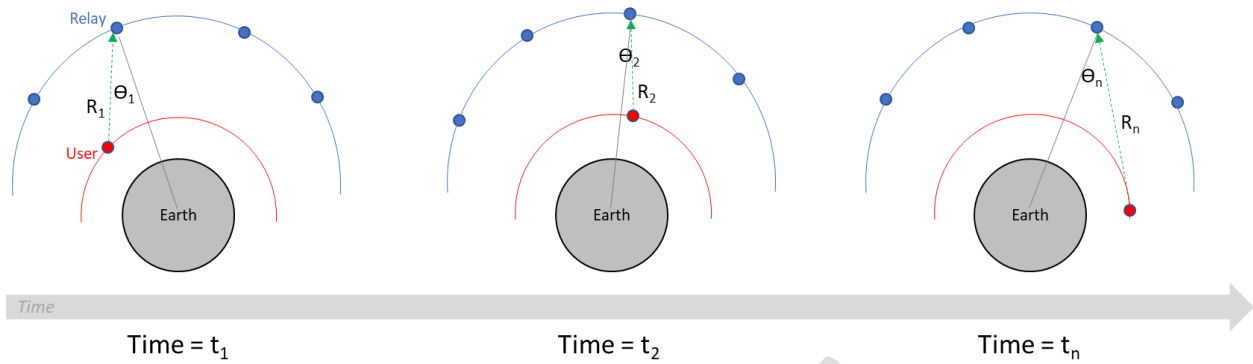


Figure 5. RF Coverage – Impacts of Orbital Geometry

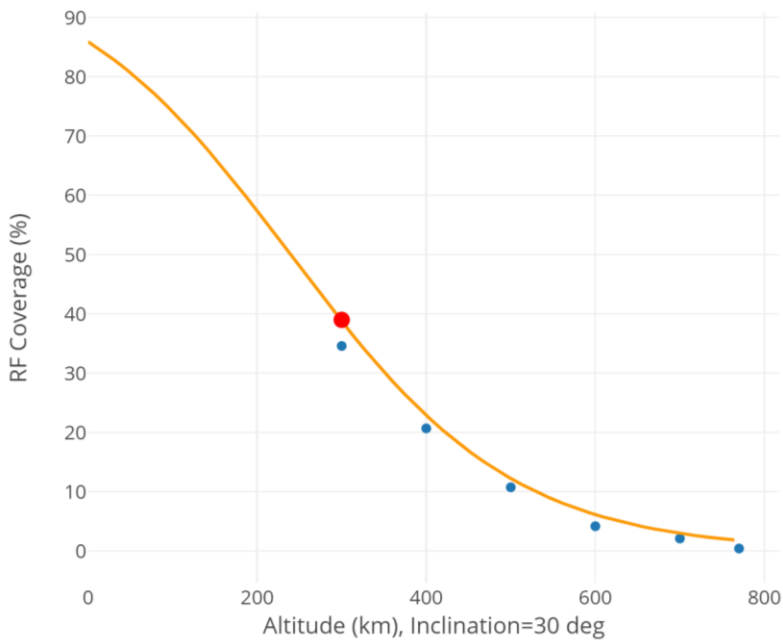


Figure 6. Illustration of RF Coverage Results and Regression Fit for IridiumNext – User Inclination 30-deg, Varying Altitude (km)

This metric conveys, at a top level, the applicability of a given commercial system for a user need, by providing a sense for how well supported the user might be. This is denoted as RF coverage opportunity because it is (a) based on a notional user transmit definition aligned with the respective commercial system FCC filings and associated link analysis, and (b) does not yet include the impacts of network and mobility management functions that could reduce the coverage time in which data flow is actually feasible.

4.2.1 Objective

Based on user input, describing the orbital parameters of the mission, the CART determines the projected RF coverage provided by each commercial system, based on regression models trained on coverage statistics for a set of reference users.

4.2.2 Inputs/Outputs

CART model results references:

- The primary CART reference is the set of coverage data for each commercial system and reference user pair, the result of RF link modeling described above.

CART user input:

- User mission orbital parameters to sufficiently define the orbit –
 - altitude (km)
 - inclination (deg)

CART output:

- Projected RF Coverage (%) provided by each commercial system based on the input defining user mission orbit

4.2.3 Algorithm Description

The RF Coverage estimate uses the regression model-based template. A precondition for processing is the altitude compatibility check (described in Section 3.3.1). The user provides the basic orbital mission parameters. A beta regression model is trained on the results of physical link modeling, and the predicted coverage value is provided based on the regression model results.

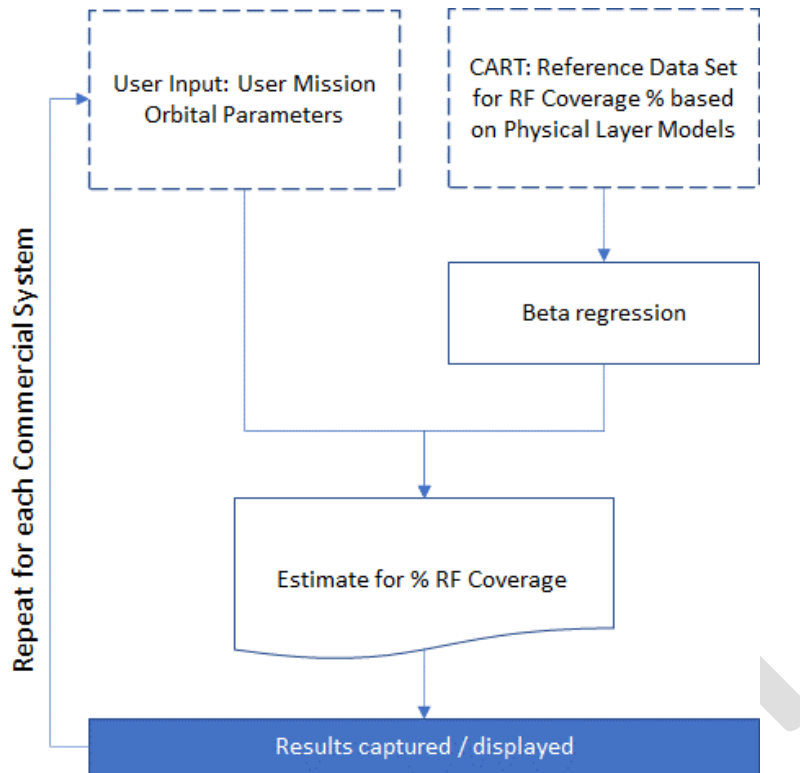


Figure 7. Logic Flow: RF Coverage

4.2.4 Assumptions/Limitations

1. The RF coverage results from the physical link model are based on a set of assumptions for the user RF transmitter capability consistent with the FCC filings for each respective commercial system. As such they are representative only and are intended for comparative purposes. The user burden evaluation algorithms in Section 5.0 provide additional reference points.

4.3 RF Coverage Gaps

From the physical link model, information is derived not only to support RF coverage percentage over time, as used in the preceding algorithm, but also maximum and average gap times and distributions thereof.

4.3.1 Objective

In CART, the intent is to present how a commercial system may impact a user's ability to meet its latency requirements. The basis of this algorithm is the assertion that the statistical characteristics related to gap time can be used as a metric to determine significant *contributions* achievable latency.

Latency, as defined in [3], is the allowable time to deliver data, “typically measured from the time of platform measurement to the time of delivery to its destination. The network portion is measured typically from the time of receipt of data from the platform to time of delivery to the user MOC.” For the purposes of this algorithm, we consider how the distribution of gaps in RF coverage could contribute to total latency as shown in Figure 8. Following the RF coverage calculation method described in the prior section, gaps represent times when the received power and link margin are insufficient.

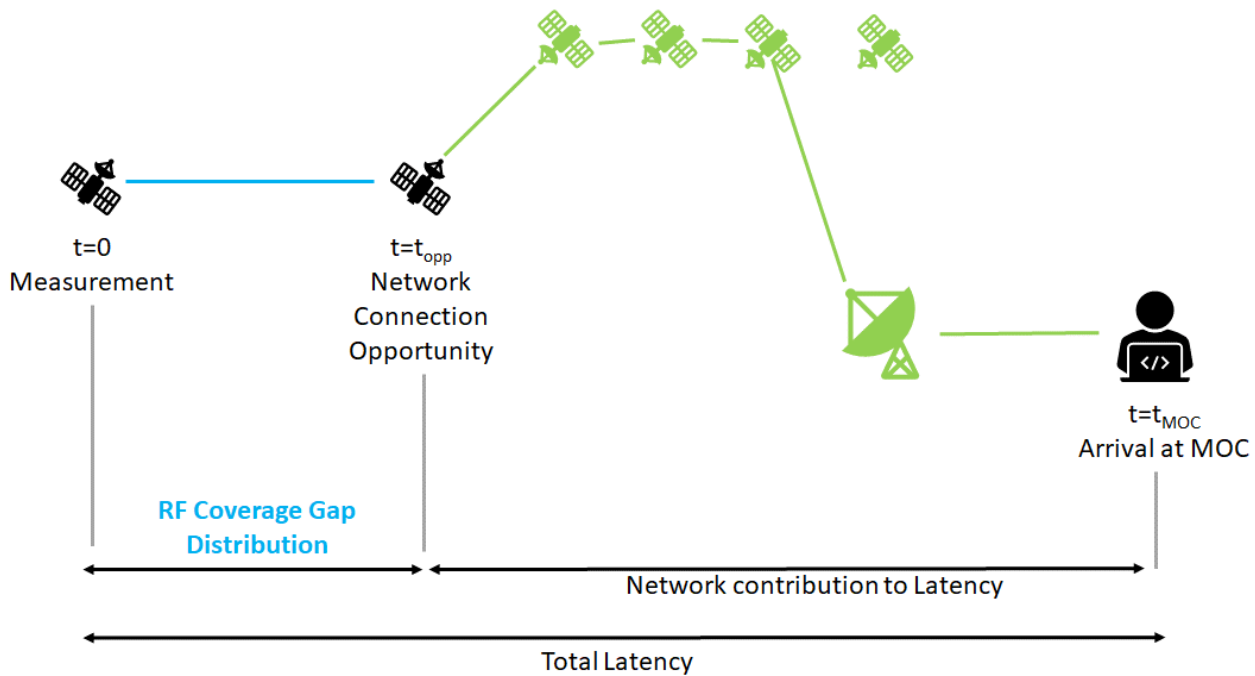


Figure 8. RF Coverage Gaps

Although some missions may have a quantitative latency requirement, most missions, particularly in a planning phase, can describe their latency in qualitative categories. The qualitative categories from [3] and their associated descriptions are used as a basis for this algorithm.

4.3.2 Inputs/Outputs

CART model results references:

- The primary CART reference is the set of RF coverage gap data for each commercial system, the result of physical link modeling.

CART user input:

- User mission orbital parameters to sufficiently define the orbit –
 - altitude (km)
 - inclination (deg)
- Tolerable gap in RF coverage may be entered directly (minutes)

CART output:

- Estimated average gap in RF coverage
- Is the average gap less than the user defined tolerable gap in RF coverage? Yes/No
- **Under Development:** additional metrics are being developed for integration into CART. Metrics may include maximum gap, median gap, time-averaged gap, as well as graphical information including running average gap, and histograms of gap durations for individual model runs (user altitude/inclination pairs).

4.3.3 Algorithm Description

The RF Coverage Gap estimate uses the regression model-based template. A precondition for processing is the altitude compatibility check (described in Section 3.3.1). The user provides the basic orbital mission parameters as well as desired operational latency or threshold value. Regression models are trained on the results of physical link modeling, and the predicted average gap value is provided based on the regression model results. Each commercial system's regression is selected and tuned based on the results. This estimate is compared against the user provided objective or threshold and the user is alerted to whether the gap times indicate that their tolerable gaps in RF coverage may not be achievable.

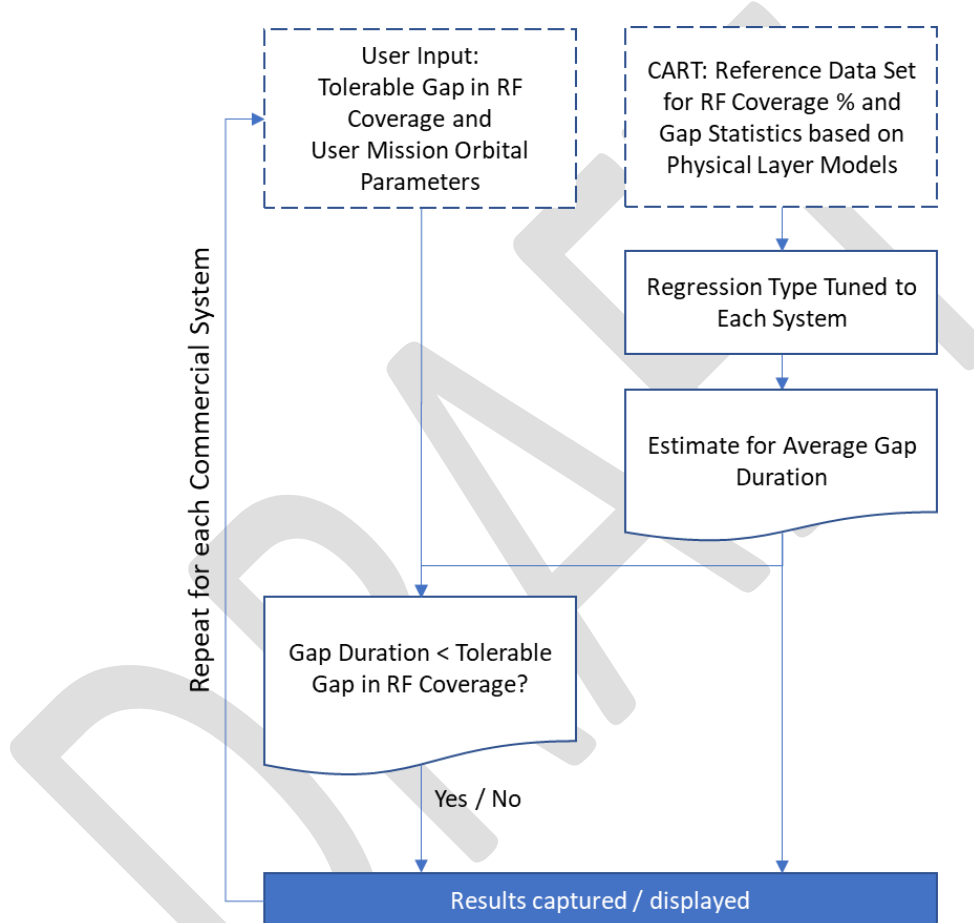


Figure 9. Logic Flow: RF Coverage Gap

4.3.4 Assumptions/Limitations

1. The logic flow makes use of relationships between qualitative performance (e.g. “moderate” latency) to numeric values that can be compared against characteristics of the commercial system. Relationships have been defined as noted in the input/out description, but these assumptions may be altered in the CART code if needed.

4.4 Effective Communication Time

Availability, as defined in [3], is how persistent access to the network is. This is a value typically expressed as a ratio or percent; however, qualitative terms are often used. The qualitative terms are often used interchangeably, and their associated descriptions are used as a basis for this algorithm:

- Availability: Reasonable, Reasonable-High, High
- Persistence: None, Periodic (hourly/daily), Regular, More Frequent, Persistent (near continuous)

For the purposes of this algorithm, we assert that effective communication time is analogous to availability. Referring back to Figure 4, effective communication time is the results of multiple factors including RF coverage (time with sufficient power), signal acquisition time, and network registration and other network processing effects. Effective communications time is therefore determined by Equation 1:

$$\text{Effective Communication Time, } T_{EC} = T_{RF} - T_{aq} - T_{net} \quad (\text{Equation 1})$$

Where T_{RF} = Time with enough RF power to establish a communications link,

T_{aq} = Acquisition Time to Acquire the Signal,

T_{net} = Time required to register into the network, and losses associated with network efficiency/inefficiency.

The starting point is the RF coverage model results (previously described) as well as the results of signal acquisition modeling (Matlab) as input to the evaluation. The Matlab Simulink model uses the range-rate and doppler information derived from the physical model, as well as system reference data (frequency, modulation, data rate) to inform an estimate of signal acquisition time. Subsequently, the network model determines the impacts of network processing and handovers as packet flow is simulated between the user and the relays.

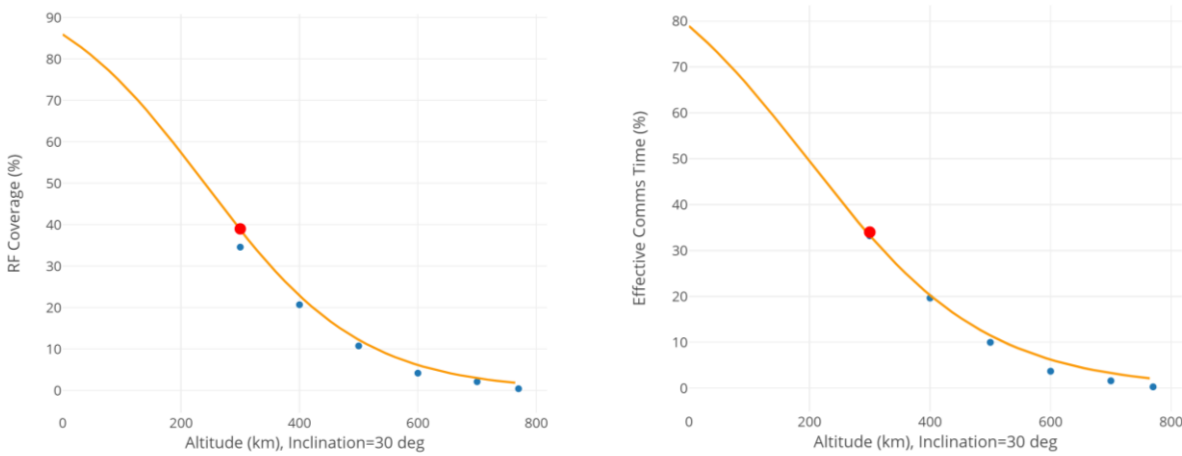


Figure 10. Sample Comparison – Effective Communications Time (right) Prediction of 34% vs. RF Coverage (left) at 39% -- for Iridium Next (User at 30-deg Inclination)

4.4.1 Objective

In CART, the intent is to determine the anticipated effective communication time and indicate how well (or poorly) that corresponds to a user's expectation for network availability/persistence.

4.4.2 Inputs/Outputs

CART model results references:

- The primary CART reference is the set of effective communication time data, represented as a percentage, for each commercial system.

CART user input:

- User mission orbital parameters to sufficiently define the orbit –
 - altitude (km),
 - inclination (deg),
- Availability/persistence expectation is selected from a set of generalized categories defined as follows. Per assumption/limitation note (2), quantitative values are required for comparison and the selected values are noted.
 - High availability / persistent: 99.9% (TBR, available at least every minute)
 - Reasonable-High availability / more frequent or regular: 96% (TBR, available at least every hour)
 - Reasonable availability / periodic: 67% (TBR, available at least every 8 hours)
 - Persistence = none: 4% (TBR, available at least every 23 hours)

CART output:

- Effective Communication Time (%)
- Availability/persistence need satisfied: Yes/No

4.4.3 Algorithm Description

The Effective Communication Time estimate uses the regression model-based template. A precondition for processing is the altitude compatibility check (described in Section 3.3.1). The user provides the basic orbital mission parameters as well as desired availability/persistence or threshold value. A beta regression model is trained on the network model results (ns-3 drawing on STK and Matlab inputs), and the predicted effective communication time value (%) is provided based on the regression model results. This estimate is compared against the user provided objective or threshold and the user is alerted to whether the effective communication time is compatible with their availability/persistence requirements.

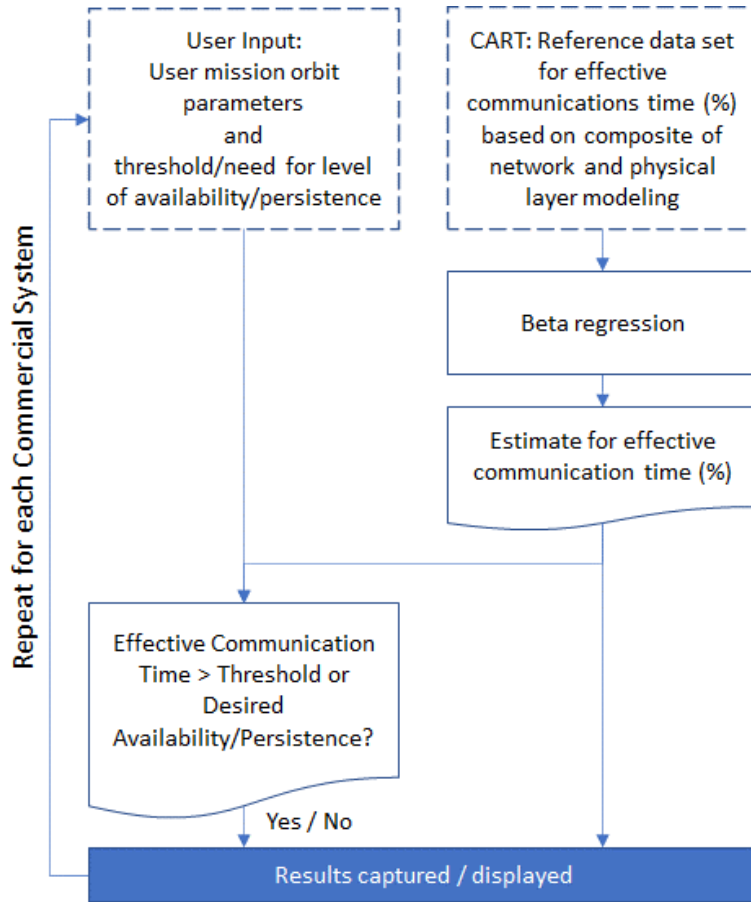


Figure 11. Logic Flow: Effective Communication Time

4.4.4 Assumptions/Limitations

1. Access is another characteristic defined as the mission need for guarantee of service at a specified time. The current methodology sets “access” aside, assuming that if the network is available, the user will have access. Effectively, this discounts any cases where the capacity of the network or its scheduling (manual or automated) would impact access.
2. The logic flow makes use of relationships between qualitative performance (e.g. “reasonable-high” availability) to numeric values that can be compared against characteristics of the commercial system. Relationships have been defined as noted in the input/out description, but these assumptions may be altered in the CART code if needed.

4.5 Throughput

Throughput, or data volume in a specified time, as defined in [3], is the amount of data generated by and received by the mission user platform in a given unit of time whether status telemetry, command uploads, or mission data that needs to be transported. “The typical driver is the mission data transported from the platform to an operations center; such data volume may range from 10s kb/day to 10s Tb/day.” Although some missions may have a quantitative throughput requirement, other missions, particularly in a planning phase, may describe their throughput more qualitatively categories. The qualitative categories from [3] and their associated descriptions are used as a basis for this algorithm.

4.5.1 Objective

In CART, the intent is to present how well (or poorly) a commercial system may meet a user's expectation for data volume transmission. Throughput is derived from the effective communication time and system data rates within the ns-3 model.

4.5.2 Inputs/Outputs

CART model results references:

- Effective communications time results

CART user input:

- User mission orbital parameters to sufficiently define the orbit:
 - altitude (km),
 - inclination (deg),
- Data volume need or threshold specified as Gb/day, or selected from generalized categories in [3] as shown in Table 1, see assumption/limitation note (1):

Table 1. Data Volume / Throughput: Qualitative Descriptors and Assumptions for Quantitative Values

Volume/Throughput, Qualitative		Quantitative Gb/day
Limited	--	0.1
Very Low	<< 100 Gb/day	1
Low	<100 Gb/day	100
Low-Moderate	500 Gb/day	500
Moderate or Modest	< 1 Tb/day	1000
Moderate-High, or Modest-to-High		5000
High	1-10 Tb/day	10000
Very High	>10 Tb/day	15000

CART output:

- Data Volume Need Satisfied: Yes/No
- Estimated Throughput (Gb/day)

4.5.3 Algorithm Description

The Throughput estimate uses the logic-based template. A precondition for processing is the altitude compatibility check (described in Section 3.3.1). The user provides the basic orbital mission parameters as well as desired data volume or throughput. CART references the effective communications time results and multiplies by the system data rate to determine the maximum possible throughput. This estimate is compared against the user provided objective or threshold and the user is alerted to whether the throughput meets their requirements.

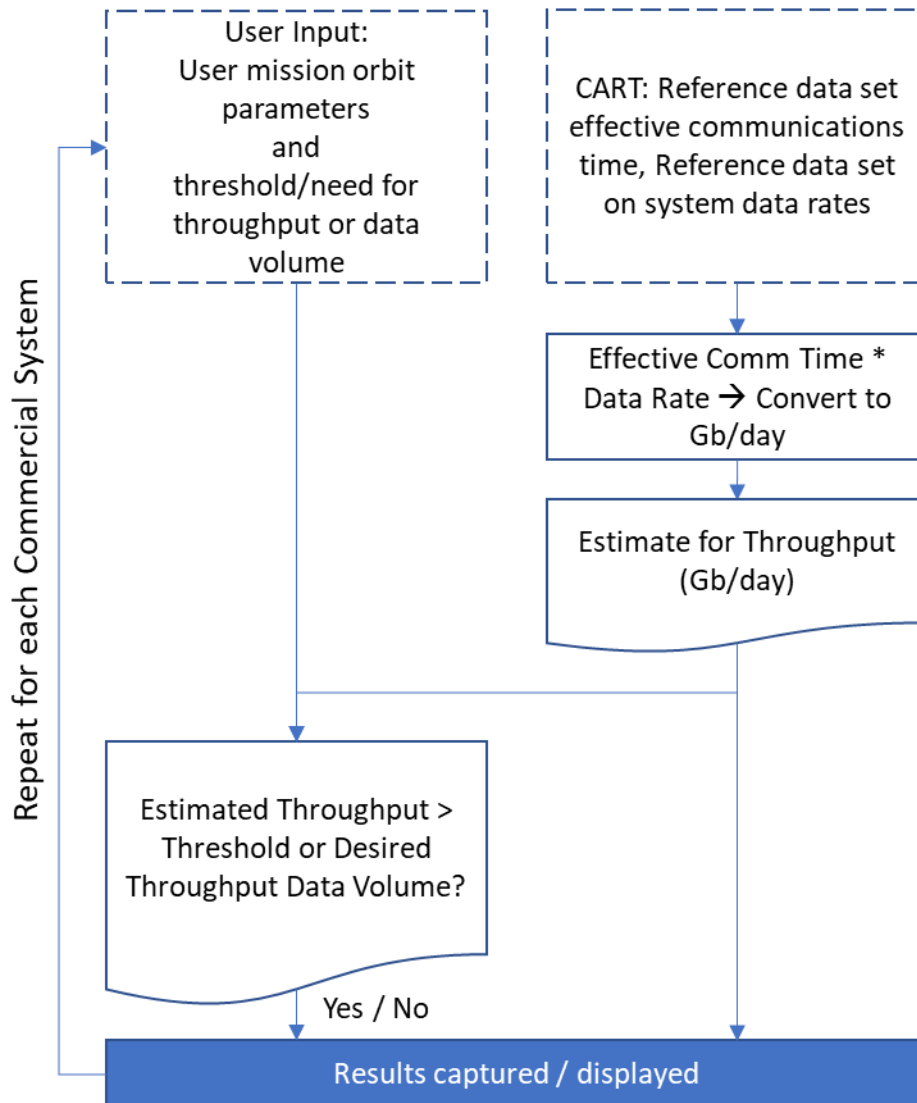


Figure 12. Logic Flow: Throughput

4.5.4 Assumptions/Limitations

1. The logic flow makes use of relationships between qualitative performance (e.g. “very-high” data volume) to numeric values that can be compared against characteristics of the commercial system. Relationships have been defined as noted in the input/out description, but these assumptions may be altered in the CART code if needed.

5.0 USER BURDEN ALGORITHMS

In the previous section, the communication service evaluation focused on the system capability relative to the user inputs such as orbit parameters and desirable characteristics (RF coverage, data volume, etc.). In this section, the resultant impacts on the user are determined and include consideration of transmission power; additional size, weight, and power impacts of the resultant antenna options and processing; and pointing requirements and impacts.

CART Algorithm Design Document

Each of the major evaluation areas is supported by one or more algorithms described in this section:

- Communications Payload:
 - Antenna size and weight for three types of antenna for any given mission parameters (i.e. Altitude/Inclination)
 - Antenna Pointing Impacts / Burden
- Navigation Needs:
 - Navigation Capability and GNSS Options

5.1 Communications Payload: Antenna Size and Weight calculation based on the mission parameters.

5.1.1 Objective

The intent of this algorithm is to estimate the antenna size and weight requirements needed to successfully establish connectivity with each of the commercial relay systems.

5.1.2 Inputs/Outputs

CART database references:

- Data base references include relay receiver parameters extracted from the FCC filing such as:
 - Frequency
 - G/T
 - Link losses such as cross polarization loss
 - Receiver implementation loss
- SN parameters from the Space Network Users Guide.

CART user input:

- Transmitter output power
- Altitude

CART output:

- Parabolic antenna size (diameter, m) and mass (kg)
- Electronically steerable antenna size (physical area, m²) and mass (kg)
- Helix antenna size as equivalent antenna height (m)
- Patch antenna size (m²)
- Dipole antenna size (m)

5.1.3 Algorithm Description

Antenna size and weight estimates are performed depending on system types. For steerable beam systems, CART currently uses a minimum EIRP requirement assessment. For fixed beams systems, CART assumes a worst-case assessment which uses the EIRP required for a terrestrial user. This limitation in antenna size and weight calculation will be removed in a future version of CART. In addition, forward G/T requirements will be compared to return EIRP requirements to detect any potential systems where the forward link drives the size of the antenna. This tradeoff is necessary as many commercial systems are designed to provide higher speed forward links than return links as internet traffic is usually forward

link dominant, i.e., large amount of date is sent to the subscriber instead of the typical NASA mission use case where the platform is the one that is sending a large amount of data on its return link.

As it can be seen from Figure 13 the algorithm starts with the user altitude and reference value of EIRP (i.e. EIRP1) and the Free space Loss, FSL, (i.e. FSL1) which is calculated for the maximum distance between the relay and the terrestrial user.

If the system is a fixed beam structure the reference EIRP (i.e. EIRP1) will be the same for any user altitude and the next step will be antenna size/weight calculation.

If the system is a steerable beam structure, first the maximum distance between the relay to the user (on a given altitude) is calculated as follow:

$$X = \frac{2(r+A_r)\cos\theta - \sqrt{(2(r+A_r)\cos\theta)^2 - 4(r+A_r^2 - r+A_u^2)}}{2} \quad (\text{Equation 2})$$

Where X is the maximum distance between the relay and the user for any altitude, A is the summation of the earth radius (r) and user altitude (A_u), B is the distance between the user altitude and the relay altitude (A_r)and θ is half cone angle derived from the FCC filing. Details of all these parameters can be found in Figure 14.

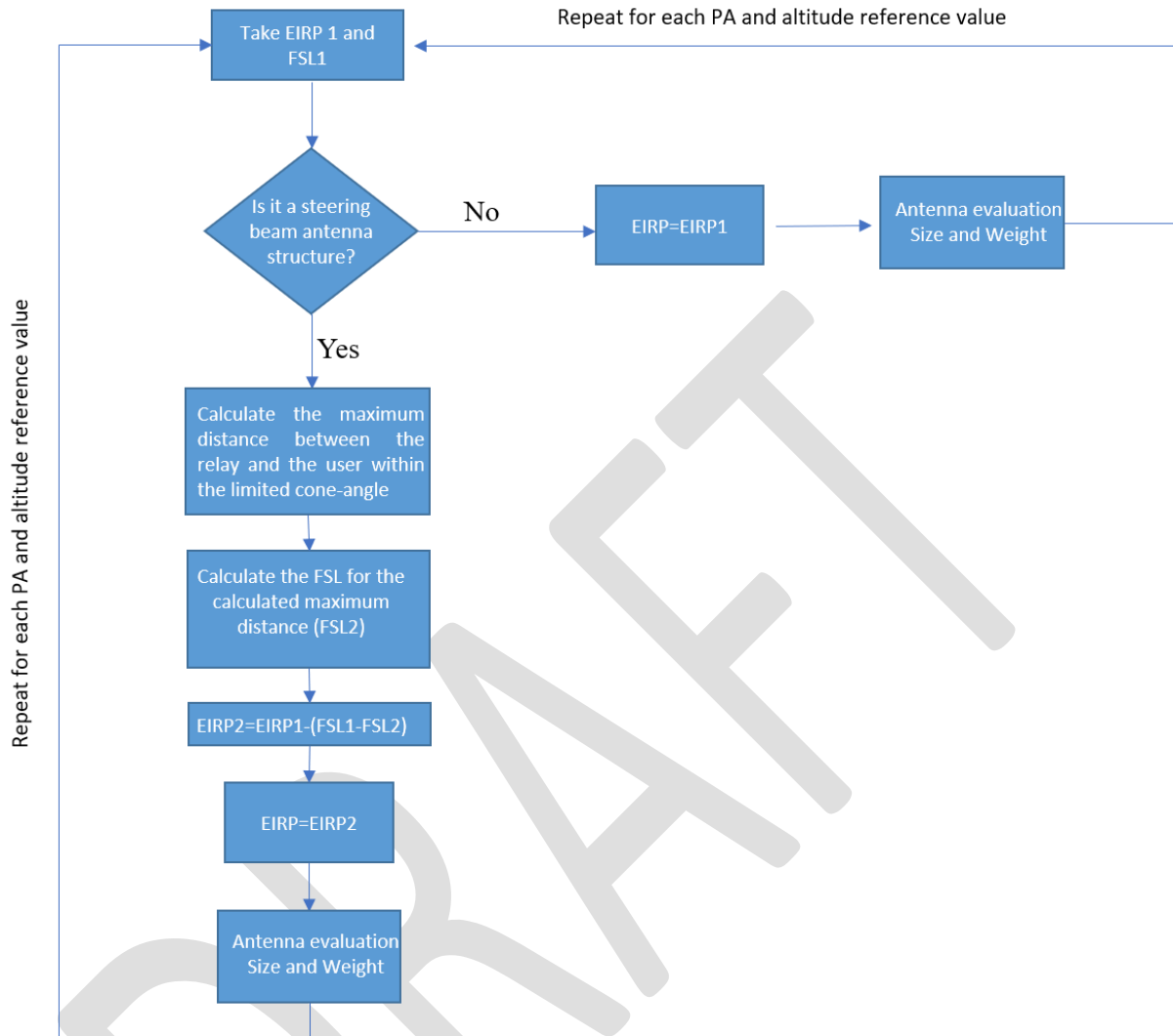


Figure 13 Logic flow: calculation of the required EIRP for any system and for any given altitude

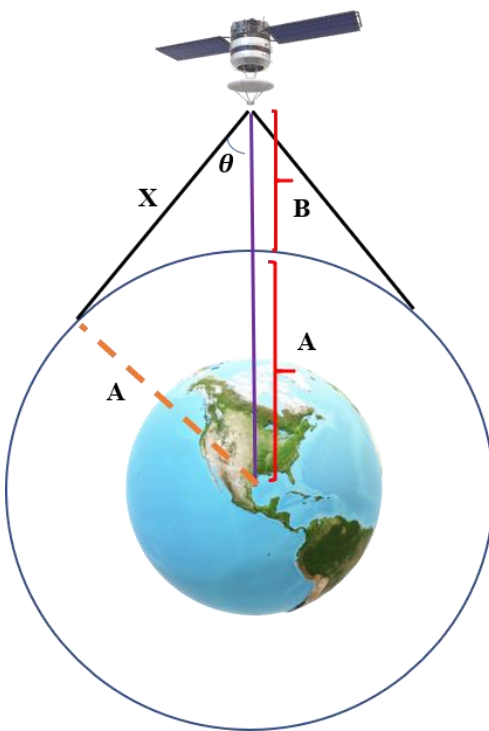


Figure 14 The geometry of the beam steerable antenna structure for the EIRP calculation

Once the maximum distance is calculated, then the Free Space Loss FSL (i.e. FSL2) is calculated. The equivalent required EIRP for the new altitude can be calculated as follows:

$$EIRP2 = EIRP1 - (FSL1 - FSL2) \quad (\text{Equation 3})$$

In order to calculate the size and weight of the antenna we need to first determine the required antenna gain. Figure 15 shows the algorithm description to determine the required antenna gain. If the antenna is a passive (i.e. parabolic or Helix), the return gain will be calculated from the difference between calculated EIRP and the user “output power” input. If the antenna is active (i.e. electronically steerable), the return antenna gain will be EIRP+20, where we have assumed a 10dBm amplifier is used for antenna elements. In the next step the return gain will be compare to the forward gain and the greater between the two determine the required user antenna gain.

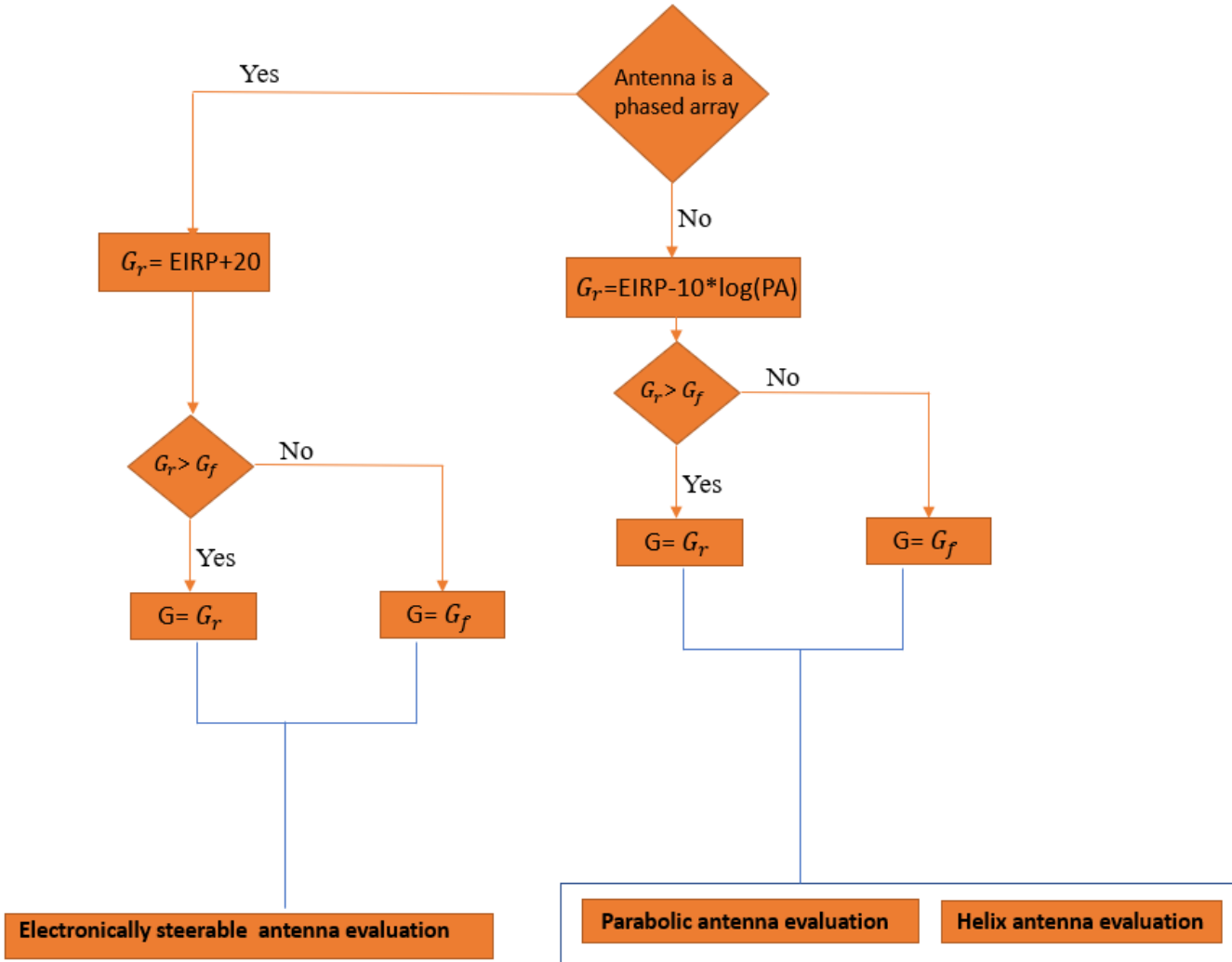


Figure 15Algorithm description to determine the antenna gain

The sections below describe the analytical details for determining the size and weight of parabolic, helix, electrical steerable, patch and dipole antennas. Figure 16 provides a summarizes the calculation process.

5.1.3.1.1 Parabolic antenna size and weight

Based on the determined user required antenna gain the parabolic antenna size and weight are calculated as follow:

$$D = \frac{\lambda}{\pi} \times \sqrt{\left(\frac{10^{10}}{k}\right)}; \quad \text{in meter} \quad (\text{Equation 4})$$

Where λ is the wavelength of the signal in meters, D is the diameter of the parabolic reflector in meters, and k is the efficiency. By assuming an efficiency of 0.55 and using knowledge of the user frequency and gain, one can derive the antenna diameter (size).

For the mass of the parabolic antenna two empirical formula were used. If the size of the antenna diameter is more than 0.6 meters the mass is calculated as:

$$W=6.674D-3.802 [4] \quad (Equation 5)$$

where D is the antenna diameter. If the diameter is less than 0.6 meters the antenna weight is calculated as:

$$W=3D^2 [5] \quad (Equation 6)$$

where D is the antenna diameter and W is the antenna mass in kg.

5.1.3.1.2 Helix antenna size and weight

Based on the determined user required antenna gain the Helix antenna size is calculated as follow:

$$H = \lambda \times 10^{(\frac{G-10.8}{10})}; \quad \text{in meter} \quad (Equation 7)$$

Where λ is the wavelength, and G is the required antenna gain.

It should be noted that the mass of the antenna is considered negligible for the Helix type. Furthermore, if the required antenna height exceeds one meter the CART will print that “Helix antenna not an appropriate solution”.

5.1.3.1.3 Electronically steerable antenna size and weight

Based on the determined user required antenna gain the electronically steerable antenna size and weight are calculated as follow:

The antenna gain is calculated as:

$$G = \text{EIRP}+20 \quad (Equation 8)$$

Where it is assumed a 10dBm amplifier is used for any single antenna element.

$$A = (N \frac{\lambda}{2})^2; \quad \text{in m}^2 \quad (Equation 9)$$

Where N is the total number of required elements and is calculated from:

$$N = 10^{(\frac{G-5}{20})}; \quad (Equation 10)$$

where N, is the total number of required elements.

A 5 dB gain for a single antenna is assumed. Moreover, the distance between elements are considered to be half of a wavelength and symmetric.

The mass of the array antenna can be calculated from;

$$M=0.9671N-0.1826 \text{ (kg)} [4]. \quad (Equation 11)$$

5.1.3.1.4 Patch Antenna size and Gain

A typical gain of a patch antenna is between 6-9 dB. In CART the gain of 8dB is assumed for a typical patch antenna. As a result, regardless of the required gain based on the user “output power” input the gain of the patch antenna is 8dB. In CART, if the required gain be more than 8 dB, patch antenna would not be a good solution, however, if the required gain be equal or less than 8 dB, the antenna size is calculated as follow:

$$W = 0.49 \frac{\lambda_0}{\sqrt{4.4}} [6] \quad (Equation 12)$$

By considering the length is equal to width in a rectangular patch antenna the overall size is:

$$Size = L \times W \quad (Equation 13)$$

In the above equation the relative dielectric constant of the patch antenna is FR4 which is a typical substrate. A general size of a patch antenna can be calculated from an experimental equation [7]:

$$W = \frac{c}{2f \sqrt{\frac{\epsilon_r+1}{2}}} \quad (Equation 14)$$

where W is the width of the patch antenna, f is the frequency and ϵ_r is the dielectric constant of the substrate

$$\epsilon_{eff} = \frac{\epsilon_r+1}{2} + \frac{\epsilon_r-1}{2} \left[\frac{1}{\sqrt{1+12(\frac{h}{w})}} \right] \quad (Equation 15)$$

where ϵ_{eff} is the effective dielectric constant, and h is the height of the substrate.

$$L = \frac{c}{2f \sqrt{\epsilon_{eff}}} - 0.824h \left(\frac{(\epsilon_{eff}+0.3)(\frac{w}{h}+0.264)}{(\epsilon_{eff}-0.258)(\frac{w}{h}+0.8)} \right) \quad (Equation 16)$$

Where L is the length of the patch antenna

5.1.3.1.5 Dipole Antenna size and Gain

Dipole antenna can be at different size and consequently different gain. However, there are two specific sizes that can be useful in terms of its efficiency, antenna pattern and gain properties.

- 1- For a dipole antenna with the size of $1.25 * \text{Lambda}$ the antenna gain is equal to 5 dB,
- 2- For a dipole antenna with the size of $0.5 * \text{Lambda}$ the antenna gain is equal to 2 dB.

Therefore based on the required gain one of the two options is displayed in CART.

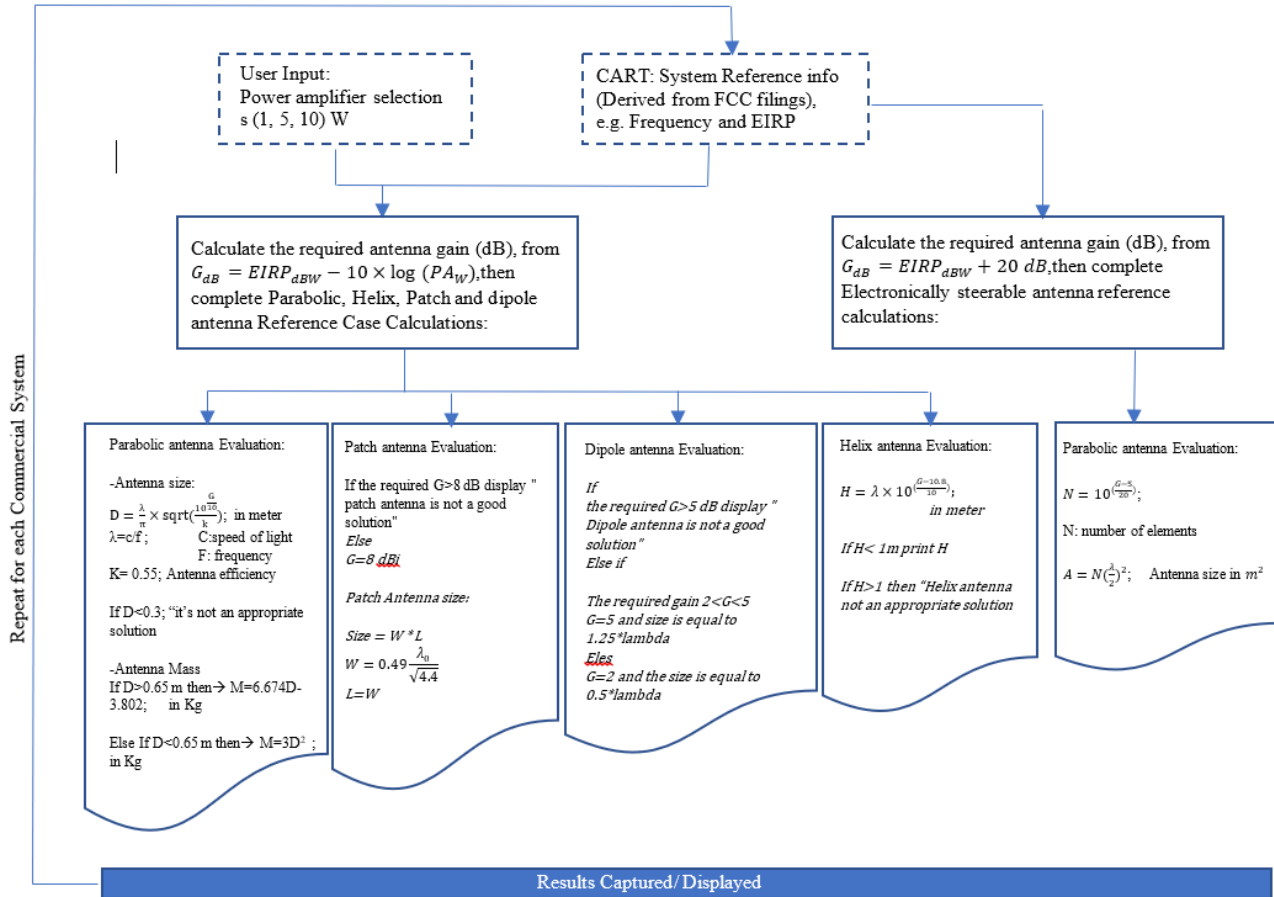


Figure 16 Logic Flow: Reference Antenna Size and Mass

5.1.4 Assumptions/Limitations

1. In our calculations, we just considered the parabolic antenna diameter, array element quantity, or helix antenna height. The antenna feed system (waveguide structure, coaxial cables, ...) is not considered in the assessment.
2. The antenna mass assessment is based on the industry reference points and the data set is currently relatively small.

5.2 Communications Payload: Antenna Pointing Impacts / Burden

One of the potential challenges with space-based relay communications, particularly if the commercial assets are non-geostationary, is the need for the user to dynamically point. Depending on the pointing rates between the bodies the user may be burdened by additional hardware, mass, complexity, or alternative systems (such as phased arrays) that may have cost implications.

5.2.1 Objective

Based on user input, describing the orbital parameters of the mission, CART provides a projected impact on the spacecraft resulting from pointing dynamics in terms of feasibility of body-pointing, mechanical pointing, or need for a phased array solution. Pointing rates vary significantly with relative orbital

geometry and speeds. The average pointing rate (deg/s) plus two standard deviations provides a reference point that captures most of the distribution of rates without forcing the user burden to be driven by maximum values. Using this reference threshold, the RF coverage time which falls below the reference is captured as an additional output.

5.2.2 Inputs/Outputs

CART model results references:

- The primary CART reference is the set of angular pointing data for each commercial system and a revised estimate of RF coverage, the result of physical link modeling.

CART stored reference data:

- Feasibility/reasonableness threshold for body pointing
- Commercial product tracking rate references, of which the critical value is the maximum

CART user input:

- User mission orbital parameters to sufficiently define the orbit –
 - altitude (km)
 - inclination (deg)

CART output:

- Projected average plus two standard deviation pointing rate (deg/sec) (pointing rate threshold)
- Feasibility of body-pointing
- Feasibility of mechanical pointing (based on a sample of industry mechanism performance)
- Estimated pointing-rate-adjusted RF coverage based on the pointing rate threshold
- **Under Development:** revised post-processing scripts to allow users to see the difference between pointing rates associated with tracking a relay during service vs. the pointing rates (or slew rates) associated with moving to a new relay.
- **Under Development:** current approach for pointing-rate-adjusted RF coverage is being revised to use a uniform threshold across all systems, vs. using the distribution of pointing rates for a given user-system combination.

5.2.3 Algorithm Description

The antenna pointing impact estimate uses the regression model-based template. A precondition for processing is the altitude compatibility check (described in Section 3.3.1). The user provides the basic orbital mission parameters. A regression model trained on the physical link model results for each system which capture pointing angle rate statistics. The data captured from this model is represented as the average pointing angle rate plus 2 standard deviations in (deg/s). This is used as a single numeric reference value for the distribution of pointing angle rates. The regression model is used to predict the reference value for a given user input case and is then compared against a set of evaluation criteria for both body pointing (evaluation 1), and mechanical pointing impacts (evaluation 2). Further, the processed results of the physical link simulations include a pointing-rate-adjusted value for RF coverage by removing RF coverage times in which the pointing rate exceeds the average plus two standard deviation threshold. A (TBD) regression model is trained on these model results, producing a pointing-rate-adjusted RF coverage estimate. Comparing the baseline RF coverage with the modified value provides insight into how

frequently the pointing rate hits peak values beyond the average plus two standard deviation reference. The integrated logic flow is shown in Figure 17.

For body pointing and slewing, industry reference points are as follows [8]:

- < 0.5 deg/sec: Impact to spacecraft is minimal; reaction wheels may be enough for small vehicles.
- > 0.5 deg/sec: Structural impact on appendages, weight and cost increases; gyros and/or thrusters are required.

Body pointing for communications purposes also must be balanced against compatibility with the science mission and observations. If time is taken away from scientific observation to point for communications, this can be viewed as another type of burden.

For mechanical pointing, several commercially available products are provided as a reference (captured in Table 2). The tracking rates for these COTS products vary from 0.02 deg/sec to 3.75 deg/sec, all exceed 4kg and 10 W requirements.

Table 2. Sample Antenna Pointing Mechanisms from Moog Inc.

Product #	Tracking Rate (deg/sec)	Slew Rate (deg/sec)	Mass (kg)	Power (W)	Reference Missions
Type 33-Large Range of Travel Variant	0.1	3	5.23	17	HALCA Mission – 830 kg spacecraft
Type 55	0.75	3	16.42	6.4 W/axis	ADEOS Mission – 3560 kg spacecraft
Type 33	0.02	0.075	4.6	17 W/axis	SOHO Mission – 1850 kg spacecraft
Type 22	3.75	--	5.44	10 W/axis	Earth observation satellites
Interorbit Link	0.06	0.4	15.6	14	Large GEO

If neither body nor mechanical pointing is feasible, the result displays an indicator that phased array solutions could be considered. The user is provided with the predicted pointing rate (deg/s) result as reference.

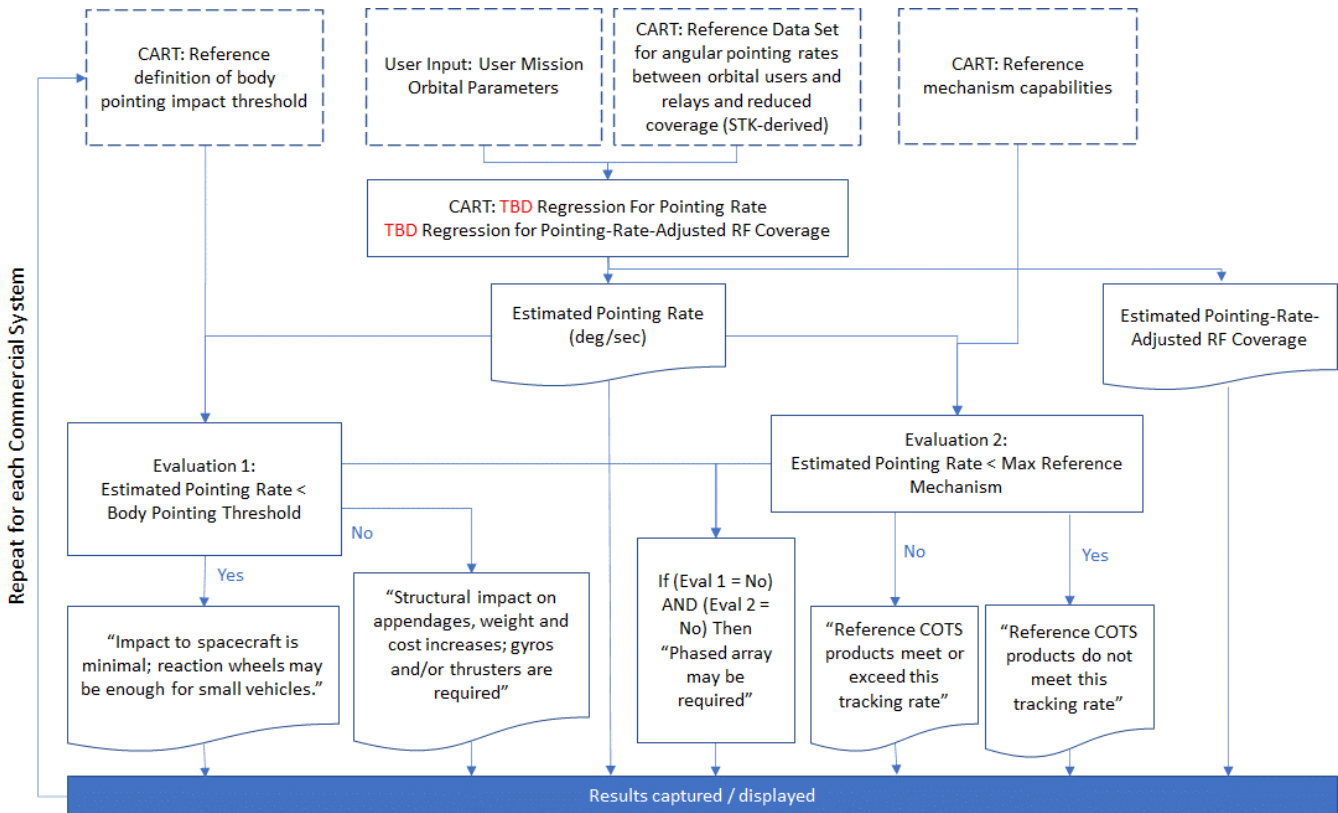


Figure 17. Logic Flow: Pointing Burden

5.2.4 Assumptions/Limitations

1. The mechanical pointing feasibility is based on industry reference points and the data set is currently relatively small; this could be expanded for more meaningful output.

6.0 OTHER ALGORITHMS

CART addresses a variety of other considerations spanning navigation, availability of the service relative to user launch date, the RF spectrum used by a commercial system relative to current regulatory efforts to allow for space-to-space use, and overarching algorithms used to rank order results for multiple systems.

6.1 Navigation Needs: Navigation Capability and GNSS Options

Navigation needs are one of the key mission use case characterizations described in NASA's future mission space communications and navigation needs documentation. Missions often use radiometric data such as doppler and ranging, provided by the communications networks. In describing the needs for the different use cases, several qualitative descriptions are made [3]: (1) "Basic" navigation – location and trajectory, (2) "More stringent" navigation requirements, (3) navigation requiring network support – typically in deep space mission use cases, and (4) cases in which no navigation requirements were specified.

Although most missions, predominantly near-Earth robotic science missions, have basic needs, there are current and future mission cases with unique and complex needs, and there is an expectation that improvements in navigation accuracy over time will enable new missions and scientific observations. Discussing navigation burden is challenging due to both the lack of specificity in quantitative requirements

(user needs are currently expressed qualitatively), and the notion that those needs will continue to increase (greater precision) over time to enable new and unique missions.

Based on review of positioning, navigation, and timing accuracy levels, and the projected commercial communications satellite capability, the following may be observed:

1. Advanced processing methods can improve on standalone GPS-based measurements, generally accepted to be ~1m position accuracy for LEO missions and several meters at GEO distance, down to centimeter-level for post-processing methods.
2. There are several available commercial off the shelf (COTS) GPS receivers with mass and power values suitable for small “disadvantaged” satellite users—carrying a GPS receiver is not a burden by itself.
3. Custom receivers, such as those developed at GSFC, are capable of weak signal tracking and can be utilized beyond the traditional GNSS space service volume.
4. *Commercial relays do not typically provide radiometric tracking services.*

6.1.1 Objective

Based on the user input, identifying the level of accuracy required, the CART determines, for each commercial constellation, if the capability exists, and if not, provides a basic assessment of GNSS feasibility as an alternate.

6.1.2 Inputs/Outputs

CART database references:

- Commercial system identification, radiometric tracking or positioning capability indicator (None, Value (m)), and associated notes as applicable
- GNSS usage and receiver implications by altitude regime

CART user input:

- User altitude, expressed in (km)
- Navigation accuracy required, expressed in (m).

CART output:

- Navigation indicator (Yes/No) for ability of each commercial system to provide radiometric tracking, and anticipated accuracy (m)
- Category of GNSS usage based on altitude, if commercial system is unable to provide position information.

6.1.3 Algorithm Description

The navigation needs assessment uses the logic-based algorithm template. A precondition for processing is the altitude compatibility check (described in Section 3.3.1). The evaluation checks the available service provided by the commercial system; the majority do not provide tracking or position services and will return a negative result. For those systems that do offer tracking or positioning, the accuracy is compared against the user need, and reported as a positive/negative result with the specifics of the service accuracy and any accompanying notation.

CART Algorithm Design Document

If the commercial system cannot meet the accuracy need, the user may need to rely on GNSS solutions, although this is not the only option. The evaluation process then indicates the applicability/usability of GNSS solutions based on altitude; providing contextual information for the CART user, as opposed to the particulars of GNSS accuracy (see assumption/limitation 1). This logic flow is depicted in Figure 18.

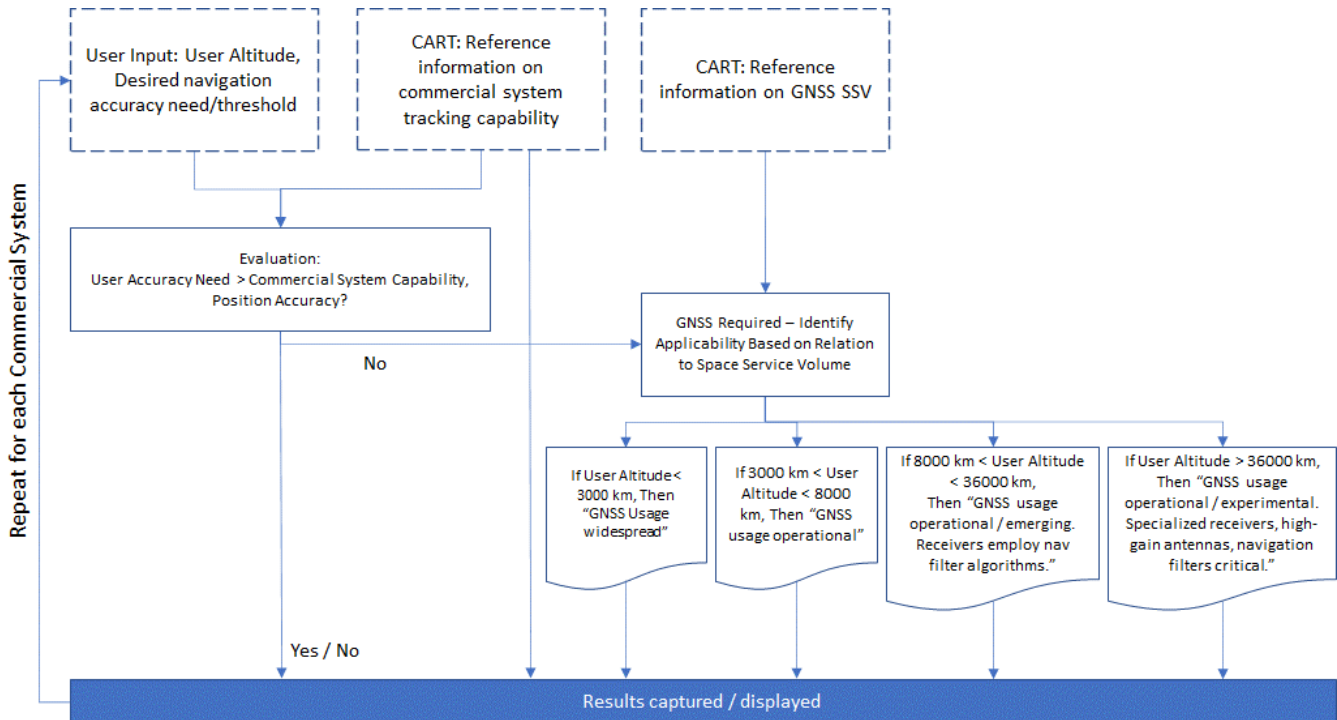


Figure 18. Logic Flow: Navigation Needs

6.1.4 Assumptions/Limitations

1. GNSS accuracy and usage is complex and outside the scope of this effort. The intent is to simply identify basic categories of GNSS applicability if the commercial system does not meet the user needs. The references related to usage and qualitative descriptors are taken from [9].

6.2 Commercial Network Status and Mission Adoption

The potential for NASA users to take advantage of commercial services is clearly dependent on the status of those networks and the time to verify performance and capability with respect to NASA needs. Currently there are a mix of existing and proposed networks and services, with an array of Initial Operating Capability (IOC) dates.

6.2.1 Objective

Compare the user input regarding expected launch or mission timeframe to the commercial system IOC and an expected lag time for the commercial services to be certified for NASA use and onboarded contractually. Provide the CART user with an indication of the resulting readiness of the network to meet their mission timeline.

6.2.2 Inputs/Outputs

CART stored reference data:

- Commercial System IOC dates (e.g. 2022)
- Assumption for time to certify and onboard (e.g. 1 year)

CART user input:

- *Either* Launch Year, *or*
- Proposal Year *and*
- Development Time

CART output:

- System IOC
- Feasible/Not Feasible to support the mission

6.2.3 Algorithm Description

The network status and mission use feasibility assessment uses the logic-based algorithm template. A precondition for processing is the altitude compatibility check (described in Section 3.3.1). The logic flow is summarized in Figure 19. The initial operating year is combined with a reference assumption for the time to certify and onboard the providers services, thus creating a “year available” date reference. This value is compared to the user’s anticipated launch date to provide an indication of the feasibility of using that system.

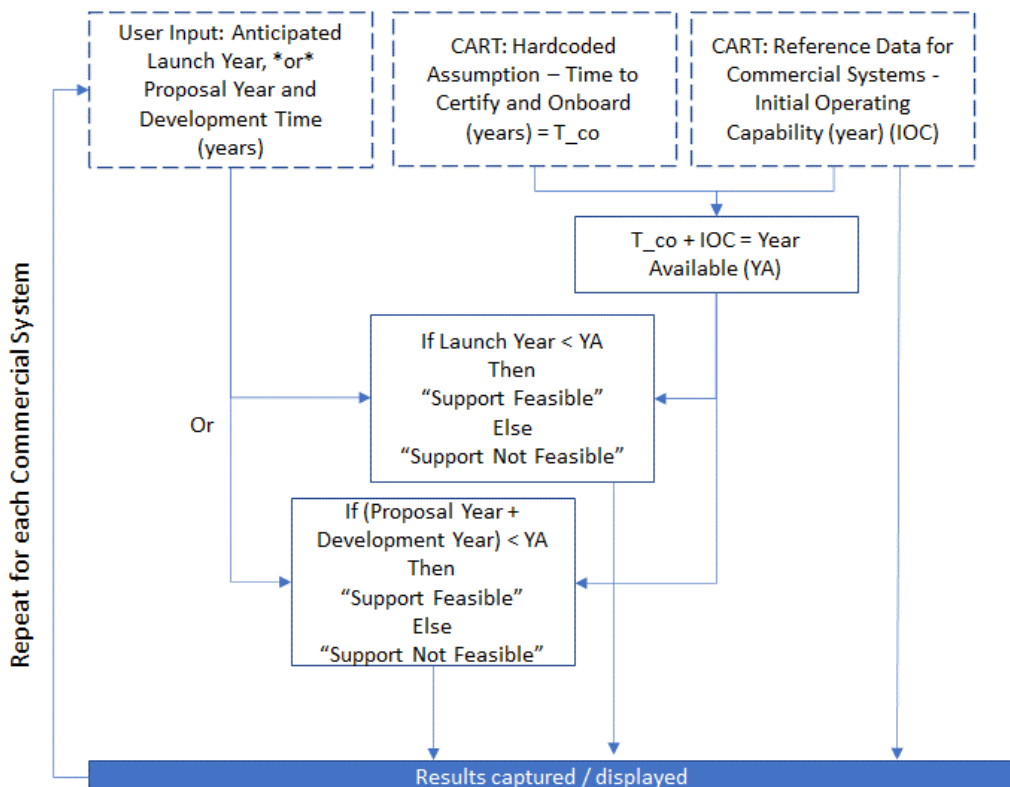


Figure 19. Logic Flow: Network Status & Mission Adoption Feasibility

6.2.4 Assumptions/Limitations

1. The generic period for onboarding and certification is fixed rather than flexible for the prototype.
2. IOC dates are based on public data and may change periodically.

6.3 Spectrum Regulatory

Another key challenge in adopting commercial space-based relay service is spectrum compatibility and authorizations. The science services frequencies used by NASA missions do not overlap with the frequency allocations used by commercial communications satellites. In general, most fixed-satellite service (FSS) and mobile-satellite service (MSS) allocations in the U.S. are for non-government use only (some of these allocations are available for Government use but are restricted to military applications). On the opposite front, most science services allocations are available for both Government and non-government use, but differences may exist in terms of priority access. From an operational standpoint, these two differences can be bridged by either (1) NASA missions adapting to use the commercial systems on commercial services frequency bands, or (2) commercial systems adapting to transmit to NASA missions on science services frequency bands. Exploiting either of these options requires resolving domestic and international spectrum regulatory issues. In that context, NASA has successfully pursued a future World Radiocommunication Conference (WRC) agenda item for the 2023 WRC to gain regulatory recognition for space-to-space user links within certain frequency bands currently allocated to the FSS and MSS.

6.3.1 Objective

The objective of this the spectrum regulatory logic flow is to provide the user with information regarding if the frequency used by the commercial system is within scope of the agenda item, or if the user is potentially at risk of receiving services on an experimental basis.

6.3.2 Inputs/Outputs

CART stored reference data:

- Commercial system Return Link Frequency (MHz)
- Commercial system Forward Link Frequency (MHz)
- Frequencies under consideration for radio regulation revision at WRC-23

CART user input:

- None.

CART output:

- Indicator for return link operation – if regulatory approval may be resolved or operation may occur only under experimental / non-protected conditions
- Indicator for forward link operation – if regulatory approval may be resolved or operation may occur only under experimental / non-protected conditions

6.3.3 Algorithm Description

The spectrum regulator assessment uses the logic-based algorithm template. A precondition for processing is the altitude compatibility check (described in Section 3.3.1). The logic flow is summarized in Figure 20. The commercial systems' frequencies are compared against a reference list for the frequencies under consideration at WRC-23 and provides the related information to the user.

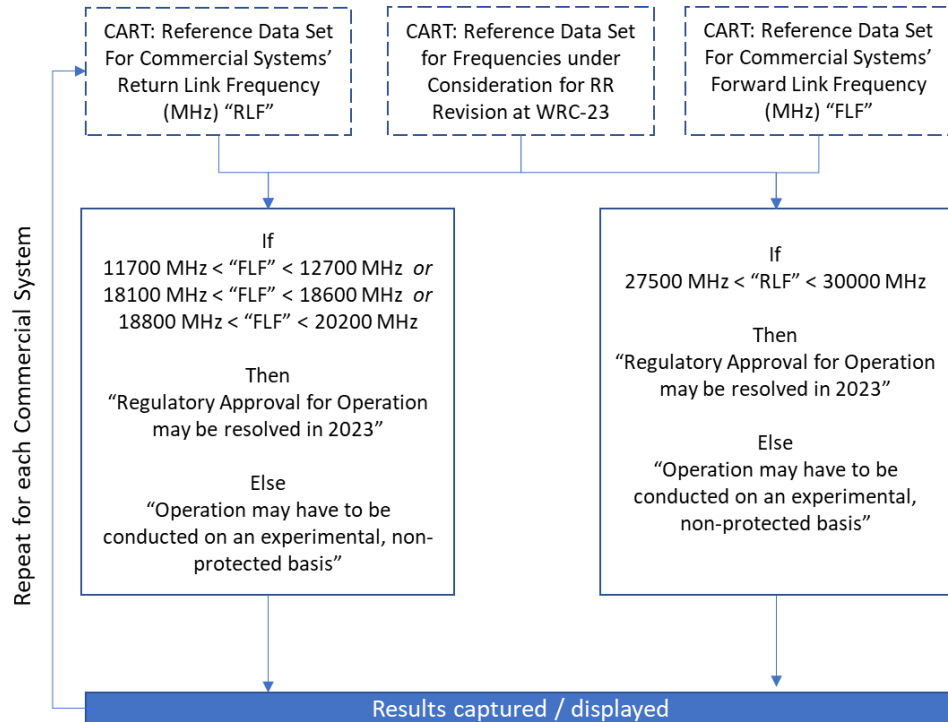


Figure 20. Logic Flow: Spectrum Regulatory Status

6.3.4 Assumptions/Limitations

- At this time, the frequencies included in the logic flow are those proposed for evaluation at WRC-23, but this may change in the intervening years and should not be considered final.

6.4 Ranking Algorithm

The “Analyze” function in CART allows the user to compare system results for a set of mission inputs. The ranking algorithm addresses how the results are displayed, to provide the user with an indication of “better” performance.

6.4.1 Objective

Allow the user to define the relative importance of various parameters and use the resultant parameter weights to rank order the system results.

6.4.2 Inputs/Outputs

CART stored reference data:

- Commercial Relay Constellation Altitude

CART analysis results:

- Results of analysis – e.g. performance parameters such as RF coverage, throughput, gaps, etc.

CART user input:

- Altitude
- Inclination
- Ranking preferences for six parameters. For each parameter, i.e. throughput, the user provides a qualitative input on the relative importance as follows:
 - *Exclude System if Not Met*; This selection is equivalent to “very important” but further indicates that the user wishes to not see any systems which fail to meet threshold needs associated with the applicable parameter. For example, if throughput requirements are critical and the user cannot tolerate an option that may not meet its throughput needs, this choice would eliminate all systems from the ranked display which fall below the threshold.
 - Very Important
 - Somewhat Important
 - Neutral
 - Somewhat Unimportant
 - Not Important

CART output:

- Results rank ordered

6.4.3 Algorithm Description

The ranking algorithm uses the logic-based algorithm template. The logic flow is summarized in Figure 21. The user is prompted to define the importance for each of the key threshold parameters: network availability, data volume, average RF coverage gap, pointing feasibility, launch date, and spectrum viability. Non-viable (altitude) systems are removed from the display. A score is created based on the weights of each parameter and the applicable pass/fail status for the system. The system with the highest score is ranked first, etc. For systems with equal scores, the tie breaker is the network availability (or effective communications time) score.

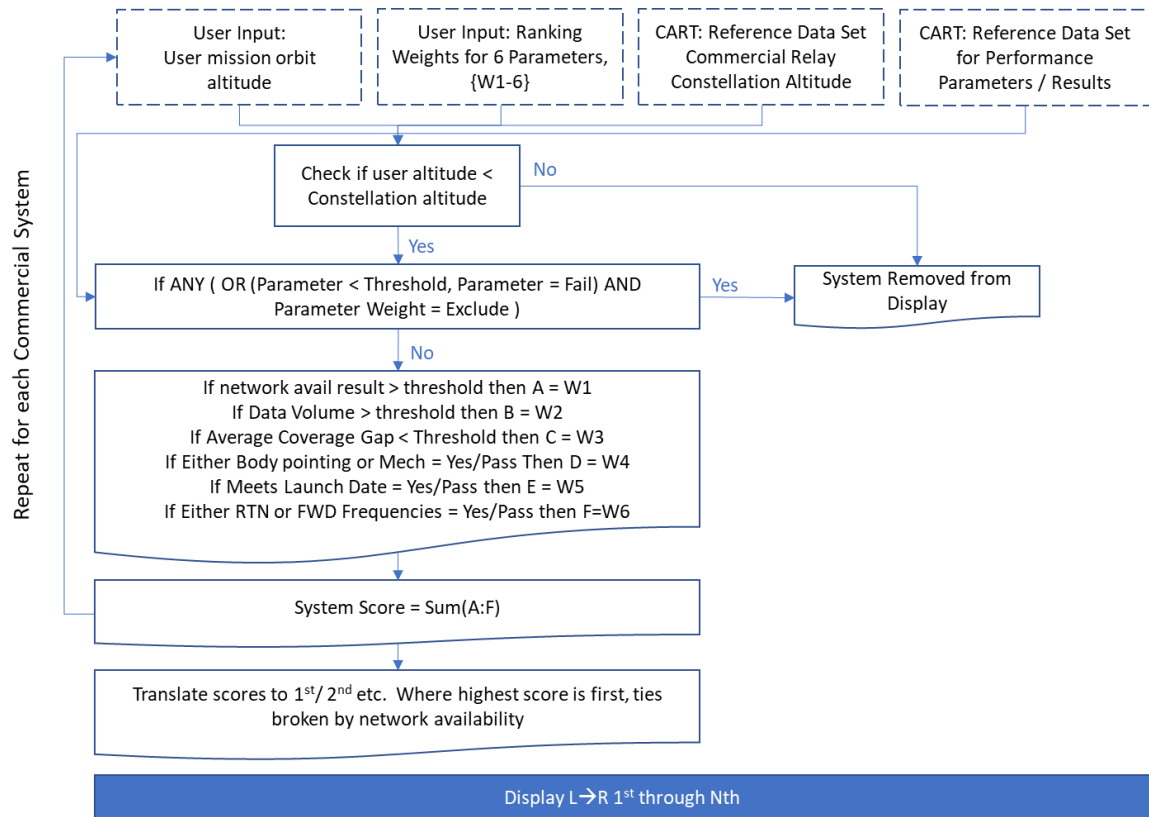


Figure 21. Logic Flow: Analyze / System Comparison Ranking

6.4.4 Assumptions/Limitations

1. None.

7.0 REFERENCES

- [1] Teltrium, "Commercial Communications and Navigation Services Study Final Report Volumes I and II," NASA, 2019.
- [2] Teltrium, "CART Use Case Document," 2019.
- [3] NASA, "Future Mission Space Communication and Navigation Needs," Version 2.0 National Aeronautics and Space Administration, Document No. NNC16ZLC002L., 2016.
- [4] D. P. A. T. K. M. Price, "Mass and Power Modeling of Communication Satellite," NASA, Cleveland , 1991.
- [5] M. O. Courseware, MIT, [Online]. Available: https://ocw.mit.edu/courses/aeronautics-and-astronautics/16-851-satellite-engineering-fall-2003/assignments/ps4_cs_solution.pdf.
- [6] By D. Orban and G.J.K. Moernaut, "The Basics of Patch Antennas, Updated," Orban Microwave Products, 2009.
- [7] K. Yazdandoost and D. Gharpure, "Simple formula for calculation of the resonant frequency of a rectangular microstrip antenna," in *1998 IEEE 5th International Symposium on Spread Spectrum Techniques and Applications - Proceedings. Spread Technology to Africa*, Sun City, South Africa, 1998.
- [8] J. R. E. D. F. P. J. J. Wertz, *Space Mission Engineering: The New SMAD*, Hawthorne, CA: Microcosm Press, 2011.
- [9] J. J. K. Parker, "Interoperable GNSS Space Service Volume (SSF)," GPS.GOV, 2018.
- [10] Y. N. H. Y. T. Takashi, "WINDS Satellite Networking Protocol for Bent-pipe Mode," *Journal of the National Institute of Information and Communications Technology*, vol. 54, no. 4, pp. 113-116, 2007.
- [11] "EXHIBIT A, Space Station Antenna Contours," Iridium-Next.
- [12] "Sched S Tech Report SpaceX," Fedearl Communication Commissions, 2019.
- [13] "Sched S Tech Report for Space-X," Fedearl Communication Commissions, 2018.
- [14] GlobalStar, "Technical and Operational Description Schedule S," FEDERAL COMMUNICATIONS COMMISSION.
- [15] "Intelsat Satellite Fleet," Intelsat, [Online]. Available: <http://www.intelsat.com/global-network/satellites/fleet/>. [Accessed 01 April 2020].
- [16] ViaSat, "ATTACHMENT A, Technical Information to Supplement Schedule S," FCC, 2015.
- [17] ViaSat, "Technical and Operational Description, Schedule S," FEDERAL COMMUNICATIONS COMMISSION, 2019.

- [18] Eutelsat, "Schedule S," FEDERAL COMMUNICATIONS COMMISSION.
- [19] OneWeb, "Technical and Operational Description, Schedule S," FEDERAL COMMUNICATIONS COMMISSION.
- [20] M. A. S. S. M. H. S. S. B. N. S. F. Ghazvinian, "Low-earth orbit satellite acquisition and synchronization system using a beacon signal". United States Patent and Trademark Office Patent US6127967A, 19 July 1999.
- [21] M. Rice, Digital Communications - A Discrete-Time Approach, Prentice Hall, 2008.
- [22] M. M. ,. S. A. F. H. Meyr, Digital Communication Receivers, Synchronization, Channel Estimation, and Signal Processing 1st Edition, Wiley-Interscience Publication, 1997.
- [23] E. W. Peter Weed, "SCaN Commercial Services Study: Status Update: Space-Based Relay Network Setup and Handovers (Memorandum #5A)," April 30, 2019.
- [24] A. J. D. &. A. G. Barnett., An Introduction to Generalized Linear Models., Chapman & Hall, 2008.
- [25] T. R. Foundation, "The R Project for Statistical Computing," The R Foundation, [Online]. Available: <https://www.r-project.org/>.
- [26] I. K. &. A. Z. Bettina Grün, "“Extended beta regression in R: Shaken, stirred, mixed, and partitioned.”," *Working Papers in Economics and Statistics*, vol. No. 22, 2011.
- [27] I. K. &. D. Firth, "A generic algorithm for reducing bias in parametric estimation.,," *Electronic Journal of Statistics*, vol. 4, 2010.
- [28] E. Claude Sammut & Geoffrey I. Webb. Springer, "Leave-one-out cross-validation," in *Encyclopedia of Machine Learning*, Springer, 2010.

APPENDIX A: RF COVERAGE ANALYSIS AND MODELING

A.1 Introduction

The first step of the physical link (OSI Level 1) connectivity analysis between a user satellite and a commercial communications relay is to perform a power requirements analysis using system specific link budgets. The link budget analysis parameters such as EIRP, G/T, and operational frequencies are derived from a combination of FCC filings, publicly available data, or custom designs, as applicable.

STK is used to turn the static analysis into a dynamic analysis that more precisely calculates distances and power values. Each relay constellation model in STK consists of numerous satellites in orbital orientation (orbital altitude, inclination, number of orbital planes, satellites per plane, etc.). The STK model is run over a long enough simulation period to reduce variations in results due to the statistical characteristics of each model by comparing coverage results for different simulation run times; that is, a higher simulation run period with a lower simulation run period time. The appropriate simulation period is defined at a point when the difference between two consecutive simulation runs yield the same coverage percentage.

The power outputs of STK are compared against a received power (Prec) threshold level to evaluate link usability. The Prec threshold is determined based on assumed desired link margin, modulation and coding scheme, and data rate.

A.2 Approach

There are two types of relay architectures used in satellite communications: 1) bent-pipe transponders and 2) regenerative transponders. The bent-pipe transponder (two hops) converts the frequency of the uplink signal issued from Earth stations, amplifies it, and downlinks the signal back to Earth stations (see Figure A - 1-1 (a)) [10]. By way of example, the Space Network (SN) and Globalstar use a bent-pipe architecture.

The regenerative transponder (one hop), on the other hand, demodulates the uplink signal from the Earth stations, converts the signal to baseband, modulates the signal, and then downlinks the signal to Earth stations (see Figure A - 1-1 (b)). Starlink is an example of regenerative transponder model.

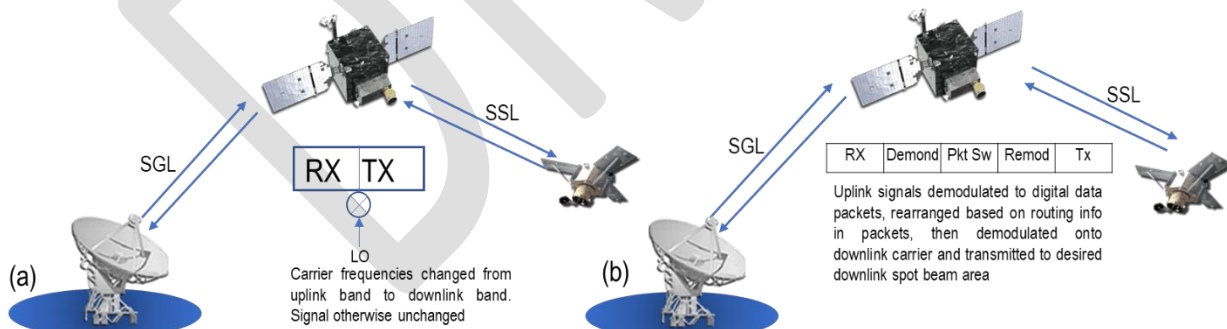


Figure A - 1. (a) a bent pipe network (b) a regenerative network model

The beam structure in the relay satellites are divided into two categories of Fixed Service Satellite (FSS) and High Throughput Satellite (HTS). The main difference between FSS and HTS is the size of their beams, or footprint, on the ground. FSS uses a wide beam covering entire continents or similarly large regions on the ground (“regional beams”) and HTS, on the other hand, uses many smaller “spot beams” with smaller footprint, each covering smaller regions. As a result, each of these smaller beams have a higher spectral efficiency and therefore can support higher speed.

Moreover, the relay systems can be categorized as shared analog bandwidth providers or digital shared capacity service providers. The shared analog bandwidth model (see Figure A-2), is a traditional model where a satellite service provider leases analog bandwidth to users for a selected amount of time. Service infrastructure can be selected by the user or purchased as a managed service from the service provider. Leased infrastructure can include any combination of ground sites or space segment. At any given time, only one user has access to a given portion of the infrastructure.

An example of this model is the direct-to-home broadcast service market. Intelsat, and Eutelsat are the systems that follow this service model.

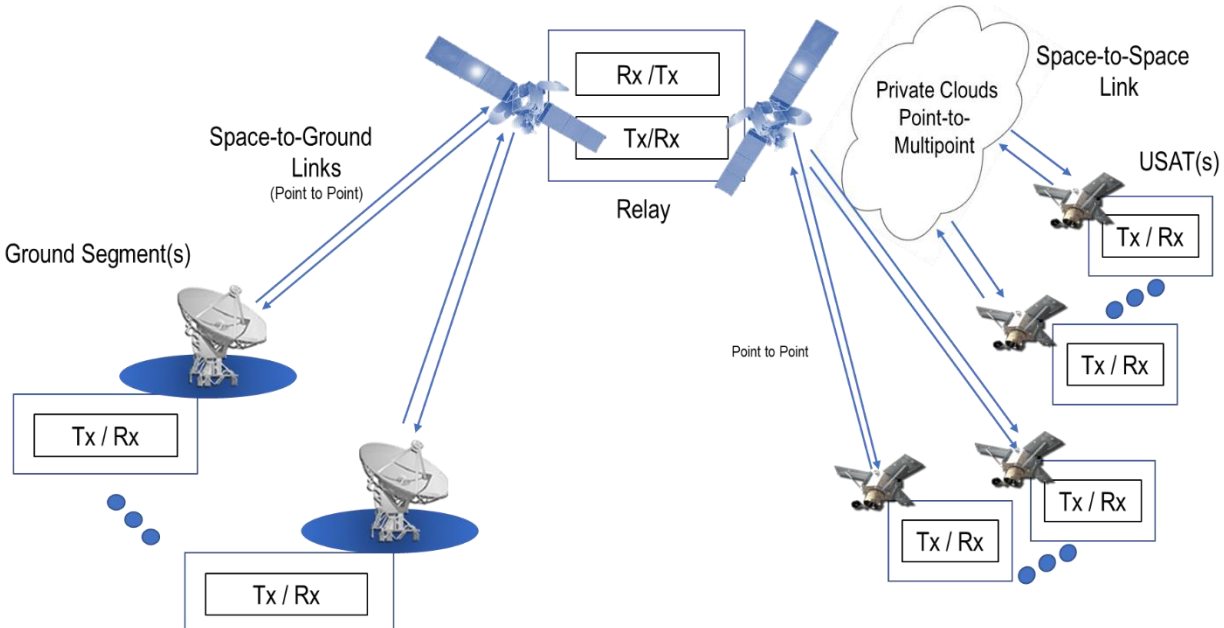


Figure A - 2. Shared Analog Bandwidth Model Architecture

Figure A - 3 shows a shared digital capacity architecture. In this model, multiple users are assigned or compete for shared connectivity resources enabled by time, frequency or code division multiple access technology and network protocols which assist in the transfer of information between source and destination. Throughput capability will be determined by the performance of all the network layers which orchestrate this process: Physical, Data Link, Network, and Transport layers.

Shared capacity service providers are modeled after today's terrestrial wireless service providers where a voice or data service is provided to subscribers that use a compliant end-user terminal. Just like in terrestrial networks, satellite digital networks may not be compatible with each other, and subscribers require equipment that is compatible with each network. Unlike terrestrial, the satellite industry has not matured to the point where multi-service provider terminals are available. Iridium, Globalstar, Inmarsat, Starlink, One Web are the systems that follows the shared capacity concept.

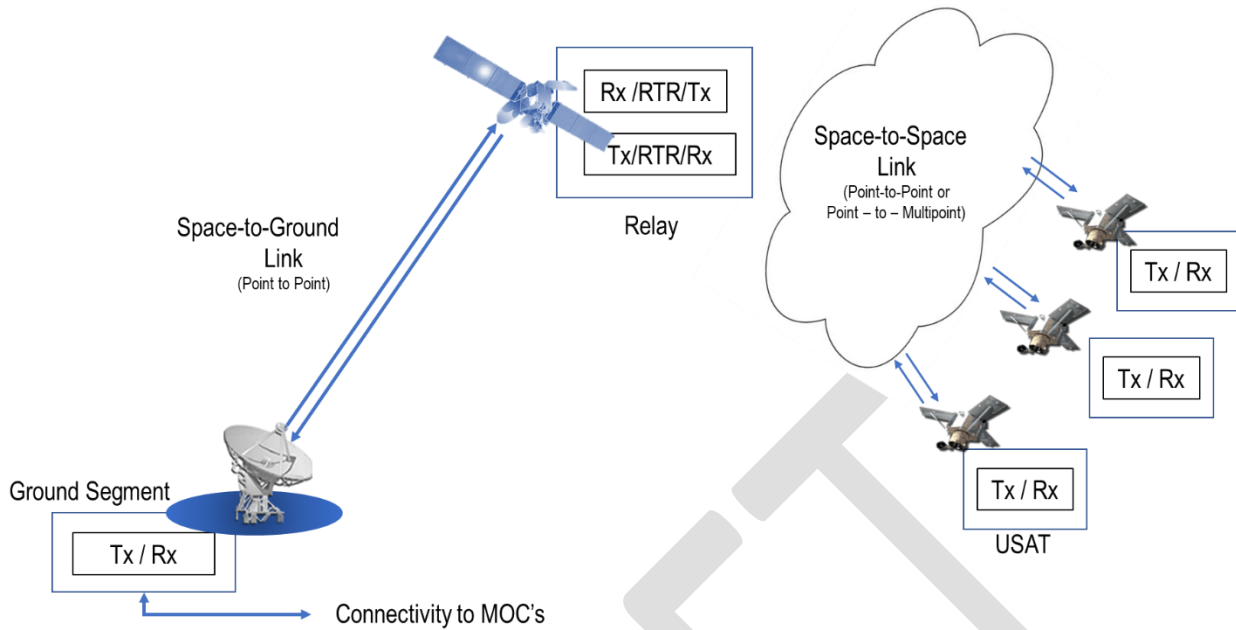


Figure A - 3. Shared Digital Capacity Architecture

Table A-1 summarizes the modeled commercial system beam structure type and service type architecture (leased RF bandwidth or digital shared capacity).

Table A - 1. Commercial System Beam Structure and Service Type Architecture Summary

Commercial System	Beam structure	Service Type Architecture
Iridium Next	48 Fixed Spot beams	Shared capacity service providers
Starlink	One fixed TT&C beam and 12 steerable beams. Out of 12 steerable beams, 8 are for Gateway communication and 4 for User terminals	Shared capacity service providers
Inmarsat-4	One global beam, 19 regional beams, 2 TT&C beams and on the order of 200 spot beams	Shared capacity service providers
One Web (MEO Configuration)	36 steerable receive beams out of which 16 for User terminals and 20 are for Gateway Communication	Shared capacity service providers
Globalstar	16 fixed spot beams	Shared capacity service providers
Intelsat	FCC filings are not available, modelled based on information from Intelsat's website	Shared analog bandwidth providers
Eutelsat	9 fixed beams, one global beam covering North America and Pacific Ocean and the other global beam covering Pacific Ocean region	Shared analog bandwidth providers
O3B	3 fixed TT&C beams, 24 steerable beams out of which 18 for user terminals, 6 are for Gateway communication	Shared capacity service providers
Viasat3	8 fixed Spot beams	Shared capacity service providers

Whether the system is a bent pipe or regenerative model, a two-hops or one-hop network, uses FSS or HTS relays, or is designed for leased RF-bandwidth service or network services, we are interested in the feasibility of return link (user and the relay satellite) connectivity throughout a users' orbit. For leased

bandwidth provider type systems, an SN-like service is assumed where a Single Carrier Per Frequency (SCPC) service is provided to each user per beam for this assessment; for network type systems the required parameter (EIRP, G/T, and operation frequencies, etc.) for this assessment is derived from a combination of FCC filings and publicly available data.

A.3 Model Description and Verification

A.3.1 Model Description

For each commercial relay system, a satellite constellation is created in STK. A custom application for building quickly building constellations was used. The input parameters for the constellation builder application are inclination, number of planes, number of satellites per plane, RAAN increment, phase offset, radius in km, and sensor type.

Once the constellation is set up, the user and the relay satellite parameters are entered according to design parameters verified using link equations (Section A.3.2) and Excel link budgets (see Section A.5).

- The relay system antenna beams are modeled based on data from the following data sources: FCC Filing Schedule S Technical Report: information about commercial relay constellation (e.g., orbit altitudes, inclination, orbital planes, number of satellites per plane, orbital plane spacing, satellite spacing in each plane) and information on transmitting and receiving beams such as frequency, gain, G/T, EIRP.
- FCC Filing Exhibits, Attachment Technical Information, Technical narratives, and available information other publicly available data as applicable for the information about the frequency bands for user terminals, gateways, gain contours and link budget calculations.

After the constellation, user satellite and relay satellite parameters are set up, the model is run. The output raw data includes the received RF power throughout the entirety of the simulation period at 1 second intervals. The raw data is compared to a calculated Prec (i.e. threshold power) to generate the coverage for each specific time within the simulation period.

A.3.2 Model Verification

In order to verify the model, the link budget analysis results were compared with STK results.

The link budget received power is calculated as:

$$P_r(dBw) = EIRP(dBw) - ((32.45) + 20 \log(f_{MHz}) + 20 \log(d_{km}))(dB) [10]$$

Where d is the maximum distance between the relay and user satellite.

Table A-2 shows the comparison between the received power calculated by the link budgets and the simulated power from STK for all relay models with 0-degree inclination and 450km user altitude.

Table A - 2. Comparison between Link Budget Received Power Calculation and STK Model

System	Representative Distances (km)	Simulated received power from STK (dBW)	Calculated Power based on link budgets (dBW)
Iridium Next	630	-116.58	-114.27
	570	-117.8	-113.5
Starlink	660	-110.19	-107.96

System	Representative Distances (km)	Simulated received power from STK (dBW)	Calculated Power based on link budgets (dBW)
Globalstar	964	-137.97	-137.92
	1710	-138.51	-137.75
One Web MEO	8050	-110.40	-110.39
	8500	-110.95	-110.86
ViaSat-3	35402	-111.80	-111.80
	43981	-113.71	-113.68
Intelsat	35338	-116.26	-116.26
	36452	-118.05	-116.53
Eutelsat	40145	-122.79	-122.5
	42003	-123.2	-122.89
Inmarsat-4	35840	-135.40	-134.61
	35860	-135.68	-134.62
O3B	7762	-106.14	-106.13
	5062	-102.42	-102.41

A.4 Systems and Configuration Parameters

A summary of the system configuration, including the orbital parameters, link budget parameters, communication link parameters and antenna model description are listed in Tables A - 3 to A - 5 for the modeled LEO, GEO and MEO satellite systems respectively.

Table A - 3. LEO System Configuration and Parameters

Systems	Iridium	Starlink	Globalstar
Orbital Parameters			
Altitude (km)	780	1110	1414
Inclination (deg)	86.4	53	52
Number of satellites per plane	11	50	3
Number of planes	6	32	8
Link Budget parameters			
Space to space Links (SSL)			
SSL frequency, MHz	1660	14500	1618
USAT EIRP, dBW	15.2	28.4	4.5
Total loss (dB) (note 1)	0.29	0.29	0.29
Space to ground link (SGL)	Note 2	Note 2	
SGL frequency, MHz	-	-	6980
Relay EIRP, dBW	-	-	-8.8
Gateway G/T, dB/k	-	-	28.4
Communication link parameters			
Modulation	QPSK	QPSK (note 3)	QPSK
Data Rate (Kbps)	512	3000	256
Eb/No (dB)	12.1(note 4)	4.2 (note 5)	4.2 (note 5)
Bandwidth (KHz)	240	125000	1230
System noise (Tsys)	570 K	530 K	397 K
Prec (dBW)	-134.3	-129.26	-141.7

Antenna beam model description	Note 6	Note 7	Note 8
Antenna model Description	Note 9	Note 10	Note 11
STK Model Development and Assumptions:	Note 12	Note 13	Note 14
Notes:			
<p>1. Assumption for the summation of multipath loss (0 dB), polarization loss (0.29 dB), atmospheric loss (0 dB), and rain attenuation (0 dB).</p> <p>2. The model is regenerative and the space to ground link is not applicable.</p> <p>3. The modulation is dynamic based on the user demands.</p> <p>4. From FCC filing link budget for 240 ksps case.</p> <p>5. Theoretical value.</p> <p>6. 48 Spot beams with the same footprint as FCC filing were modelled.</p> <p>7. User terminal steerable beam having maximum frequency with the same footprint as FCC filing was modelled.</p> <p>8. Sixteen (16) spot beams with the same footprint as FCC filing were modelled.</p> <p>9. Antenna pattern were designed based on trial and error comparison of FCC filing Antenna pattern with beam contours at the surface of the Earth on the STK.</p> <p>10. A generalized parabolic antenna with the ability of tracking the user satellite representing a phased array prototype were modeled.</p> <p>11. The orientation (azimuth and elevation angle) of each transmit and receive beam in reference to the Globalstar satellite body was computed manually using geometry and trigonometry. A parabolic antenna with the maximum peak gain derived from Schedule S was chosen.</p> <p>12. See Appendix A.4.1.</p> <p>13. See Appendix A.4.2.</p> <p>14. See Appendix A.4.3.</p>			

Table A - 4. GEO System Configuration and Parameters

Systems	Intelsat	Inmarsat-4	ViaSat	Eutelsat
Orbital Parameters				
Sub-satellite point	100W, 130E, and 10E	24.9E, 143.5E, 63.9E, 98.4W	89W, 209W and 31E	133W, 140E, 12W
Number of satellites	3	4	3	3
Link Budget parameters				
Space to space Links (SSL)				
SSL frequency, MHz	14125	1650.5	30000	14041
USAT EIRP, dBW	48.4	11	47.38	48.14
Total loss (dB) (note 1)	0	0	0	0
Space to ground link (SGL)				
SGL frequency, MHz	11575	3600	42500	Note 2
Relay EIRP, dBW	47.2	0.5	72.7	Note 3
Gateway G/T, dB/k	40.3	35.6	42 (note 4)	10.6
Communication link performance				
Modulation	QPSK	16QAM	QPSK	QPSK
Data Rate (Kbps)	80000 (note 5)	492	100000	3000
Eb/No (dB) (note 4)	4.2	4.2	4.2	4.2
Bandwidth (KHz)	120000	200	50000	3600

Systems	Intelsat	Inmarsat-4	ViaSat	Eutelsat
System noise (Tsys)	580.76	583 K	1380 K	439.54 K
Prec (dBW)	-117.33	-137.3	-112.71	-122.65
Antenna model description	Note 6	Note 7	Note 8	Note 9
STK model development and assumptions:	Note 10	Note 11	Note 12	Note 13

Notes:

- Assumption for the summation of multipath loss (0 dB), polarization loss (0 dB), atmospheric loss (0 dB), and rain attenuation (0 dB).
- The are 14 TX beams with different frequency ranges from 2.26 GHz to 12.75 GHz.
- There are 14 TX beams with different EIRP value ranges between 45 dBW to 57.6 dBW.
- Assumption.
- Data rate is tailorable. Link and transponder dependent.
- Theoretical value.
- Multiple spot beams that cover America, Asia, Europe and Africa regions were modeled. Center frequency of Intelsat 35e was assumed for receive beam frequency. Parabolic antenna was considered for modelling receive beam antenna. Same receiver parameters were assumed for all GEO satellites.
- Multiple spot beams (190 beams) with different Azimuth and elevation angles were designed to cover the entire satellite's field of view.
- A parabolic antenna with the ViaSat's contour on the Earth as a beam were designed to be able to continuously track the user satellite
- Global beam that's covering North America and Pacific Ocean region was modelled. Antenna beam is designed to be steerable. Sensor cone angle of 8.6 deg was assumed such that it covers the entire satellite's field of view and matches with the respective coverage area from the filings. A parabolic antenna with the peak gain of 37.03dB is selected.
- See appendix A.4.5.
- See appendix A.4.6.
- See appendix A.4.7.

Table A - 5. MEO System Configuration and Parameters

System	One Web MEO	O3B
Orbital Parameters		
Altitude (km)	8500	8062
Inclination (deg)	45	0
Number of satellites per plane	20	7
Number of planes	8	1
Space to space Links (SSL)		
SSL frequency, MHz	50200	30000
USAT EIRP, dBW	39.2	58.65
Total loss (dB) (note 1)	0.29	0.29
Space to ground link (SGL)		
SGL frequency, MHz	42500	-
Relay EIRP, dBW	52.3	-
Gateway G/T, dB/k	50 (note 2)	-
Communication link parameters		
Modulation	QPSK	QPSK

System	One Web MEO	O3B
Data Rate (Kbps)	25000	100000
Eb/No (dB)	4.2 (note 3)	4.2(note 3)
Bandwidth (KHz)	490000	500000
System noise (Tsys)	501.87 K	630.96 K
Prec (dBW)	-110.9	-112.61
Antenna model Description	Note 4	Note 4
STK Model Development and Assumptions:	Note 5	Note 6
Notes:	<ol style="list-style-type: none"> 1. Assumption for the summation of multipath loss (0 dB), polarization loss (0.29 dB), atmospheric loss (0 dB), and rain attenuation (0 dB) 2. Assumption. 3. Theoretical value. 4. A generalized parabolic antenna with the ability of tracking the user satellite representing a phased array prototype were modeled. 5. See Appendix A.4.8 6. See Appendix A.4.9 	

For all relay systems the transmit power derived from the peak gain, max EIRP, and maximum system noise temperature values were considered for all receive beams. The antenna efficiency for all relay system with parabolic antennae is assumed 55% and the polarization was not considered in the models. Specifics on each system model and assumptions are as described in Sections A.4.1 through A.4.8.

A.4.1 Iridium Next

The STK multibeam transmitter and receiver objects were used to model the transmit and receive antennas, transmitters, and receivers for Iridium Next beams. Since the antenna gain pattern was not available in a tabular format, the antennas for the transmit and receive antenna beams were created in STK as follows:

- The orientation (azimuth and elevation angle) of each transmit and receive beam in reference to the Iridium Next satellite body was computed manually using geometry and trigonometry.
- The Exhibit A in the FCC filings [11] beam contours at the surface of the Earth were assumed to represent the -3dB contour.
- Through trial-and-error, it was determined that a parabolic antenna in conjunction with the peak gain from the Schedule S closely approximates the contour of each Iridium Next beam on the Earth's surface.

A.4.2 Starlink (SpaceX)

Multibeam transmitter and receiver objects were used to model SpaceX transmitters and receivers. SpaceX was not modelled as per new 2020 filings based on customer direction. The RF parameters were the same in both the filings; the primary changes were the number of satellites and the altitude of the constellation. The receiver beam characteristics were referenced from the Schedule S tech report of October-2019 filings [12]. (Only user terminal beams were modelled). [13]

The SpaceX Starlink model has 3 user-terminal receive beams that differ in frequency, polarization and gain. Out of these, the beam with the maximum frequency was considered since all are having same footprint on the Earth's surface. The chosen beam parameters are:

Name: RX12

Frequency: 14.475 GHz

Antenna, Peak gain: Parabolic, 35.7dB

Through trial-and-error, it was determined that a parabolic antenna in conjunction with the peak gain of 35.7 dB from Schedule S gives the reliable power levels between transmitter and receiver objects.

A.4.3 Globalstar

The STK Multibeam Receiver object was used to model user terminal receive beams. Antenna beam patterns were created as follows:

- The orientation (azimuth and elevation angle) of each transmit and receive beam in reference to the Globalstar satellite body was computed manually using geometry and trigonometry.
- Through trial-and-error, it was determined that a parabolic antenna in conjunction with the peak gain from the Schedule S [14] closely approximates the contour of each Globalstar beam on the Earth's surface.

A.4.4 Intelsat

Three GEO satellites with sub-satellite points of 100W, 130E, and 10E were designed to cover America, Asia, Europe and Africa continent regions respectively. Multiple receive spot beams were used to fully cover the regions. The receiver parameters were taken from the Intelsat website [15]. For G/T the average value of Intelsat 33e satellite and highest System noise temperature of Intelsat 29e satellite was assumed. Center frequency of Intelsat 40e was assumed for receive beam. Same receiver parameters were assumed for all GEO satellites

A.4.5 Inmarsat-4

Out of global, regional and spot beams, designing multiple spot beams to cover the satellite service area was chosen because of high gain of spot beam(42dB) and contour data availability. The STK Multibeam Receiver object was used to model the user terminal spot beams and Spot beam parameters such as frequency, gain was taken from the Schedule S document for Inmarsat F1. Subsatellite points of four Geo satellites are: 24.9E, 143.5E, 63.9E, 98.4W

Antenna beam patterns were created as follows:

- Multiple spot beams (190 beams) with different Azimuth and elevation angles were designed to cover the entire satellite's field of view.
- Through trial-and-error, it was determined that a parabolic antenna in conjunction with the peak gain from the Schedule S closely approximates the contour of each Inmarsat-4 beam on the Earth's surface.

Because of limited information, it was also assumed that the rest of the satellites had the same beam structure as the F1 GEO.

A.4.6 ViaSat-3

Three GEO stationary satellites was positioned with sub satellite points of 88.9W, 208.9W and 31.1E degrees such that all satellites are spaced equally. Since the information in the FCC documents is not enough for modelling, approach of designing single receive beam of B-type (between user and ViaSat) for each GEO Satellite was selected.

Through trial-and-error, it was determined that a sensor with a cone angle of 8.6618 degrees and having complex receiver model object with a parabolic antenna approximates contours of ViaSat-3 on the Earth's surface. The beam parameters are: 30 GHz, Parabolic, 53.79 dB (Frequency, Antenna, Peak gain).

System noise temperature was taken from the Technical Annex document of 2015 FCC filings [16] and G/T value for receiver was from the 2019 Schedule S [17].

A.4.7 Eutelsat

Eutelsat 133WA satellite was modelled based on FCC filings [18] and replicated the satellite's receiver characteristics to two other satellites whose orbital location was chosen from the Eutelsat website such that all three Geo satellites are equally spaced in the orbit. The orbital location of three satellites are: 133 degrees West longitude, 140 deg East, and 12 deg West. Out of two steerable beams and 9 fixed beams, modelling of one steerable beam was chosen based on service regions of steerable beams and lack of pointing information for fixed beam modelling. The steerable beam parameters were referenced from the Schedule S document.

Antenna beam patterns were created as follows:

- Sensor cone angle of 8.6 deg was assumed such that it covers the entire satellite's field of view and matches with the respective coverage area from the filings.
- Through trial-and-error, it was determined that a parabolic antenna in conjunction with the peak gain of 37.03dB from the Schedule S closely approximates the contour of Eutelsat4 beam on the Earth's surface.

A.4.8 One Web-MEO

The STK multibeam transmitter and receiver objects were used to model the transmitting, receiving beams of user terminals. One Web-MEO has 16 user-terminal receive beams that differ in frequency, polarization and gain. Out of all those, the beam with the maximum frequency was considered since all are having same footprint on the Earth's surface.

- Through trial-and-error, it was determined that a parabolic antenna in conjunction with the peak gain of 55.1dB from the Schedule S [19] closely approximates the contour of each One Web MEO beam on the Earth's surface.
- Although an intermediate configuration of 160 satellites was modeled, the constellation in MEO was proposed to have a final deployment of 32 orbital planes each having 80 satellites.

A.4.9 O3B

Seven O3b mPOWER satellites were modelled. The STK multibeam transmitter and receiver objects were used to model the transmitting, receiving beams of user terminals. Out of all user terminal beams, the beam with the maximum frequency was considered since all are having same footprint on the Earth's surface.

- Through trial-and-error, it was determined that a parabolic antenna in conjunction with the peak gain of 35dB from the Schedule S closely approximates the contour of each One Web MEO beam on the Earth's surface.

A.5 Link Budgets

(Reserved)

A.6 Terrestrial Case Approach and Discussion

A.6.1 General Approach

The general approach for Terrestrial User Cases a facility is inserted into the current STK scenario with a transmitter child object. For systems that operate above the frequency of 18 GHz the rain model detailed in ITU-R-618 is used as it allows STK to use the rain, cloud, and fog statistical attenuation models that are detailed in that document. In the case of systems that have an operational frequency below 18 GHz the Crane 1985 rain attenuation model is used. The facility is positioned using geodetic coordinates with a starting point at latitude 0° longitude 0°. The properties (i.e. EIRP, Frequency, and Data Rate) of the transmitter child are the same as the user satellite transmitter child for all low earth orbit satellite systems. Geosynchronous satellite systems each have their own unique EIRP that is based off the difference between the best and worst case received isometric power. This difference is then added to the EIRP and accounts for the rain attenuation loss that each system experiences. The run time for each scenario was set for an interval of 24 hours with a time step of one epoch second. For each terrestrial user in the scenario the link information reports contain the time, strand name, beam ID, received isometric power, elevation, and azimuth of the facility with respect to the relay satellites. For geosynchronous systems, the facilities coverage stops between latitudes 60° to 70°, respectively. However, for low earth orbit systems, the coverage is either global or stops at latitude 80° with a coverage gap around the polar regions of the Earth. Once the desired STK model parameters have been entered the incriminations for both latitude and longitude are determined by the user. The geosynchronous terrestrial models used in this approach had their latitude increased and/or decreased by 30° and their longitude increased and/or decreased by 60° with a total of 49 points per system. While systems that are low earth orbit has their latitudes increase and/or decrease by 20° and had their longitude increase and/or decrease by 60° with a total of 72 points per system.

A.6.2 Rain Model Notes

The Crane 1985 rain model uses the updated atmospheric distribution tables that were introduced in 1985 along with the updated rain region map introduced in 1982. The world globe is divided into 12 rain regions. The Crane model in STK refers to the Global Crane Attenuation Model. The model calculates the amount of rain attenuation by dividing the globe into various rain regions. These rain regions along with the object's instantaneous position and outage percentage are used to determine the point-path

rain rate. It should be noted that the calculation of the rain attenuation is dependent upon the rain rate, 0 deg. isothermal height, specific attenuation tables, transmitter frequency, ground station to satellite elevation angle, ground station position and elevation, and curvature of the earth. The model was verified to be dynamic by taking two separate link budgets at two different ground sites in different regions of the world. The first ground site was in Svalbard, Norway (low rain rate) and the other located at Kennedy Space Flight Center located in Florida (high rain rate). The two link budgets for each site were then generated in STK with and without the Crane rain model. The difference between the received isotropic power for each link budget was then compared. The calculated rain attenuation loss matched the rain attenuation loss simulated by STK and the two ground sites had different attenuation losses due to their locations being in different regions of the world.

APPENDIX B: SIGNAL ACQUISITION ANALYSIS AND MODELING

B.1 Introduction

A varying degree of signal dynamics (i.e., Doppler) is induced by the relative motion of the relay satellite and the LEO user mission (Figure B - 1). The experienced Doppler and its rate of change impact the time a user satellite receiver will take to acquire and track the received signal. The user must first resolve the uncertainty between the transmitted frequency and the actual received frequency while handling any additional shifts during this acquisition process. Once the signal is successfully acquired, signal tracking becomes critical. The ability of the system to track the signal is a function of the signal to-noise ratio and the signal dynamics, commonly measured in terms of the residual root mean square (rms) phase tracking error. The phase error is comprised of error due to thermal noise, and error due to Doppler Rate, or the rate of change of range rate, i.e., acceleration.

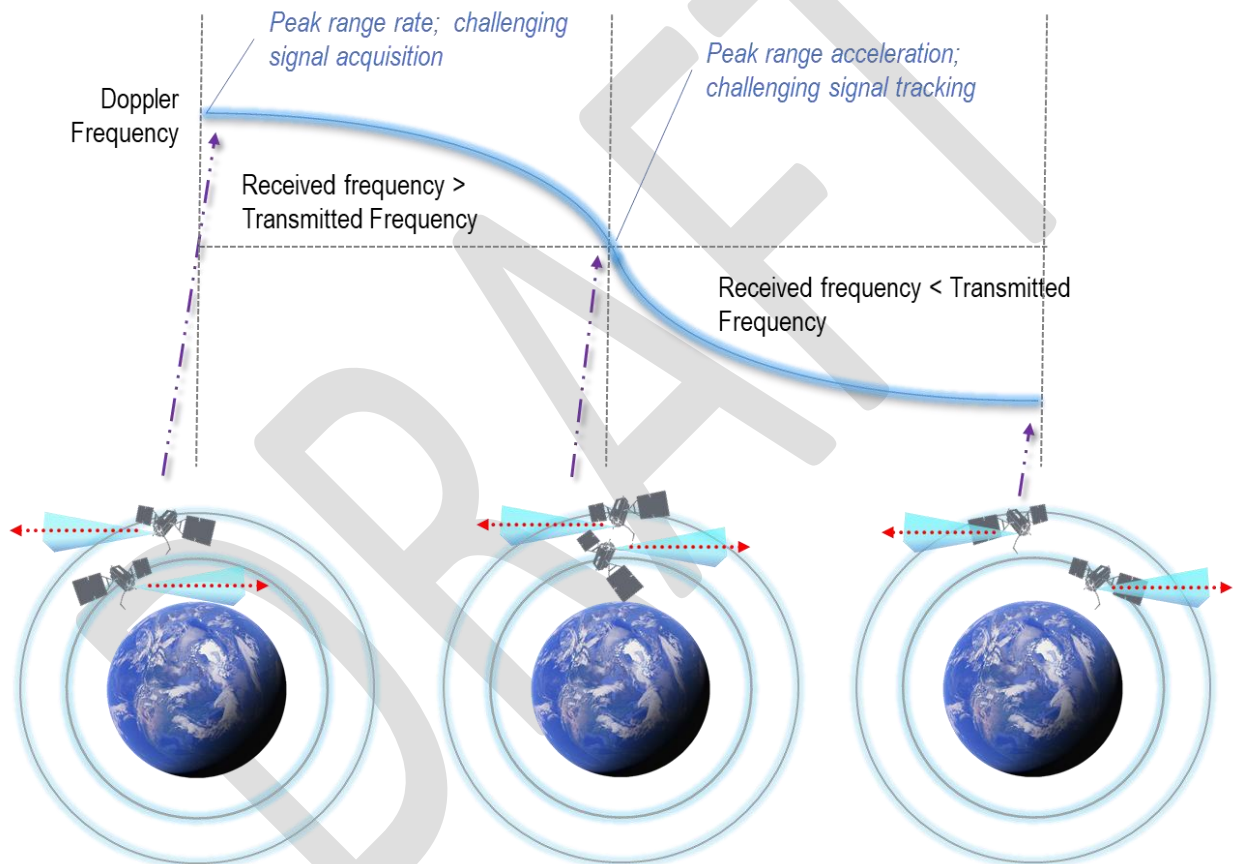


Figure B - 1. Doppler Frequency for LEO to LEO Communications

The SN uses ephemeris information of both the relay and user satellite to estimate forward and return Doppler shift and its rate of change so it can then pre-compensate forward signals prior to transmission from the ground. Similarly, it uses the same information to estimate the location and dynamics of return signals to aid in acquisition [20]. The pre-compensation of the forward signal reduces the complexity of the user satellite transponder as signals in the forward direction are received at near its expected frequencies.

With the exception of bent-pipe satellites, GEO commercial satellite systems where NASA has the opportunity to provide its own ground infrastructure to replicate today's SN ground functionality, the

NASA LEO user will need to search for the forward signal through the entire frequency uncertainty range prior to attending frequency synchronization. Note that the size of the frequency uncertainty window of the return signal can be decreased by using onboard GPS to estimate the location of the commercial relay satellites as a function of time and the corresponding signal dynamics of the forward signal.

Table B - 1 summarizes the forward Doppler frequency shift and Doppler rate (range acceleration) that will be experienced by three representative missions with respect to the Iridium, OneWeb and Globalstar commercial relay constellations.

Table B - 1. Average and Maximum Doppler Shift for Selected Systems

Commercial Constellation		Average Doppler Shift (KHz)			Maximum Doppler Shift (KHz)			Average Range Acceleration (m/s ²)			Maximum Range Acceleration (m/s ²)		
System	Altitude/ Inclination	ISS	IRIS	SWIFT	ISS	IRIS	SWIFT	ISS	IRIS	SWIFT	ISS	IRIS	SWIFT
OneWeb	1200 km/ 88 deg	72.7	38.9	116.5	300.8	333.7	326.2	53.8	19.2	178	164	167	227
Iridium	780 km/ 86 deg	33	14.3	27.9	70	66.1	58.1	147.2	35	297.2	472	166	737
Globalstar	1441 km/ 52 deg	13.2	26.3	15.7	55.3	65.7	40.9	18.3	81	24.1	137	257	91

Approximate orbital parameters for reference:
 ISS: 52-deg inclination, 400-km altitude
 IRIS: 97.9-deg, 670-km
 SWIFT: 21-deg, 550km

B.2 Approach

A mathematical assessment to determine the best approach to predict the estimated amount of time a receiver requires to lock to a signal under the conditions summarized in Table B - 1 was first performed. Based on this mathematical analysis, a MATLAB model was then developed to expand the process of estimating the performance of searching for the forward signal in a maximum frequency uncertainty window (i.e. coarse signal acquisition) and the follow-up function of pulling in the signal and achieving signal tracking (i.e. fine signal acquisition) and symbol synchronization.

Figure B - 2 is a high-level view of the developed MATLAB model. Section B-3.1 provides the details of the mathematical analysis performed to support the development and verification of the MATLAB model. Section B-3.2 provides a detailed description of the MATLAB model and simulation results. The developed model can be expanded to include signal distortions and in-channel interferers for which signal recovery impacts cannot be analyzed analytically.



Figure B - 2. MATLAB Model Overview

Using this modeling approach, we demonstrate that an FFT coarse estimator can be used to predict the Doppler shift frequency without having access to its ephemeris or that of the relay (s). This version of the model, this is used as a pass or fail test only based on the modulation order and Signal-Noise-Ratio (SNR) value. The fine signal acquisition stage compensates for both carrier frequency and phase rotation.

B.3 Model Description and Verification

B.3.1 Mathematical Analysis

For the fine acquisition component of the signal acquisition process the user mission receiver will most likely use a Phase Lock Loop (PLL) to acquire and track the phase and frequency of the input signal. A PLL consists of three main components: 1) phase detector, 2) the loop filter, and a 3) Voltage-Controlled Oscillator (VCO). See Figure B - 3 [21].

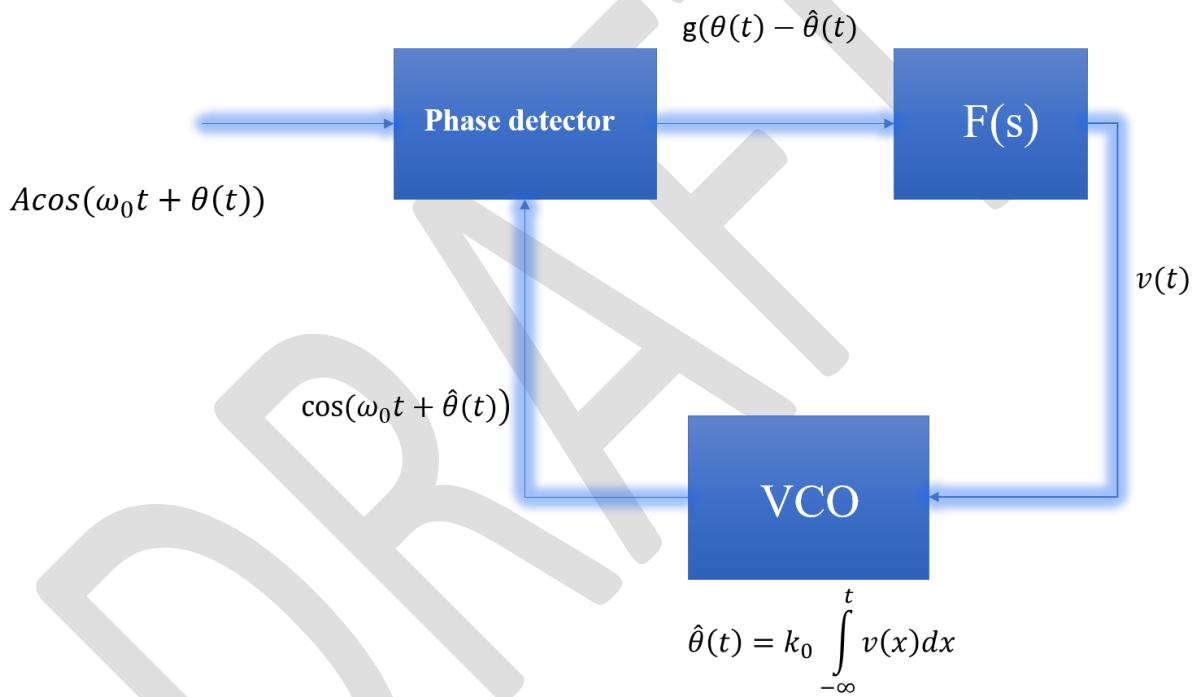


Figure B - 3 Basic Structure of PLL

The input to the loop is the sinusoid represented by:

$$x(t) = A\cos(\omega_0 t + \theta(t)) \quad (1)$$

The output of the VCO is represented by:

$$y(t) = A\cos(\omega_0 t + \hat{\theta}(t)) \quad (2)$$

The phase detector output is a function $g(\cdot)$ of the phase difference between the two inputs $g(\theta(t) - \hat{\theta}(t))$. We call the difference the phase error $\theta_e(t)$.

The phase error is filtered by the loop filter to produce a control voltage $v(t)$ that is used to set the phase of the VCO. The VCO output is related to the input $v(t)$ via the phase relationship.

$$\hat{\theta}(t) = k_0 \int_{-\infty}^t v(x) dx \quad (3)$$

Where k_0 is a constant of proportionality, called the VCO gain, that has unit radians/volt.

The loop adjusts the control voltage $v(t)$ to produce a phase estimate $\hat{\theta}(t)$ that drives the phase error to zero. When the phase error is positive $\theta_e(t) > \hat{\theta}(t)$, it means the phase of the VCO output lags the loop input and the controlled voltage must be increased. The positive phase error produces a control voltage $v(t)$ that is also positive at the loop filter output. The positive control voltage increases the phase of the VCO output $\hat{\theta}(t)$, thus producing the desired result. Likewise, when the phase error is negative, the voltage is negative.

The PLL operation is characterized using both phase error $\theta_e(t)$ and $\hat{\theta}(t)$. After some Laplace domain algebra, the transfer functions for the phase error and VCO output phase can be represented as equations (4) and (5) respectively:

$$G_a(s) = \frac{\theta_e(s)}{\theta(s)} = \frac{s}{s + K_0 K_p F(s)} \quad (4)$$

$$H_a(s) = \frac{\hat{\theta}(s)}{\theta(s)} = \frac{K_0 K_p F(s)}{s + K_0 K_p F(s)} \quad (5)$$

In which K_p and K_0 are the proportional and integrator gain constant.

Ideally, the PLL should produce a phase estimate that has zero phase error. This characteristic, together with the phase error transfer function, will be used to determine the desirable properties of the loop filter. The phase estimate transfer function, or loop transfer function, is used to characterize the performance of the PLL.

We define two inputs to the PLL. The first one is when Loop input differs from the VCO output by a simple phase difference $\Delta\theta$ (i.e. $\theta(t) = \Delta\theta u(t)$). The slope of the line is the frequency of the input sinusoid which means the frequency does not change. This response is so called step response and the Laplace transform of the input is $\Theta(s) = \frac{\Delta\theta}{s}$.

For the second case, the input sinusoid differs from the VCO output by a frequency shift of $\Delta\omega$ rad/s. The frequency offset is modeled by observing that $\cos((\omega_0 + \Delta\omega)t) = \cos(\omega_0 + \Delta\omega t)$. As a result the input is $\theta(t) = (\Delta\omega)t u(t)$, and is so called ramps response which is represented by the Laplace transform of $\Theta(s) = \frac{\Delta\omega}{s^2}$. (6)

Figure B - 4a), and Figure B - 4b) below, represents the graphical representation of the step response and ramp response respectively.

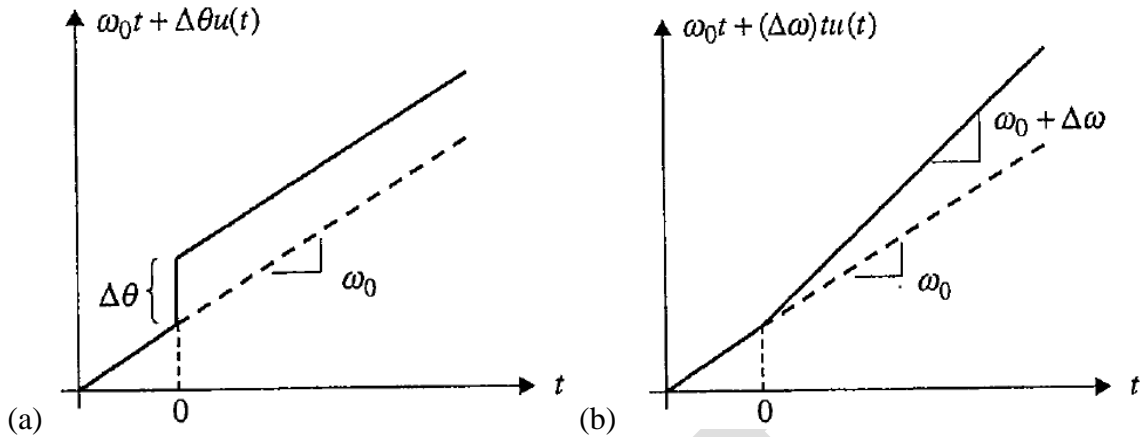


Figure B - 4 (a) step response (b) ramp response

The properties of the phase error are used to determine the desirable characteristics of the loop filter.

For example, for a step response with the transform function according to Figure B - 5.

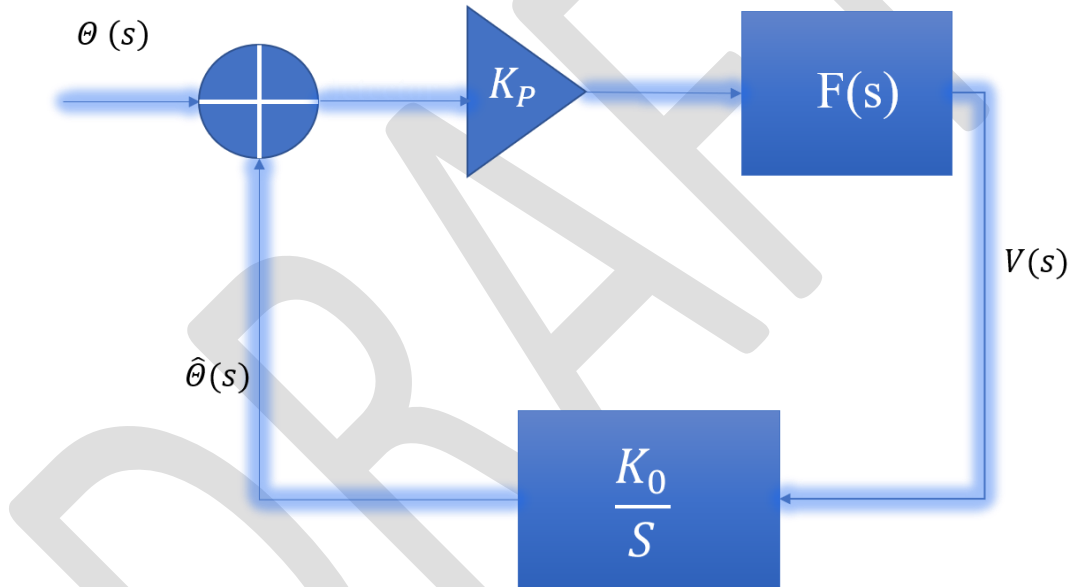


Figure B - 5. Frequency Domain PLL

The transform function can be written as

$$G_a(s) = \frac{\theta_e(s)}{\theta(s)} = \frac{s}{s + K_0 K_p F(s)} \quad (7)$$

and as we derived for the input step response $\theta(s) = \frac{\Delta\theta}{s}$, one can write error function as:

$$\theta_{e,step}(s) = \frac{\Delta\theta}{s + K_0 K_p F(s)} \quad (8)$$

The steady-state phase error may be obtained by computing the inverse Laplace transform and taking the limit as $t \rightarrow \infty$. However, this approach requires knowledge of the loop filter transfer function $F(s)$. An alternative approach is to use the final value theorem for Laplace transforms. Applying the final value theorem, the steady state phase error is:

$$\theta_{e,step}(\infty) = \lim_{s \rightarrow 0} \{s\theta_e(s)\} = \lim_{s \rightarrow 0} \left\{ \frac{s\Delta\theta}{s + K_0 K_p F(s)} \right\} = 0 \text{ if } F(0) \neq 0. \quad (9)$$

This means that if the loop filter has a nonzero DC gain, the steady state phase error for a step input is zero.

A loop filter that can satisfy this condition is as follows:

$$F(s) = K_1 + \frac{K_2}{s} \quad (10)$$

This is the proportional plus integrator filter and it produces a second order PLL. By varying the constant value of K1 and K2 we will be able to control the loop response (i.e. bandwidth and damping factor).

Any PLL requires a nonzero period to reduce a phase error to zero. During the initial stages of acquisition, the input voltage to the VCO is adjusted to produce an output whose frequency matches that of the input. This initial phase of the acquisition process is called frequency lock. Theoretically, the acquisition time for a loop to be able to lock the signal can be approximated as:

$$T_{PL} \approx \frac{1.3}{B_n} \quad (11)$$

Figure B - 6 shows the estimated acquisition time for phase lock versus different loop bandwidth based on the theoretical formula.

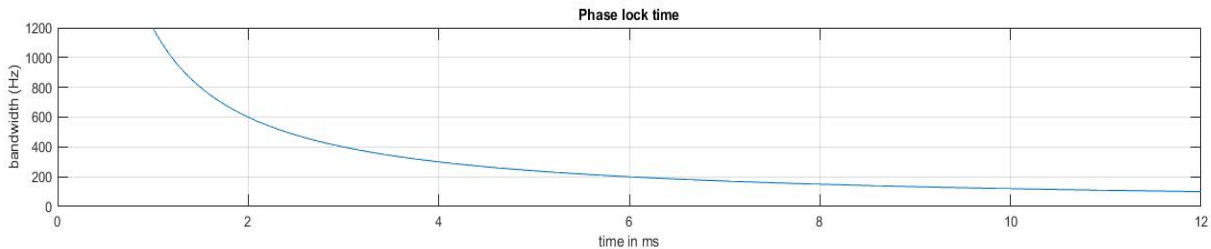


Figure B - 6. Estimated Acquisition Time for Phase Lock Versus Different Loop Bandwidth

B.3.2 MATLAB Model Description

The MATLAB model was developed to expand the process of estimating the performance of searching for the forward signal in a maximum frequency uncertainty window (i.e., coarse signal acquisition) and the follow-up function of pulling in the signal and achieving signal tracking (i.e., fine signal acquisition) and symbol synchronization. The developed MATLAB model consists of three main parts (i.e. transmitter, channel, and receiver). In the transmitter a bit generator generates the data, after modulation (e.g. QPSK, 4QAM, 16 QAM), it passes through a Root Raised Cosine (RRC) filter for shaping before transmitted to the receiver through an Additive White Gaussian Noise (AWGN) channel. The AWGN model includes the ability of changing the SNR level and to induce a Doppler frequency, allowing us to represent the different orbital dynamics of the various user-constellation pairs.

At the receiver, the signal passes through an Automatic Gain Control (AGC) unit and an RRC filter prior to it being processed by the coarse frequency and fine frequency synchronizer. The coarse frequency synchronizer takes an FFT over the received signal to detect the Doppler shift; the fine frequency synchronizer removes any residual frequency and phase shift.

Figure B - 7 shows the block diagram of the Simulink MATLAB model. The sections below describe the internal of each of the receiver main blocks.

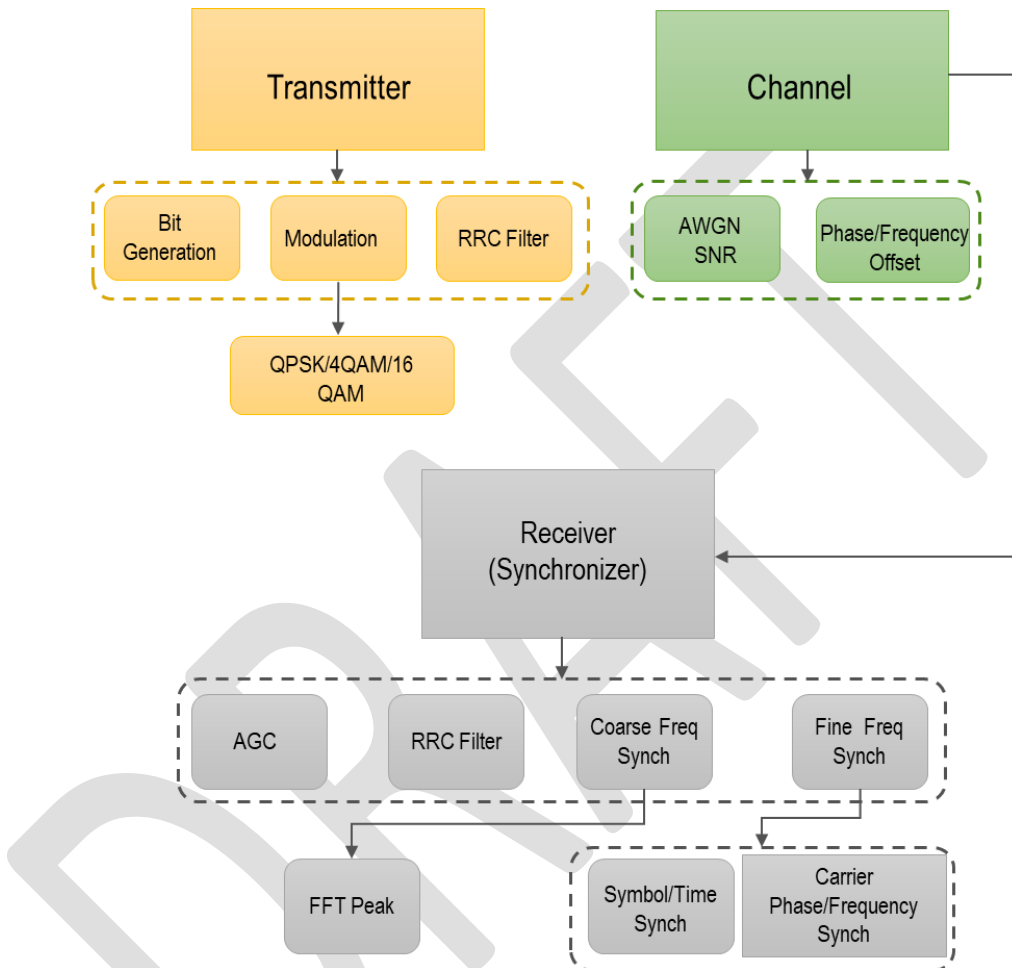


Figure B - 7. Block Diagram of the Signal Acquisition Model

B.3.3 Coarse Frequency Estimator

The first part of the signal synchronization function at the receiver is the coarse frequency compensation. This subsystem corrects the input signal with a rough estimation of the frequency offset.

There are two different common methods for coarse frequency estimation. The first method is autocorrelation which can be implemented by a FIR filter and an accumulator. The second method is an FFT peak detector which sweeps over the spectrum of the input signal to find the peak.

In this model we have used the FFT method. However, even if the coarse frequency compensation module estimates the major frequency offset, there is still a residual frequency offset. Usually the remaining frequency offset causes a rotation of the constellation. Figure B - 8. depicts the FFT peak detector used in the developed Simulink model.

The estimation of frequency depends on the number of FFT bin (NFFT) and the Eb/No or signal to carrier ratio at the receiver. The resolution of the estimate is the frequency spacing between two adjacent FFT points. There is a trade-off between speed and accuracy of the signal acquisition. The larger the FFT bin is, the closer the estimation of Doppler frequency will be. However, a larger FFT size also incurs a higher computational burden.

As described in reference [1], if the carrier to noise is high enough, we can estimate the signal with high probability. As an instance for Iridium we showed by taking 1024 FFT bins, and by knowing the carrier to noise for the Iridium signal ring alert is C/No = 67.8 dB-Hz we will have a very high probability of detection of $C/N = 67.8 - 10 \cdot \log(1024/2) = 41.9$ dB.

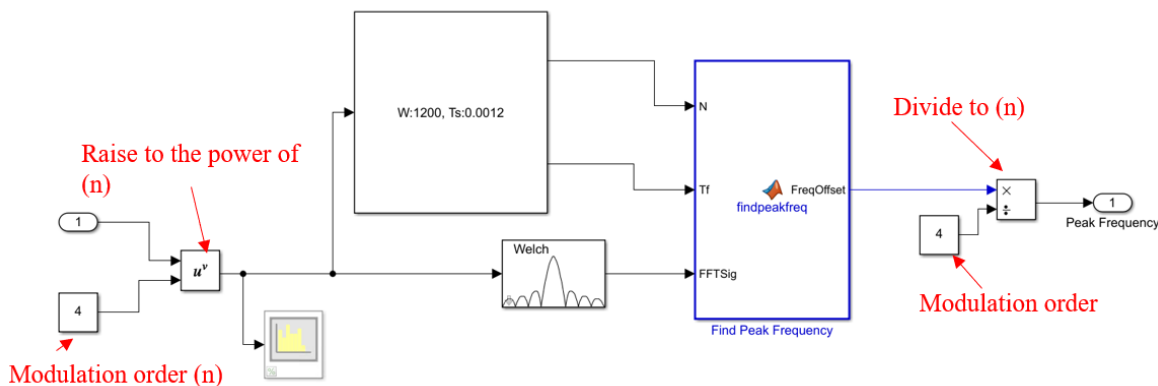


Figure B - 8. Simulink Block Diagram of FFT Coarse Frequency Estimator

Figure B - 9. (a) depict the constellation diagram of QPSK modulation after RRC filter and AGC for an 80KHz Doppler shift. Figure B - 9. (b) and (c) show the constellation diagram after coarse frequency synchronization for different number NFFT=256 and NFFT=1024 bins, respectively. It can be seen from the figure that the more accurate estimation has been achieved by using higher resolution for FFT bin.

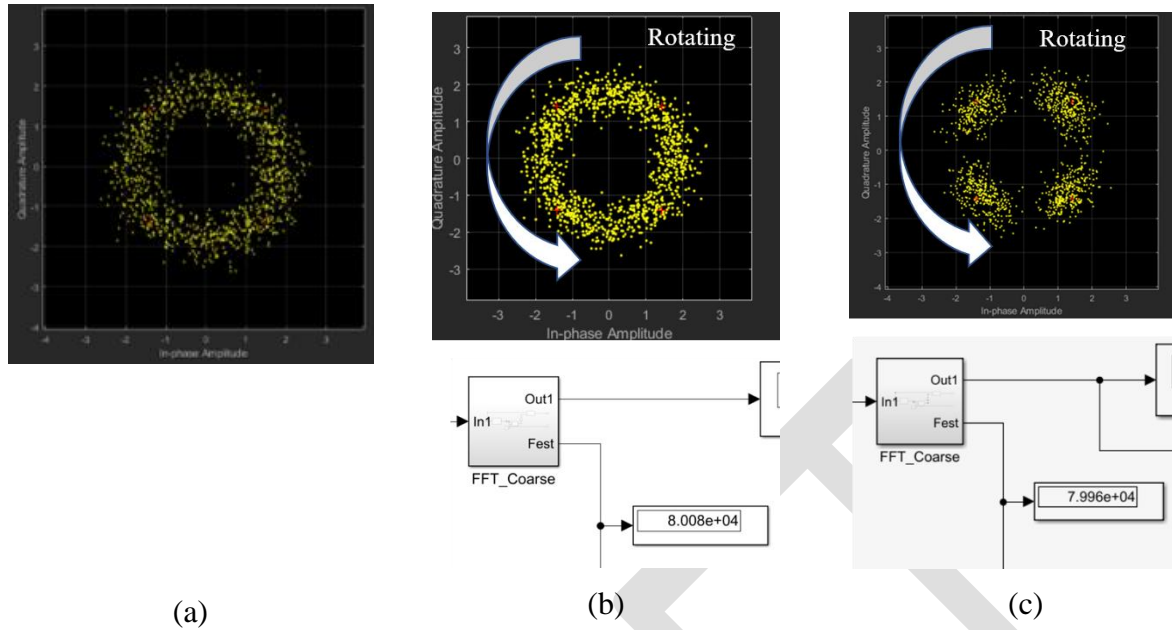


Figure B - 9. (a) constellation before FFT (b) FFT bin =256 (c) FFT bin=1024

B.3.4 Fine Frequency Estimator

The residual frequency after FFT coarse frequency needs to be compensated for both carrier frequency and phase rotation. The fine frequency subsystem is divided into two parts: 1) symbol/time synchronization and 2) carrier phase/frequency synchronization. The receiver must know the sample frequency and where to take the samples within each symbol interval. As a result, the timing recovery consists of an algorithm to estimate the Time Error Detection (TED) and a timing correction using a VCO or an interpolation filter. Carrier frequency/phase synchronization is carried out by using a PLL (second order Costas loop) frequency estimation. Figure B - 10. depicts the Simulink model of the fine frequency synchronization.

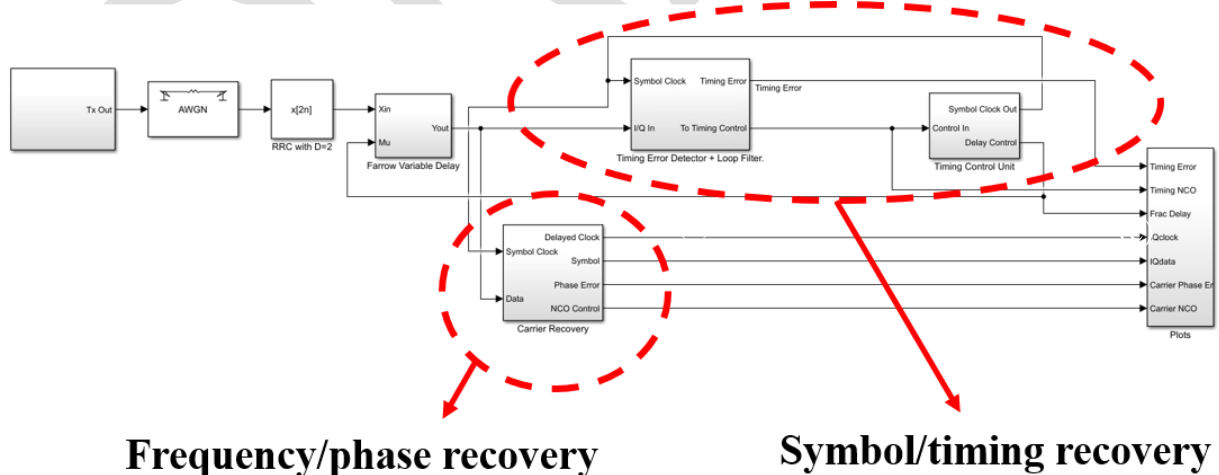


Figure B - 10. Simulink Block Diagram of the Fine Frequency Estimation

B.3.5 Time/Symbol Recovery

The time recovery loop consists of an Interpolator, a Timing Error Detector (TED), a digital loop filter, and a Numerically Controlled Oscillator (NCO). The interpolator computes the intermediate values between the adjacent signal samples. In this model, a Polynomial Interpolator, which can be derived using Lagrange's interpolation formula, is used. The interpolator is implemented using a time varying Finite Impulse Response (FIR) filter. See Figure B - 11.. The TED compares received waveform with the locally generated signal in every symbol period. Spectral estimation maximum likelihood is used in this model for TED. A second order loop filter that tracks the phase and frequency offset and has a stable close form transfer function is used in this model. The NCO controls the estimated timing of the loop which is fed to the time-variant FIR linear interpolator. m is called the basepoint index and μ is called the fractional index.

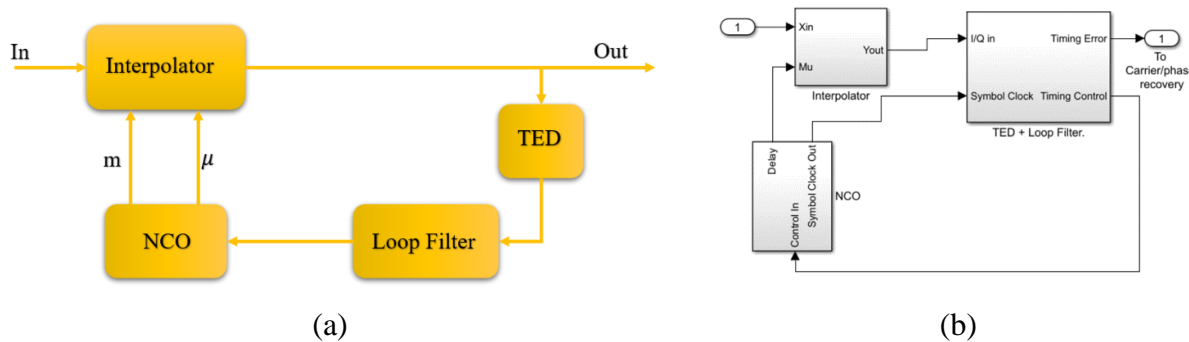


Figure B - 11. (a) shows the block diagram (b) shows the Simulink model for the time/symbol recovery.

Conceptually, symbol synchronization is the process of estimating a clock signal that is aligned in both phase and frequency with the clock used to generate the data at the transmitter.

The role of symbol timing synchronization is to move the samples to the desired time instants. Another name for “moving” samples in time is interpolation. The interpolator farrow filter is depicted in Figure B - 12 and the implemented structure is showed in Figure B - 13.

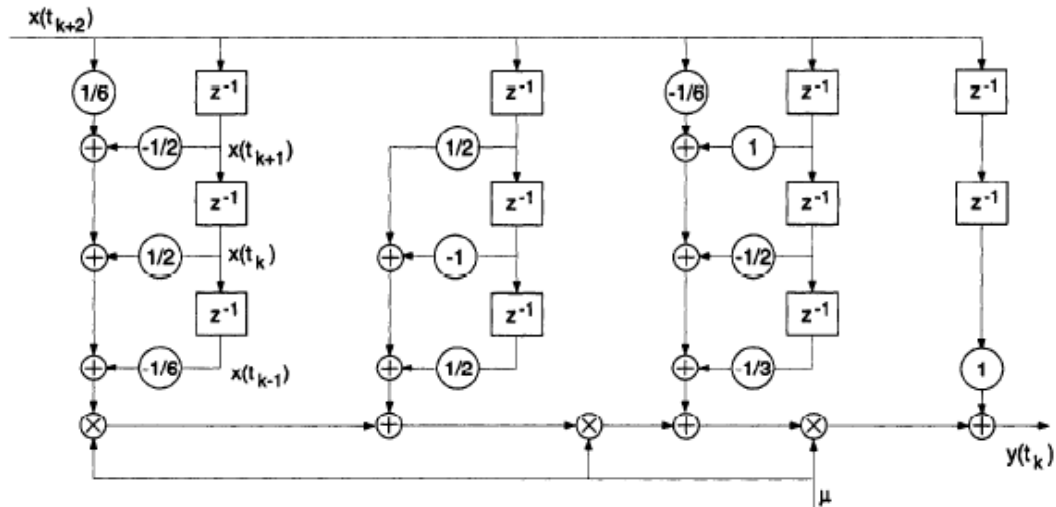


Figure B - 12. Farrow Interpolator Filter

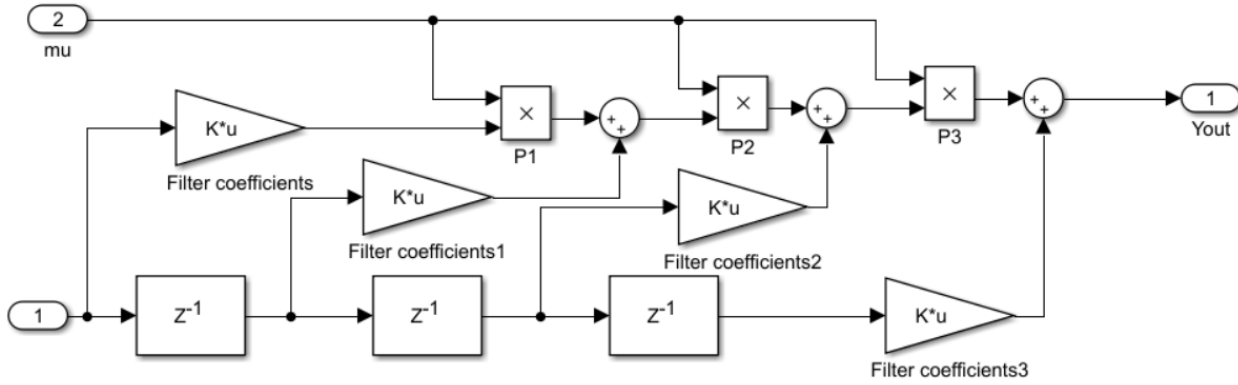


Figure B - 13. Farrow Interpolator Filter Implemented in MATLAB

In this model the time estimation or symbol recovery was done by using spectral estimation. The approach to obtain estimator for the synchronization parameters is that the likelihood must be averaged over the unwanted parameters. The objective function for the synchronization parameters (θ, ε) is given by:

$$L(a, \theta, \varepsilon) = \exp \left\{ -\frac{2}{\sigma_n^2} \operatorname{Re} \left[\sum_{n=0}^{N-1} a_n^* z_n(\varepsilon) e^{-j\theta} \right] \right\} \quad (12)$$

The estimate of ε is obtained by removing the unwanted parameters a and θ in equation (12).

Figure B - 14. shows the algorithm proposed by Meyer [22] and Figure B - 15. shows the implemented model in Simulink.

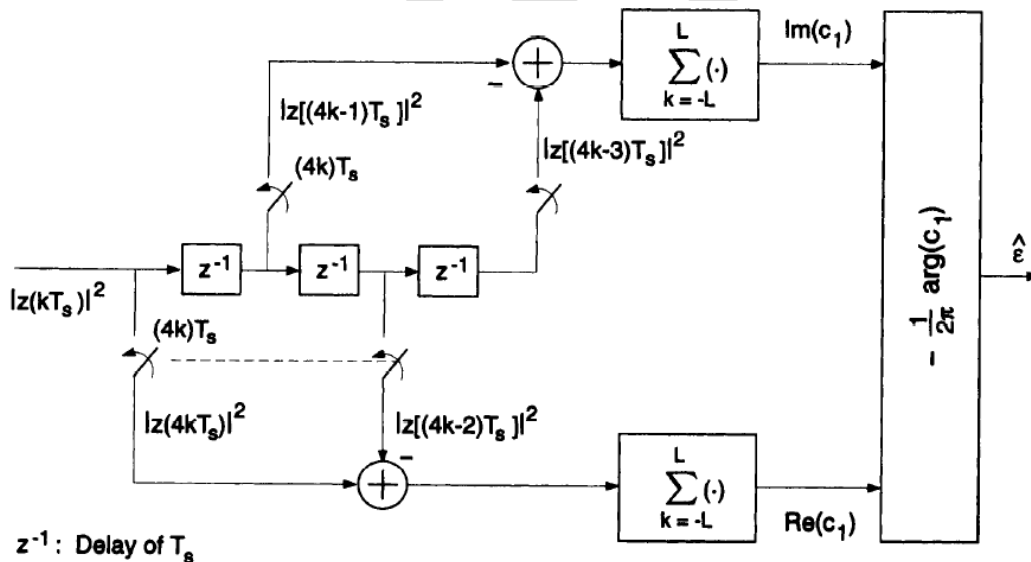


Figure B - 14. Time Error Detector Algorithm

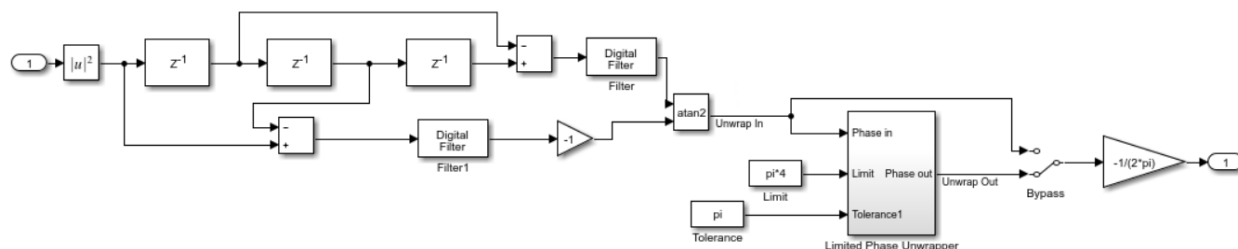
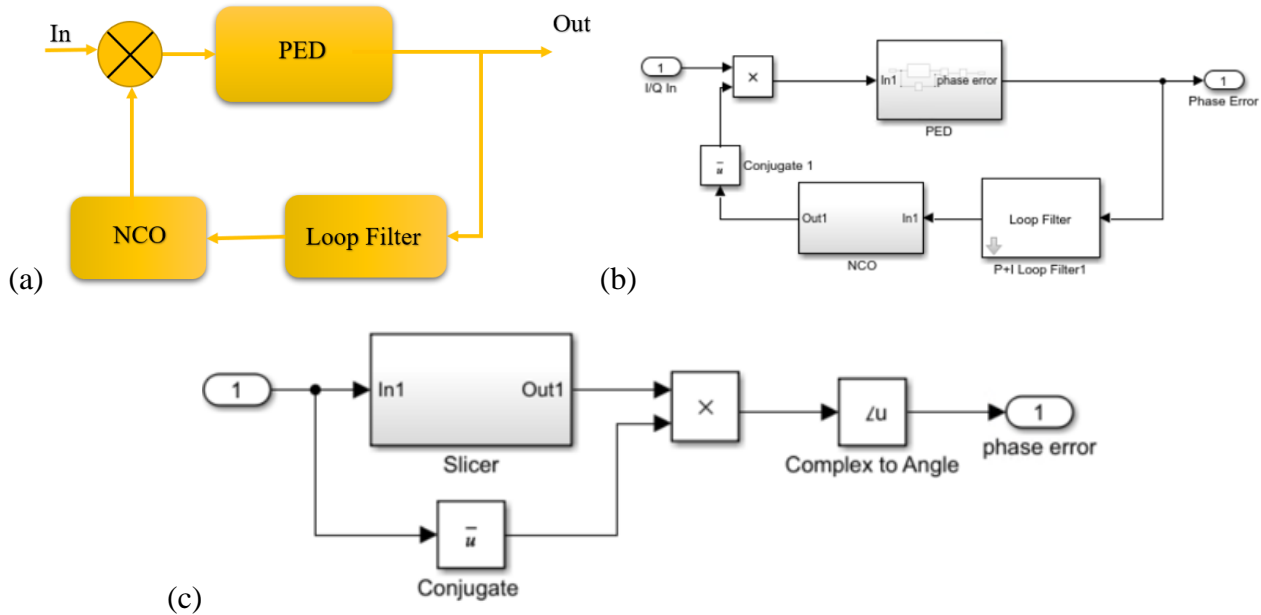


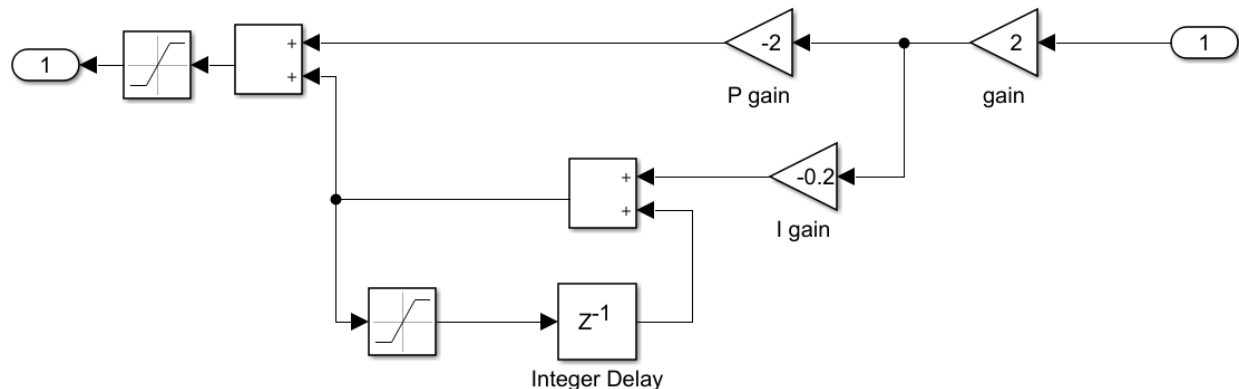
Figure B - 15. TED Implemented in MATLAB

B.3.6 Carrier/Phase recovery

The fine carrier recovery is the combination of frequency recovery (residual frequency after coarse frequency) and phase recovery as a result of transmission delay and thermal noise (i.e. AWGN). Figure B - 16. (a) shows the block diagram of the fine carrier recovery which consists of Phase Error Detector (PED), a loop filter and an NCO. The Simulink model is shown in Figure B - 16. (b) and the PED block diagram is depicted in Figure B - 16. (c) as well.

**Figure B - 16. Carrier/Phase Recovery Subsystem**

A second order Costas loop filter is used in this model. The loop parameters (e.g. loop bandwidth and damping factor) governed the accuracy and acquisition time. The details of the loop filter and NCO can be found in Figure B - 17. and Figure B - 18., respectively. A proportional integral second order Costas loop is used in this model. The gains in this block determine the bandwidth and damping factor of the loop and ultimately the maximum “pull-in” frequency and acquisition time.

**Figure B - 17. Loop filter Used in Frequency/Phase Synchronizer Block**

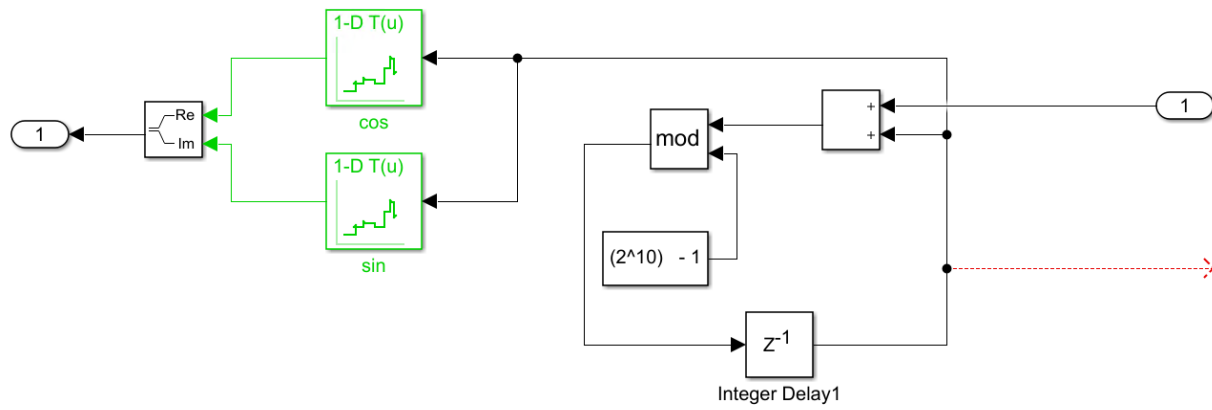


Figure B - 18. Numerical Control Oscillator

B.3.7 Simulation Results

In this section different simulation results are presented to assess the variability in results based on input signal characteristics (e.g. different doppler frequency, modulation type, noise, etc.).

Figure B - 19. through Figure B - 21. depicts the convergence time for a QPSK signal for three different doppler frequency of 1 KHz, 10 KHz, and 20 KHZ respectively. Each figure consists of two separate plots. 1) the carrier phase error which represents the required convergence time for phase error to reach the minimum possible value (i.e. phase error of 0 degree) and 2) the carrier frequency recovery which represents the required convergence time for the NCO to synchronize to the Doppler shift.



Figure B - 19. Carrier Recovery and Phase Error Convergence for Doppler Frequency of 1KHz

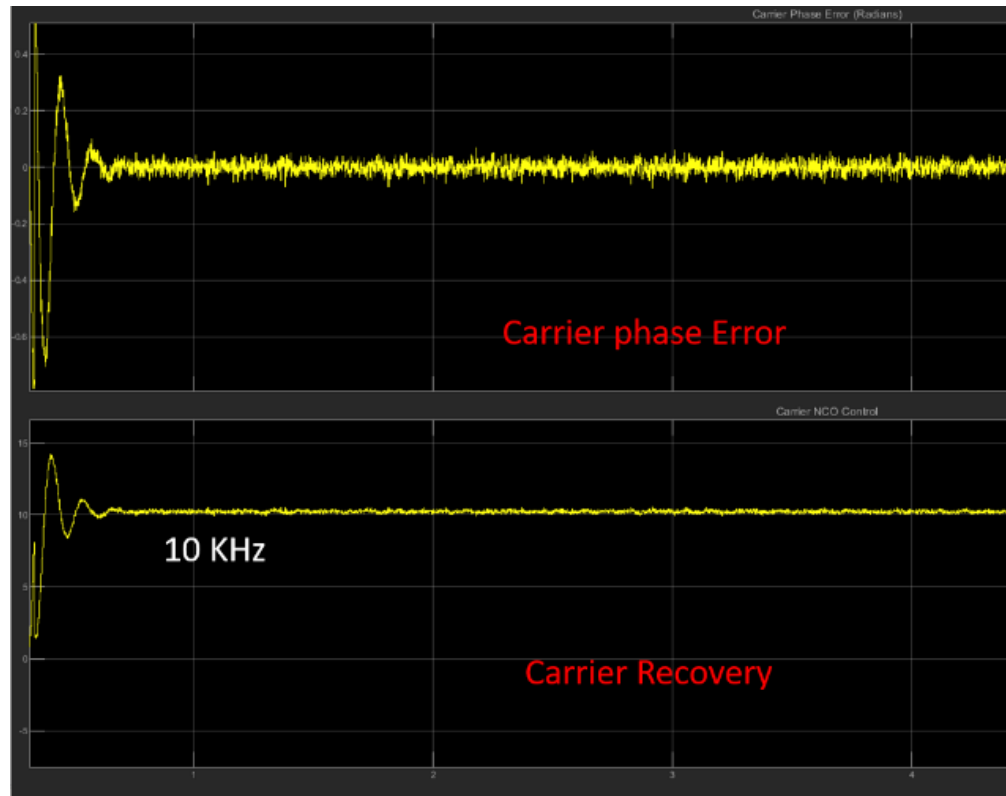


Figure B - 20. Carrier Recovery and Phase Error Convergence for Doppler Frequency of 10KHz

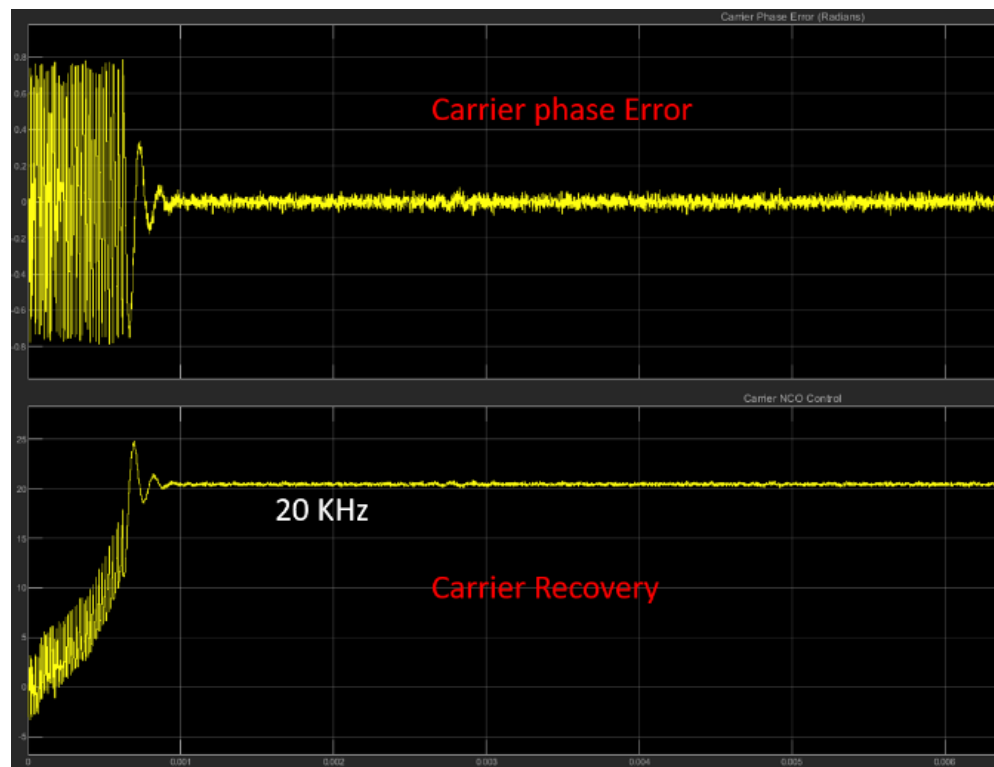


Figure B - 21. Carrier Recovery and Phase Error Convergence for Doppler Frequency of 20KHz

In order to have a better understanding of the convergence time, a comparison between carrier frequency recovery for 200Hz, 1KHz, 5KHz, and 20KHz frequency shifts is assessed. An SNR of 20 dB and QPSK Modulation is used. The results are presented in Figure B - 22.

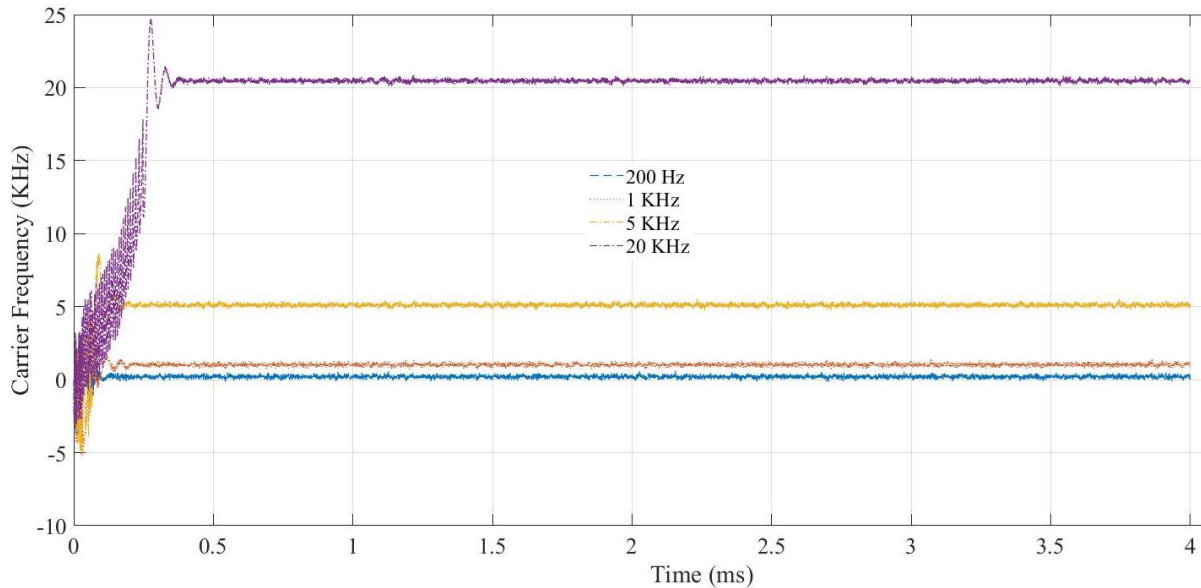
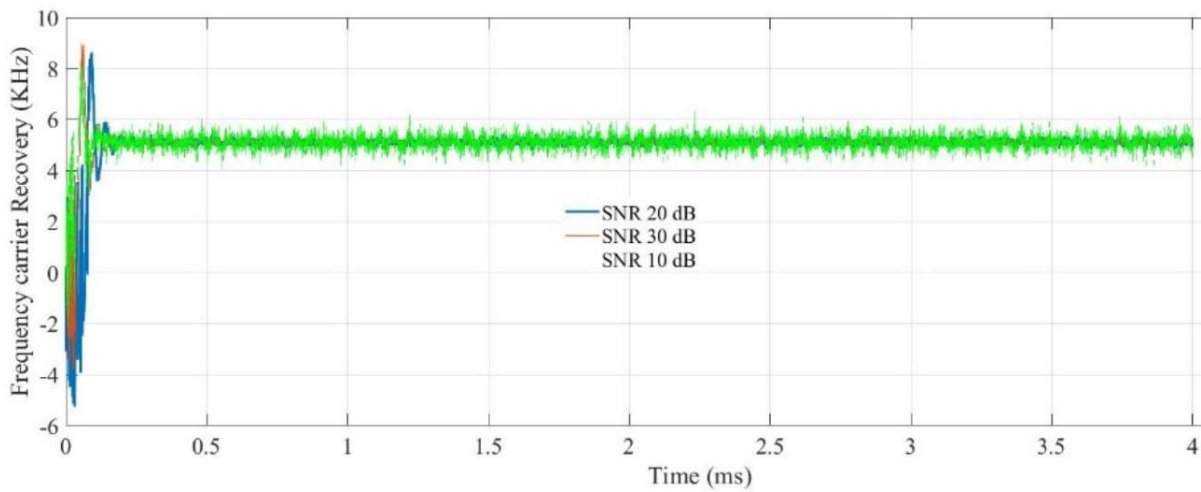


Figure B - 22. Carrier Frequency Convergence Time Comparison for Different Doppler Shift

The effect of AWGN or signal to noise ratio was also evaluated. Three SNR values (10, 20, and 30dB) were used in the simulation. By increasing or decreasing the SNR, the acquisition time does not change significantly. Decreasing SNR introduces more noise into system which consequently degrades the BER. Figure B - 23. shows the effect of signal to noise ratio on the accuracy of the carrier acquisition for a frequency offset of 5 KHz, on a QPSK modulated signal.



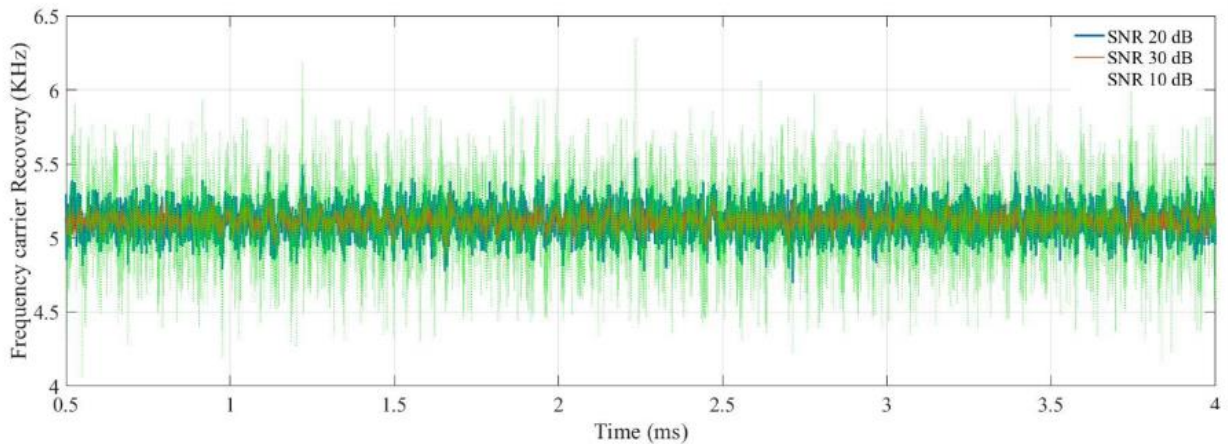
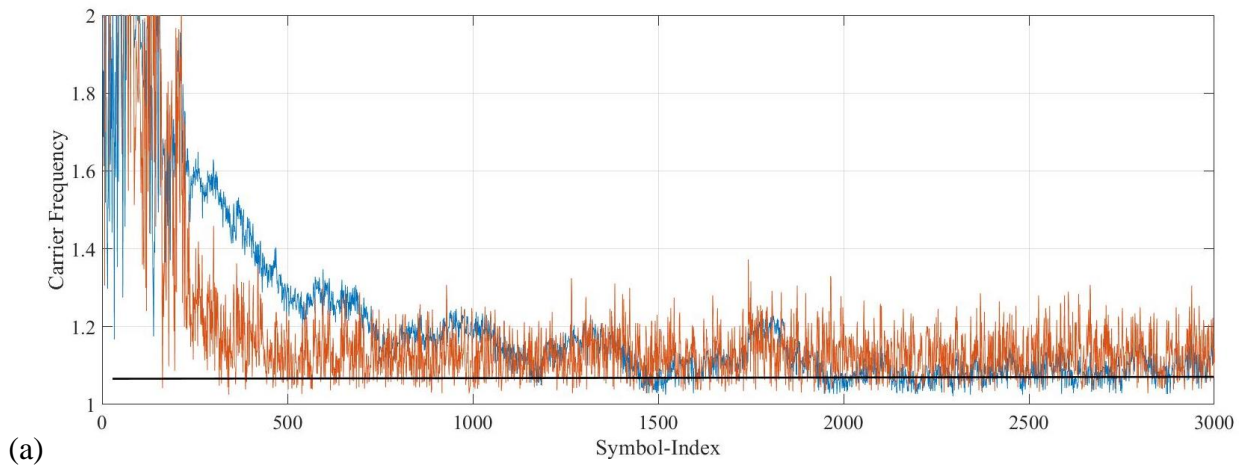


Figure B - 23. Effect of the Signal to Noise Ratio on the Accuracy of the Carrier Frequency Acquisition

One of the most important part of the fine signal acquisition process is the loop bandwidth and its related parameters which define the maximum “pull-in” range, convergence time and accuracy of the signal. By increasing the loop bandwidth, we will be able to compensate for a larger residual frequency after coarse signal synchronization. However, increasing the loop bandwidth allows more noise into the system and as a result lowers the BER ratio. See Figure B - 24 (a). In order to have a better comparison of the acquisition time for two different loop bandwidths, we have increased the SNR from 20 dB to 40 dB. Figure B - 24 (b) shows the comparison between two loop bandwidths; T_{acq1} has a wider bandwidth compare to T_{acq2} .



(a)

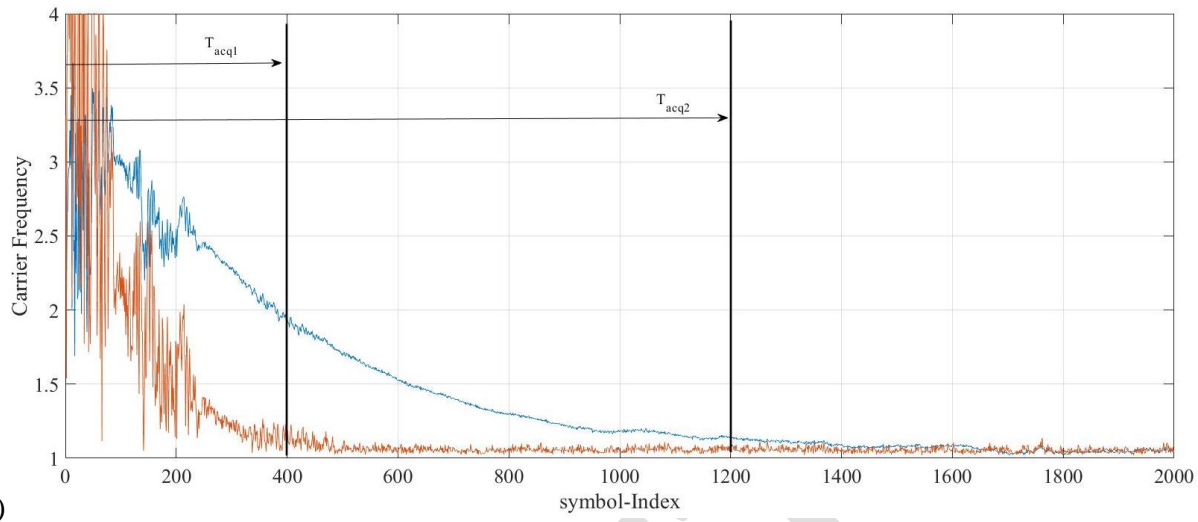


Figure B - 24. Effect of (a) Loop Bandwidth on the Convergence Time (b) the SNR on the Acquisition Time

B.3.8 Verification Results

The verification results for three sample Doppler frequencies are summarized in Table B - 2, reflecting the graphical results captured in Figure B - 25., Figure B - 26., and Figure B - 27.. A 256 Ksps, QPSK signal is modeled, representative of the Iridium system. As the results indicate, for a high SNR of 20 dB, the signal is acquired almost instantaneously. Comparing the MATLAB model with the theoretical value shown in Figure B - 6 one can understand the acquisition time is in the order of few milliseconds. However, it should be noted that the theoretical value is based on just phase lock response and for an ideal channel while in the developed MATLAB model symbol/time synchronization is taken into account and an additive white gaussian noise is added to channel as well.

Table B - 2. Estimated Signal Acquisition Time for Sample Doppler Frequencies for a QPSK System, SNR=20 dB, loop bandwidth \approx 50 KHz and 512 ksp.

Doppler Frequency	Required Symbol-Index for Convergence	Acquisition time	Analytically Computer Acquisition Time
1 KHz	1074	4.19 ms	TBD
20 KHz	1210	4.72 ms	TBD
50 KHz	2246	8.76 ms	TBD

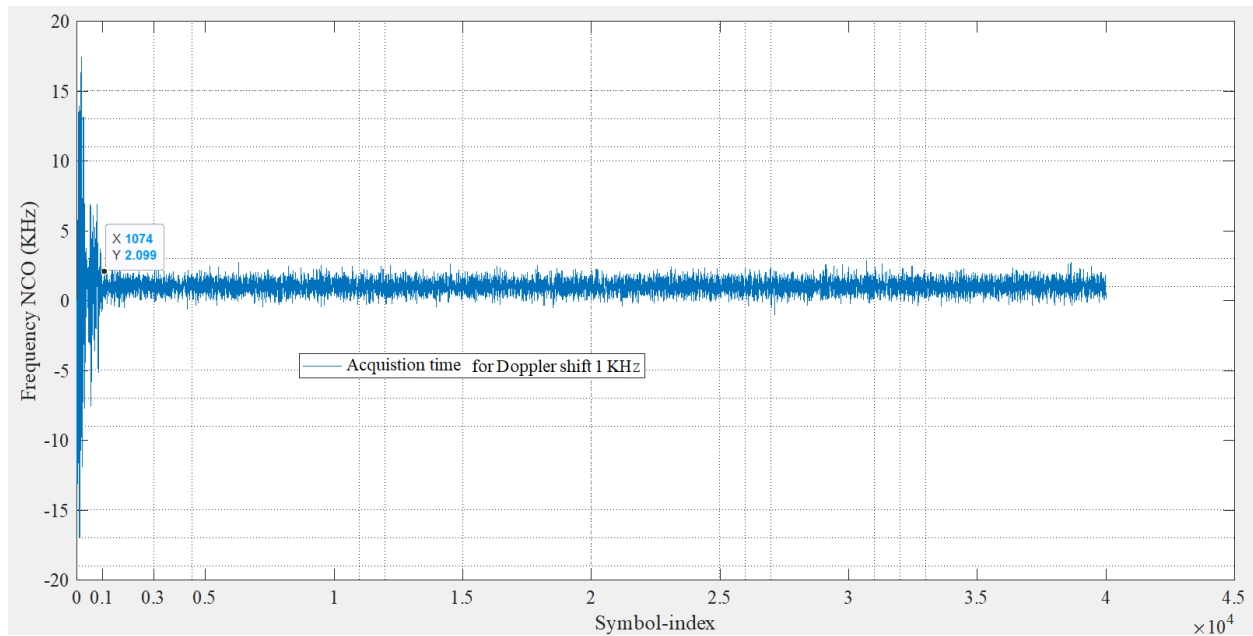


Figure B - 25. Acquisition Time Results for Doppler shift of 1 KHz as a Function of Symbol-Index

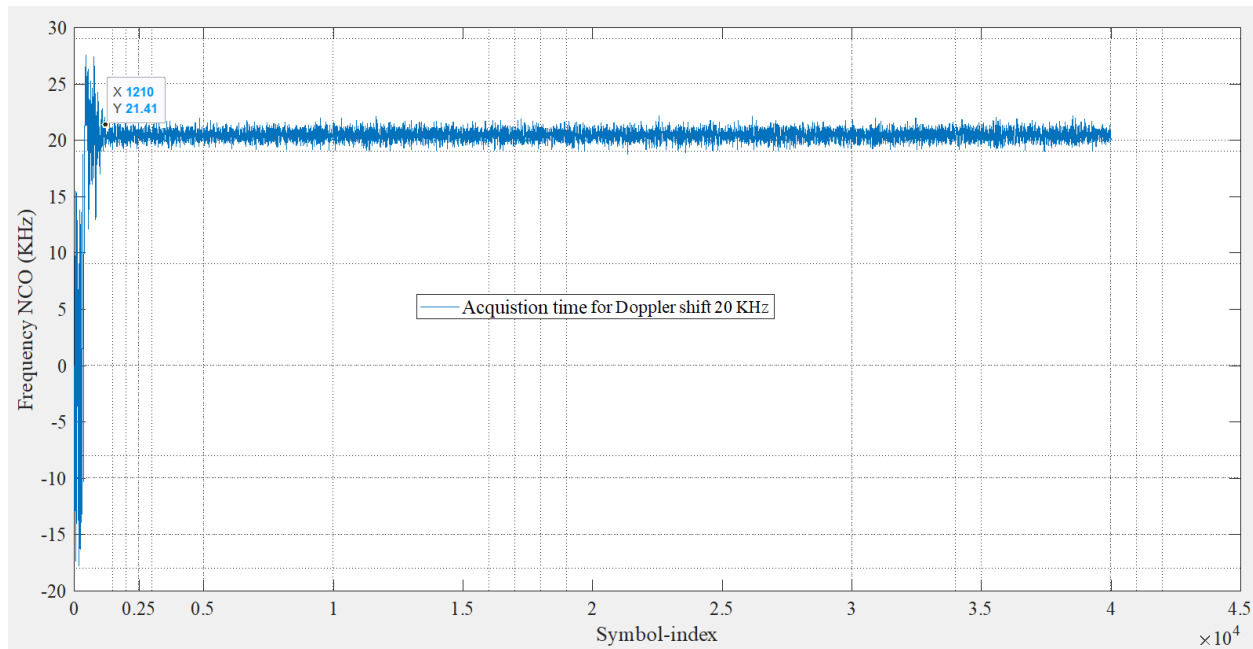


Figure B - 26.. Acquisition Time Results for Doppler shift of 20 KHz as a Function of Symbol-Index

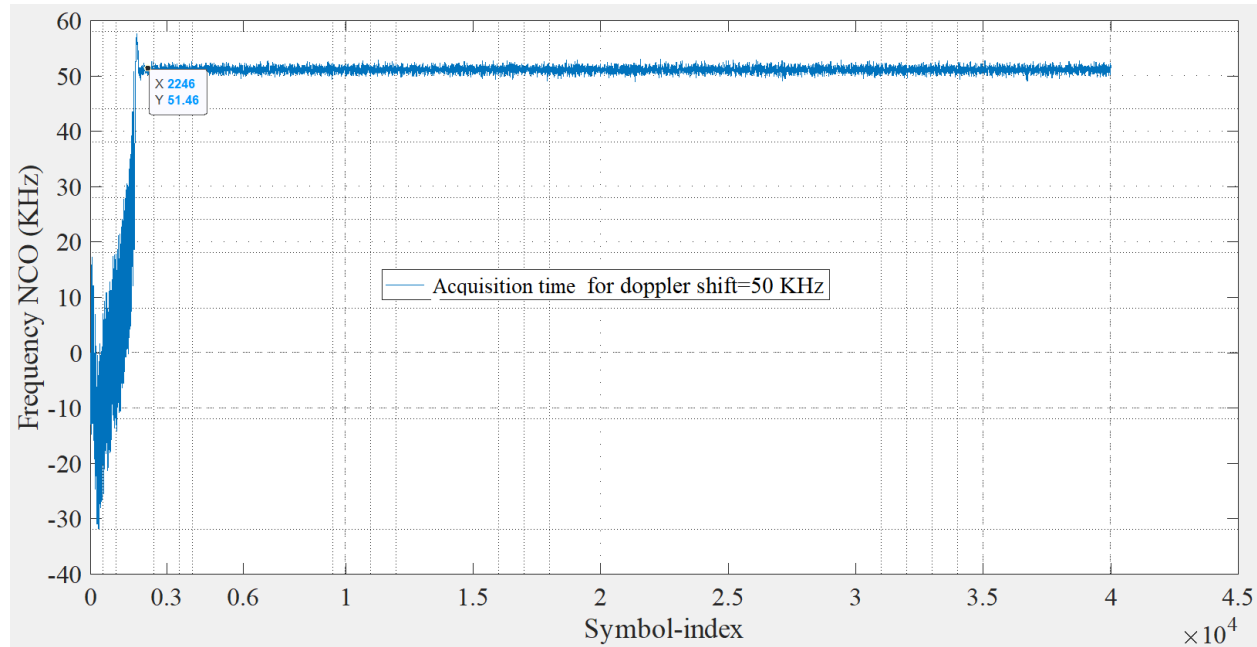


Figure B - 27. Acquisition Time Results for Doppler shift of 50 KHz as a Function of Symbol-Index

B.4 Modeled Systems and Configuration Parameters (TBD)

Table B - 3 shows the summary of estimated acquisition time for a 256 ksps QPSK signal with lower SNR values of 12.6 dB and 4.5 dB which correspond to 10e-5 uncoded and rate $\frac{1}{2}$ coded waveform, respectively. The rate $\frac{1}{2}$ coded signal is representative of the Iridium forward link. For this case, fine tuning has a maximum range of 6 KHz with an acquisition time of 507 millisecond. As such, the receiver will depend on coarse tuning to detect the signal within this frequency range or an onboard GPS receiver must be used to estimate the location of both the user satellite and the relays in the constellation. Note that for each Doppler frequency, the loop bandwidth parameters were modified to synch to the signal. Note that these results are representative of Iridium. Additional results for other systems are pending.

Table B - 3. Estimated Signal Acquisition Time for a QPSK, 256 ksps Signal

Signal to Noise Ratio	Maximum Doppler Frequency	Acquisition Time
4.5 dB (10e-5, Rate $\frac{1}{2}$ Convolutional Coded)	6 KHz	507 ms
12.6 dB (10e-5 Uncoded)	50 KHz	125 ms

Table B-4 shows the summary of estimated acquisition time for 6 systems based on the maximum Doppler frequency the developed MATLAB model can synchronize. For each system, the modulation and code rate and corresponding signal to noise ratio is listed as well.

Not that, for all systems with the same modulation order, the maximum doppler frequency is the same and the difference between the acquisition time is due to the data rate. Figure B-28, and B-29 Represents the convergence time (represented by symbol index) for two modulation of 16PSK with code rate 2/3 and QPSK with code rate $\frac{1}{2}$ respectively.

It can be found the convergence time for the two plots are very close and that is based on the fact that the loop filter is the same for the two systems.

Table B - 4. Estimated Signal Acquisition Times

Signal to Noise Ratio	Doppler Frequency	Acquisition Time (ms)
SNR=13 dB (16 PSK, 2/3 code rate) Iridium 512 Kbps	29 KHz	96
SNR=4.5 dB, QPSK ½ code rate Globalstar 256 Kbps	59 KHz	200
SNR=4.5 dB, QPSK ½ code rate OneWeb MEO 25 Mbps	59 KHz	2
SNR=4.5 dB, QPSK 0.83 code rate Inmarsat 50.492 Mbps	59 KHz	106.2
SNR=4.5 dB, QPSK 0.83 code rate ViaSat-3 100 Mbps	59 KHz	0.5
SNR=4.5 dB, QPSK 0.83 code rate Eutelsat 0.3 Mbps	59 KHz	17.42
SNR=4.5 dB, QPSK 1/2 code rate Intelsat 80 Mbps	59 KHz	0.625

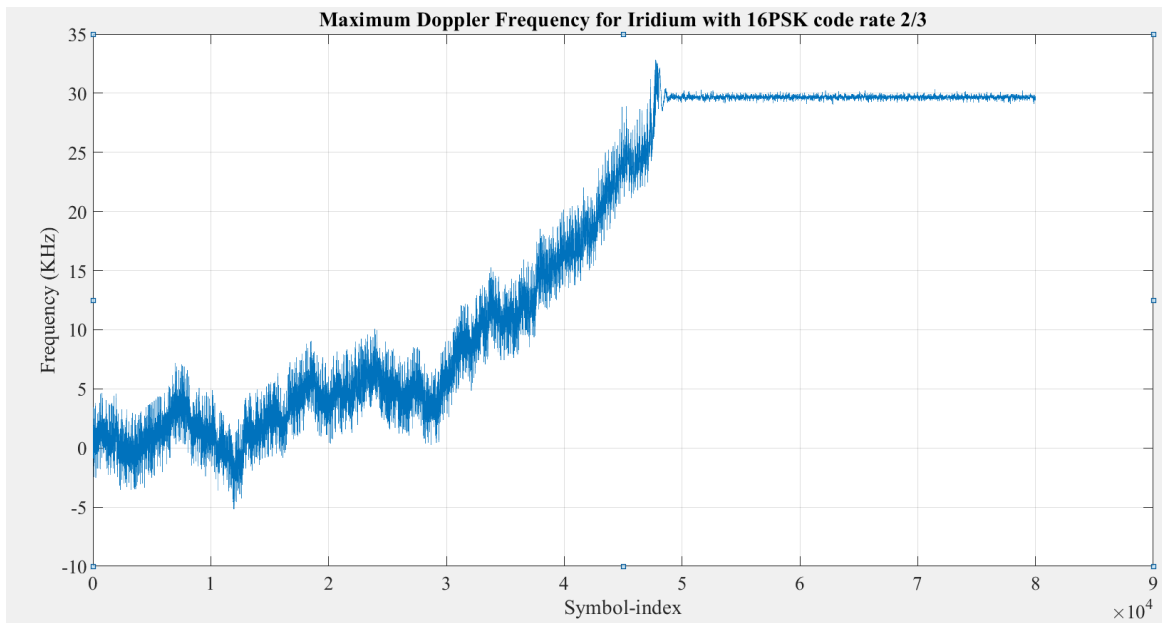


Figure B - 28. Acquisition Time Results for Doppler shift of 29 KHz for 16PSK code rate 2/3 (Iridium next)

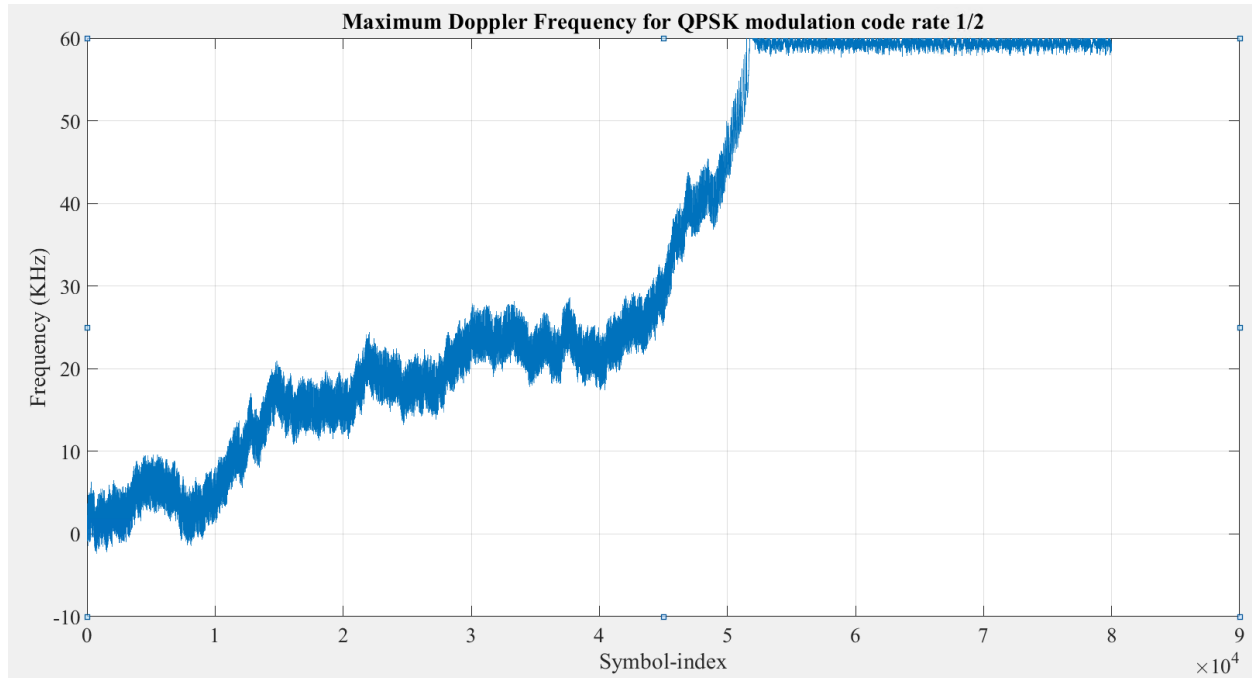


Figure B - 29. Acquisition Time Results for Doppler shift of 59 KHz for QPSK code rate 1/2

APPENDIX C: NETWORK MODELING

C.1 Introduction

A number of the commercial relay systems that are part of this study have been designed as extensions of ground networks to support terrestrial users traveling at maximum speeds of a jet aircraft. These systems follow a cellular structure coverage concept to optimize frequency reuse in order to increase system capacity and signal power to the subscriber. There are inherent inefficiencies when these types of network architectures are used to support a NASA LEO mission which travel several times the speed of the highest speed terrestrial user for which these systems were designed to support, particularly in regards to network service initiations and handovers as shown in Figure C-1. The purpose of network modeling is to estimate the impact that a mismatch in subscriber speed will have on the expected throughput of these systems after enough RF power is received in both the forward and return direction (see Appendix A).

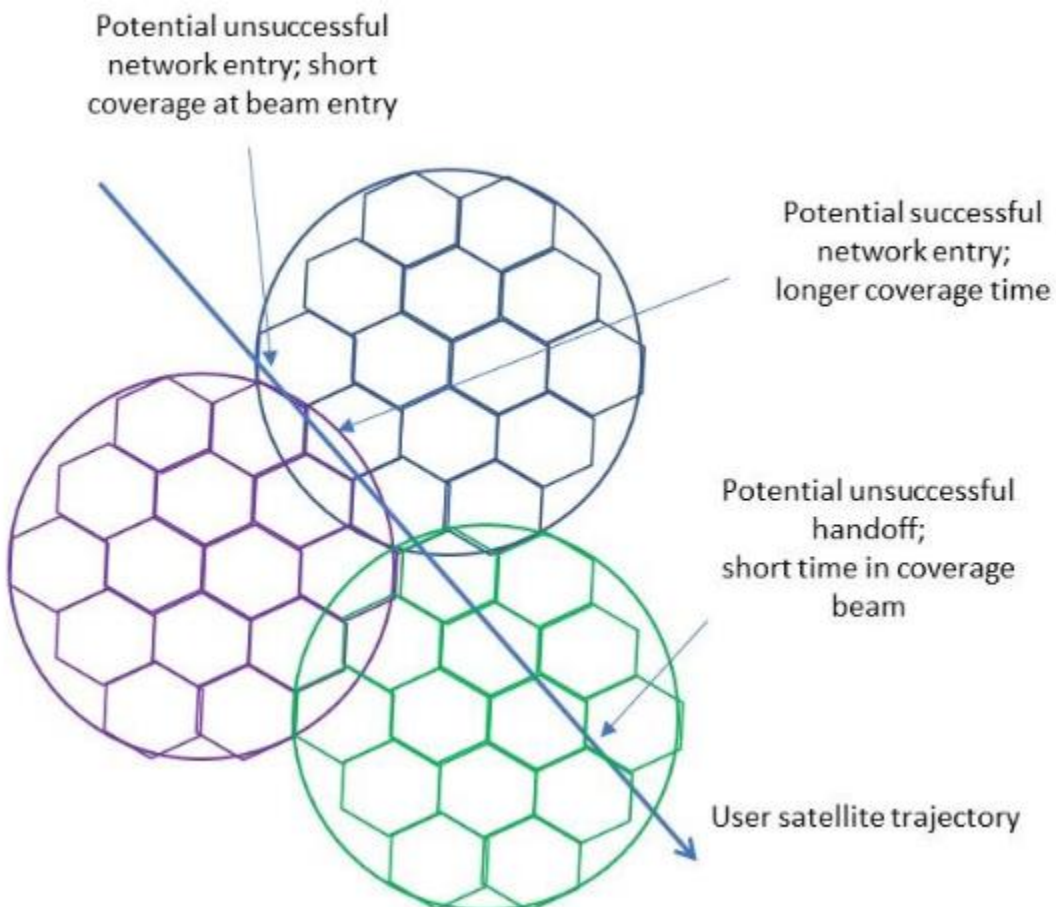


Figure C - 1. Potential service inefficiencies of a user quickly moving through a satellite network's terrestrial-based cellular structure

C.2 Approach

Table C-1 lists the systems that are part of this study which adhere to a network design construct and the network standard (or variant of the standard) which the system is based on. For the purpose of this study, our focus is to model GSM, IS-95 and LTE type satellite systems. We also need to model both regenerative

CART Algorithm Design Document

transponder and bent-pipe transponder type of systems. Therefore, we are potentially looking at 5 different network models:

- GSM / Regenerative transponder model (Iridium)
- GSM / Bent pipe transponder model (Inmarsat-4)
- IS-95 / Bent pipe transponder model (Globalstar)
- LTE / Regenerative transponder model (SpaceX Starlink)
- LTE / Bent pipe transponder model (OneWeb Starlink)

Table C - 1. Commercial System and Corresponding Network Standard

System	Network Standard	Relay Satellite Architecture
Iridium	GSM	Regenerative Transponder
Starlink	LTE	Regenerative Transponder
OneWeb	LTE	Bent Pipe Transponder
Globalstar	IS-95	Bent Pipe Transponder
Inmarsat-4	GSM	Bent Pipe Transponder

Figure C-2 depicts a network system's communications functions using the Open Systems Interconnection (OSI) conceptual model. The analysis of the performance of the physical link is analyzed in Appendix A. This appendix describes the models, verification and results for the systems identified in Table C-2.

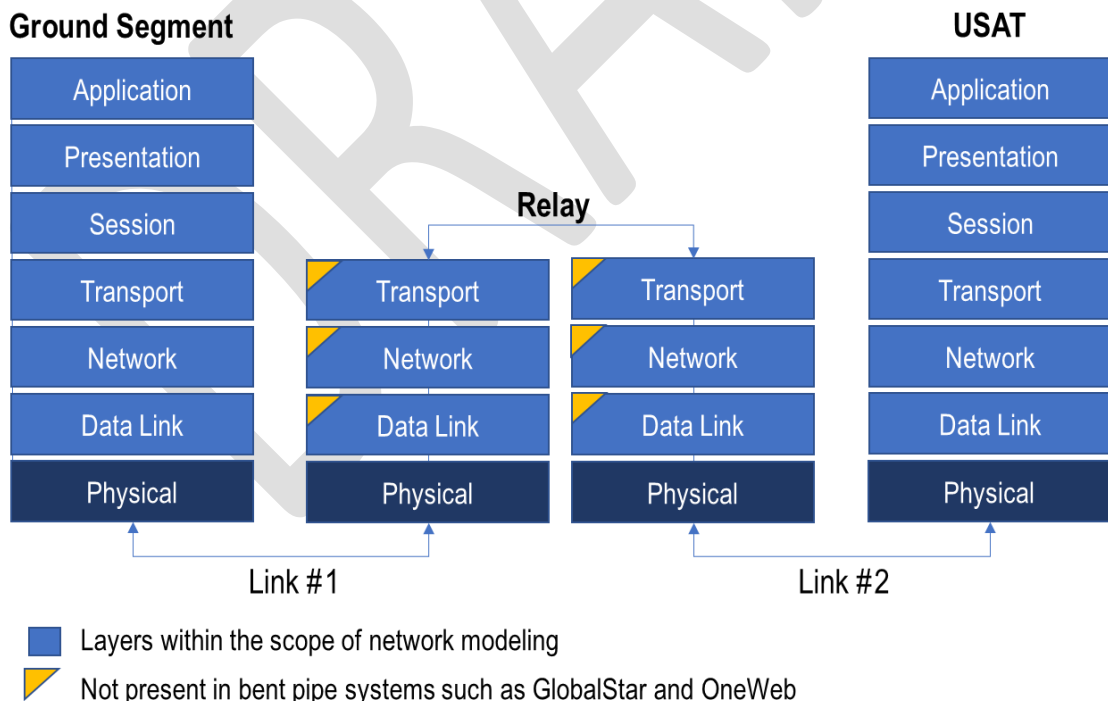


Figure C - 2. Network View using the OSI Conceptual Model

Modeling every interaction of the protocols on each layer is not a practical solution as it creates unneeded complexities including lengthy development time and slow simulation time. As is common in modeling and simulation, the selected model requirements are selected by targeting the impacted functionality.

To determine the specific modeling needs for the upper 6 network layers, an assessment of the impact user speed has on each of these layers is first performed based on the functionality mobility standards such as GSM and LTE implement in each of these layers. This assessment is summarized in Table C-2 which identifies of layers 3 and 4 as potential problem areas. These two layers are, therefore, the emphasis of our network modeling effort with an initial focus on layer 3. The modeling of layer 4 will be addressed at a later time. Moreover, we address only the modeling approach for the Iridium GSM / Regenerative transponder model. After verification of these results, our initial model will be modified as necessary for the remaining systems to be modeled.

Table C - 2. Network Layers Expected Performance Impact

OSI Layer	Functions Performed	Expected Impact / Modeling Need
Application	This layer provides application services for file transfers, e-mail, and other network software services. Telnet and FTP are applications that exist entirely in the application level. (e.g., WWW browsers, NFS, SNMP, Telnet, HTTP, FTP)	Generation of arbitrary data for transfer. Functions this layer need to be modeled as measurement of throughput is performed at this layer.
Presentation (Layer 6)	Translation between Application and lower layers. (e.g., encryption, ASCII, EBCDIC, TIFF, GIF, PICT, JPEG, MPEG, MIDI)	Encryption, serialization, compression are all ignored in the effort of determining generalized network deliverance capacity. Functions in this layer do not need to be modeled.
Session (Layer 5)	Manages connectivity sessions, back and forth communications between application. (e.g., NFS, NetBios names, RPC, SQL)	Ability to “recover” service due to temporary Prec drops is currently not implemented. The model uses a simple incremental counter to distinguish unique sessions and separate overlapping service management protocols. Functions of this layer need do not need be modeled.
Transport (Layer 4)	Prepare and ensure packet delivery between hosts; is responsible for end-to-end error recovery and flow control. It ensures complete data transfer. (e.g., TCP, UDP)	Effects of segmentation, acknowledgements, and resending packets. TCP, or a variant, will need to be modeled because the large number of handoffs require an acknowledging that information has been received at both ends. Not currently included.
Network (Layer 3)	Routing of packets across multiple nodes toward destination, managing node to node connectivity. (e.g., AppleTalk DDP, IP, IPX)	On mobile networks, this layer is responsible for is responsible for the management of an established connection and of the associated activities in the radio network. These tasks can be subdivided into 1) Call control management, 2) Mobility management MM, 3) Radio resource management. The performance impact on this layer is expected to be significant.
Datalink (Layer 2)	Controls how the subscriber on the network gains access to the physical channel (Media Access Control – Mac). Controls frame synchronization,	On the MAC, access to the physical channel will be impacted by the combination of satellite delay of short contiguous frequencies. However, this layer is expected to be tuned for satellite communications and any additional performance degradation will be

OSI Layer	Functions Performed	Expected Impact / Modeling Need
	flow control and error checking (Logical Link Control - LLC). (e.g., DDI, ATM, IEEE 802.5/ 802.2, IEEE 802.3/802.2, HDLC, Frame Relay)	minimal. Error Correction is ignored in the effort of determining generalized network performance under acceptable Prec levels.

C.3 Model Description and Verification

C.3.1 Model Description

For this study, the open source tool ns-3 is used. To model the mobility impact, a simplistic handover-initiated data flow was implemented as a means of refining RF coverage to estimate effective communication time and data throughput. The data flow is only active during periods of RF coverage defined at times when the dynamic link analysis indicates Prec levels are above the threshold required for the user-to-relay communications link at specified Bit-Error-Rate (BER). Each of these periods begins with a handshake procedure that is required to complete before the data stream is established. This results in the network model constantly being in one of four states:

- Passive, wherein no packets are transferred between nodes.
- Data Transfer, wherein data packets are being transferred from the User node to a Relay, which forwards them to the Gateway node.
- Service Initiation, which transitions the network from the Passive to Data Transfer states.
- Handoff, which transfers the User node's connection to a different Relay node (i.e. satellite) or beam.

The current model consists of one user node switching service between two relay nodes which forward information to a gateway node as shown in Figure C-3. Nodes are given instructions for “service status” and “handshake” procedures, wherein each coverage period begins with the user node initiating a handshake procedure with a targeted relay node, which sends acknowledgements upon receiving handshake packets and establishes a service “session”. Upon receiving the relay’s acknowledgement, the user node initializes a packet-generating application and begins to send data packets periodically via simplified UDP-like protocol until the coverage period ends, as depicted in Figure C-4. Any packets “in transit” when the coverage period ends are dropped by the relay agent upon reception. When the physical link model reports a change or disruption in satellite or beam service, ns-3 responds by updating the user node’s session value to prevent responses to any incoming replies, and canceling any queued packet sending events, and changing the user node’s targeted relay when appropriate. To allocate time for network registration procedures, the relay node schedules its reply to be sent at after a delay corresponding to the type of handshake (beam-beam vs. sat-sat handovers vs. service initiation). This delay is currently a static time for each handshake type based on previously performed studies on GSM and LTE based networks, specifically Iridium, Inmarsat-4, and OneWeb. Later versions of the model will incorporate results from signal acquisition analysis in MATLAB into these delays (Appendix B). If the coverage period ends before the service acknowledgement is received, the user agent updates its coverage session and ignores the acknowledgement packets belonging to previous coverage sessions.

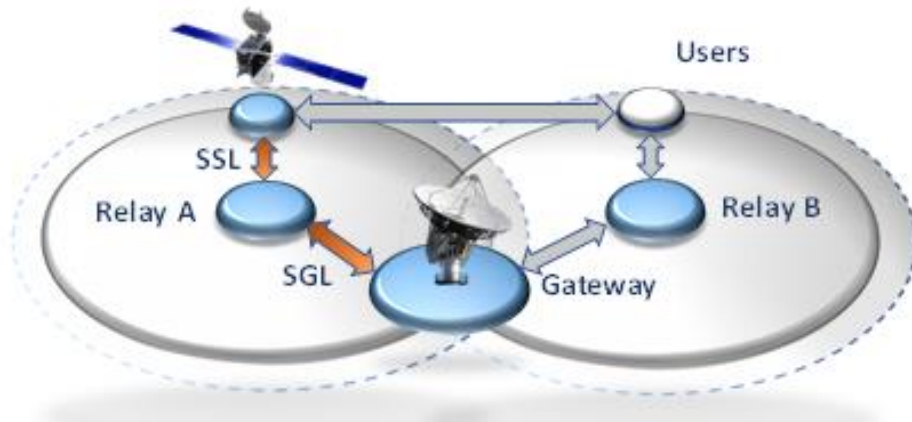


Figure C - 3. Space Based Network Communications Architecture Concept

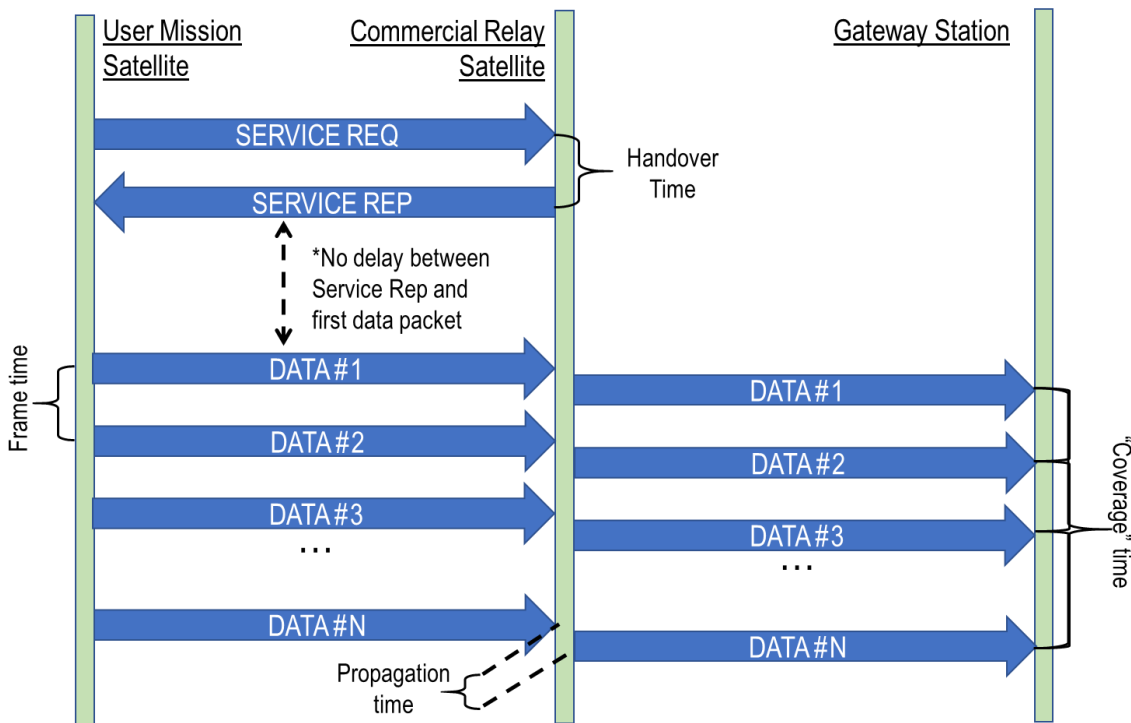


Figure C - 4. Depiction of data transfer and effective service time calculation in ns-3

Service Initiation

Service initiations consist of the time required for the network to acquire the user request signal, “attach” the user to the network, and for the PDP sequence required to begin the data exchange. Rather than simulating all the protocols involved within these procedures within the context of ns-3, each network is given a static time representing the “worst case” service initiation delay experienced by a user, i.e. the longest expected time. When the network transitions from the Passive state to the Data Transfer state, the User node sends a request containing a session ID to a Relay node, which then schedules a reply containing the same session ID to be sent after a delay corresponding to the modeled network’s service initiation time. Once the User node receives the reply, it ensures that the packet’s session ID matches its current

session and begins the data transfer. The logical process deciding whether to perform a service initiation or handoff is depicted in Figure C-5.

Data Transfer

To calculate throughput, once the user node is “connected” to a relay, it transmits a data packet every 90ms to achieve an effective data rate equal to the network’s provided input. In the case of Iridium, this is a packet size of 5760 bytes to achieve Iridium’s advertised data rate of 512kb/s. For consistency, and due to lack of clarity on many systems’ frame structures, Iridium’s 90ms frame timing is implemented on all networks modeled in NS3. These data packets are recorded at each node they pass through, and a summation of these packets’ bytes received by the gateway node is considered the network’s total throughput for the simulation. Likewise, effective communication time is calculated by a running summation of the difference in time between each data packet’s reception at the gateway node and that of its preceding data packet within the session. This effective communication time statistic can be considered a refinement of the RF coverage reported by the physical link model, since it is controlled by its STK counterpart but is exclusive of both the service initiation time and time during which transmitted packets will not reach the relay before the coverage period ends due to propagation. In other words, the effective communications time produced by the network model “trims” the beginning and end times of the RF coverage based on handshake times and propagation respectively. The current model only observes impacts between the user and relay nodes; once a packet is received at the relay node and the packet’s session ID matches the active session, the packet is immediately and instantaneously transmitted to the Gateway node which logs the packet’s size and reception time. Additionally, the current model contains no error modeling, so all packets are assumed to be transmitted flawlessly. There is no representation of network traffic and queuing times.

Propagation time is currently a static value across each network, specifically the maximum value observed in the physical link model across runs for all users. Additionally, the STK input file sometimes contains redundancies showing that the user satellite is connecting to a relay-beam combination that it is already connected to. This is an artifact of the STK 1 second reporting resolution, wherein the simulation reported a loss of service for a duration less than the reporting resolution. These artifacts are ignored in the ns-3 model, potentially resulting in up to an additional 11 successful packets per occurrence.

Handoffs

Network handoffs are implemented similar to service initiations. In addition to using different delay values for Beam-to-Beam and Satellite-to-Satellite handovers when scheduling the relay’s response, the Satellite handover carries an additional instruction for the User node to change which relay node it sends its request to. This currently serves no functional purpose since packets are only processed based at each node based on their session ID, but in future versions this will allow better implementation of timing effects due to differing propagation times and routing updates. For networks boasting seamless handoffs, a delay value of zero is applicable, resulting in only up to one *additional* data packet as the handshake procedure is completed instantaneously, and the Data Transfer timing is reset. The logical process deciding whether to perform a service initiation or handoff is depicted in Figure C-5.

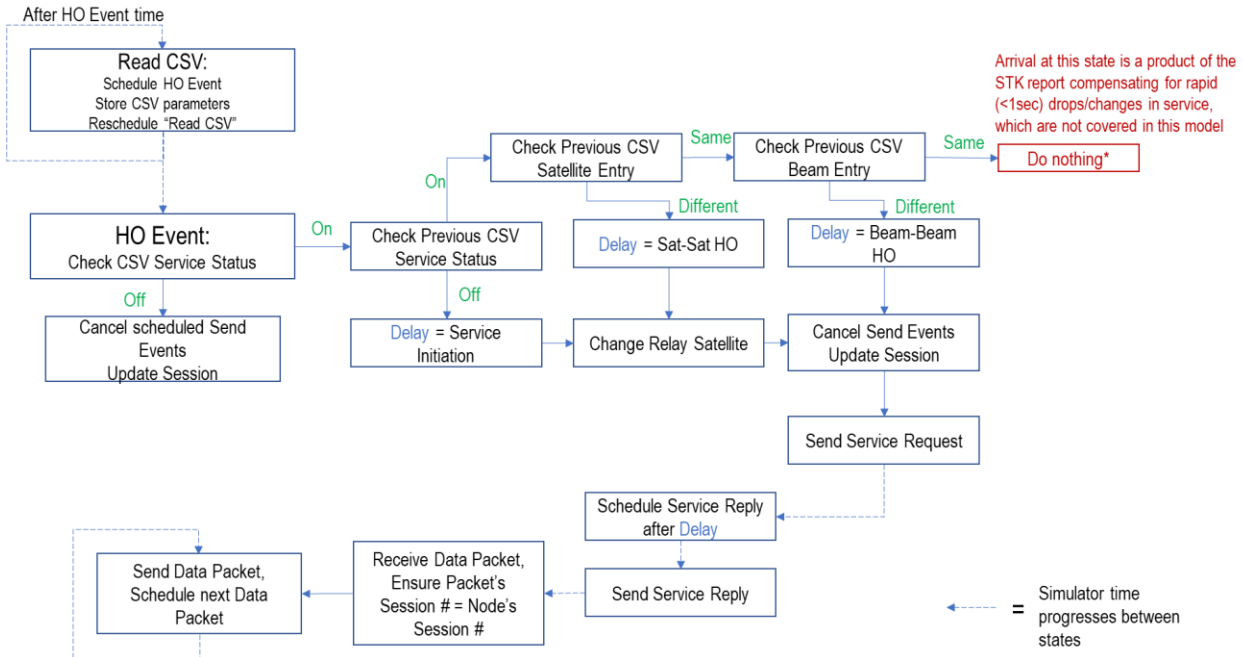


Figure C - 5. Detailed depiction of ns-3 decision making process based on physical layer model input

C.3.2 Model Verification

(Reserved)

C.4 Systems and Configuration Parameters

Currently there is only one configuration for any user/network modeling combination. This is because the necessary information regarding the physical link layer is entirely provided by the STK input file, and the extent of the model is to observe the impacts of service initiations and handovers; which are contained to three static numbers per network representing Service Initiations, Beam-to-Beam handovers, and Satellite-to-Satellite handovers, based on previous work regarding network handover impacts on serviceability [23]. This handshake simplification is designed to represent the “worst case” handovers/service initiations expected for each network. Using this method spares the program from needing to model literal back and forth protocols such as signal acquisition and registration by abstracting them together and allowing inputs that are more generalized and therefore flexible, and can be used to represent any type of service transfer such as GSM, LTE, etc. These three values are accepted as user inputs by the user when the model is run, along with the pathway to the STK input file. The network’s effective data rate is also accepted as a user input in bits per second. The model outputs a CSV document containing the network’s throughput at each simulation second to a user-provided directory and creates/appends an additional document within the directory to contain an entry for user/network combination’s effective service time.

Table C - 3. Systems, Configurations, Results (Examples)

Model Settings	System							
	Iridium	Starlink	OneWeb	Globalstar	Inmarsat-4	O3b	Eutelsat	Viasat
Propagation Delay Time	5ms	TBD	30ms	10ms	130ms	30ms	130ms	130ms
Packet Size	5.76KB	11.25MB	562.5KB	2.88KB	5.535KB	18MB	33KB	1.125MB
Frame Timing	90ms	90ms	90ms	90ms	90ms	90ms	90ms	90ms
Effective Data Rate	512Kbp	1Gbps	500Mbps	256Kbps	492Kbps	1.6Gbps	3Mbps	100Mbps
Service Initiation Time	9.55s	0.97s ^[2]	0.97s ^[2]	9.55s ^[3]	15.21s	0.97s ^[2]	15.21s ^[4]	15.21s ^[4]
Beam-to-Beam Handover Time ^[1]	0.36s	0s	0s	0s	0s	0s	0s	0
Satellite-to-Satellite Handover Time ^[1]	5.02s	0s	0.185s	0s	0s	0s	0s	0

[1] Networks with handoff times of 0 are orchestrated to be seamless, but often require some minimum amount of connectivity time to preempt handoffs. This requirement is not implemented in the current model.
[2] Using OneWeb value as a placeholder for LTE system
[3] Using Iridium value as a placeholder for GSM system
[4] Using Inmarsat-4 value as placeholder for GEO system

APPENDIX D: REGRESSION MODELS DESCRIPTION

D.1 Introduction

Appendices A-C described the physical link and network modeling used to assess performance of the various commercial (relay) systems. The simulations are run with a variety of reference users in different orbits (inclinations and altitudes). In order to extend the simulation results to predict performance for arbitrary missions as defined by CART user input, CART employs various regression models trained on these simulation results. These models serve as the statistical core of an analysis architecture that adapts automatically to changing input data. All of the regression models used by CART are variants of generalized linear models (GLMs), a generalization of familiar least-squares regression used in machine learning and experimental analysis applications, that interpolate the various modeling results used by CART to arbitrary orbital altitudes and inclinations. All GLMs compute a linear predictor, a linear combination of input variables with coefficients that are learned from data, which is then passed through a (generally non-linear) inverse link function to obtain the mean of a certain probability distribution [24]. Choosing a GLM involves choosing a parametrized family of probability distributions and a link function; for example, least-squares regression is a GLM with an identity link function and gaussian distribution family. The GLM function provided by the R stats package implements model fitting and prediction for many common GLM types and hence is being used for CART regression modeling and validation. (R is a language and environment for statistical computing and graphics. [25])

D.2 Model Descriptions

The choices of link function and probability distribution for each type of model output processed by the system are summarized in Table D - 1. These were chosen for practical reasons—for example, the beta distribution only predicts fractions between 0 and 1, and the other distributions only predict positive numbers—as well as statistical reasons. For example, waiting times between events—such as satellite handovers—are gamma-distributed under certain assumptions, and the number of events that occur in an interval of time—such as packet receptions—can be modeled with a Poisson distribution. Note that beta regression differs from typical GLMs in having two linear predictors: one for the mean of the distribution, and one for the precision, a number inversely proportional to variance that can be thought of as a confidence measure for the beta distribution; this functionality is provided by the betareg R package [26].

Table D - 1. GLM link functions and distribution families; here η denotes the linear predictor, μ denotes the mean of the distribution, and φ denotes the precision of the beta distribution

	RF Coverage (mean)	RF Coverage (precision)	Gap Duration	Effective Communication Time	Throughput	Pointing Angle Rate
Link function	$\eta = \log [\mu/(1-\mu)]$	$\eta = \log \varphi$	$\eta = 1/\mu$	Same as coverage	$\eta = \log \mu$	$\eta = \mu$ (TBR)
Distribution family	Beta	Beta	Gamma	Same as coverage	Poisson	Gaussian (TBR)

To determine coefficients of the linear predictor, η , parameters are fit using maximum likelihood (ML) estimation (the default behavior of the GLM function) for all models except the coverage model, which uses a bias-corrected version of ML as proposed by [27] and implemented in the betareg package in R. We also need to specify the terms in the linear predictor; for all models, there are terms for altitude,

inclination, their product (i.e. the interaction term), and a constant bias term. That is, for all models, we have the following expression for the linear predictor η in terms of a set of learned coefficients β_i :

$$\eta = \beta_0 + \beta_1 \cdot \text{altitude} + \beta_2 \cdot \text{inclination} + \beta_3 \cdot \text{altitude} \cdot \text{inclination} \quad (1)$$

The quality of the regression predictions will depend on two factors, among others: the number of distinct users used to fit the model and the length of time the simulations are run over. The first is intuitively obvious, as increasing the number of users reduces the types of orbit the model has never seen before. Less obviously, a larger dataset for training the model allows us to use more expressive model structures (e.g. adding quadratic terms to the linear predictor) without risking overfitting.

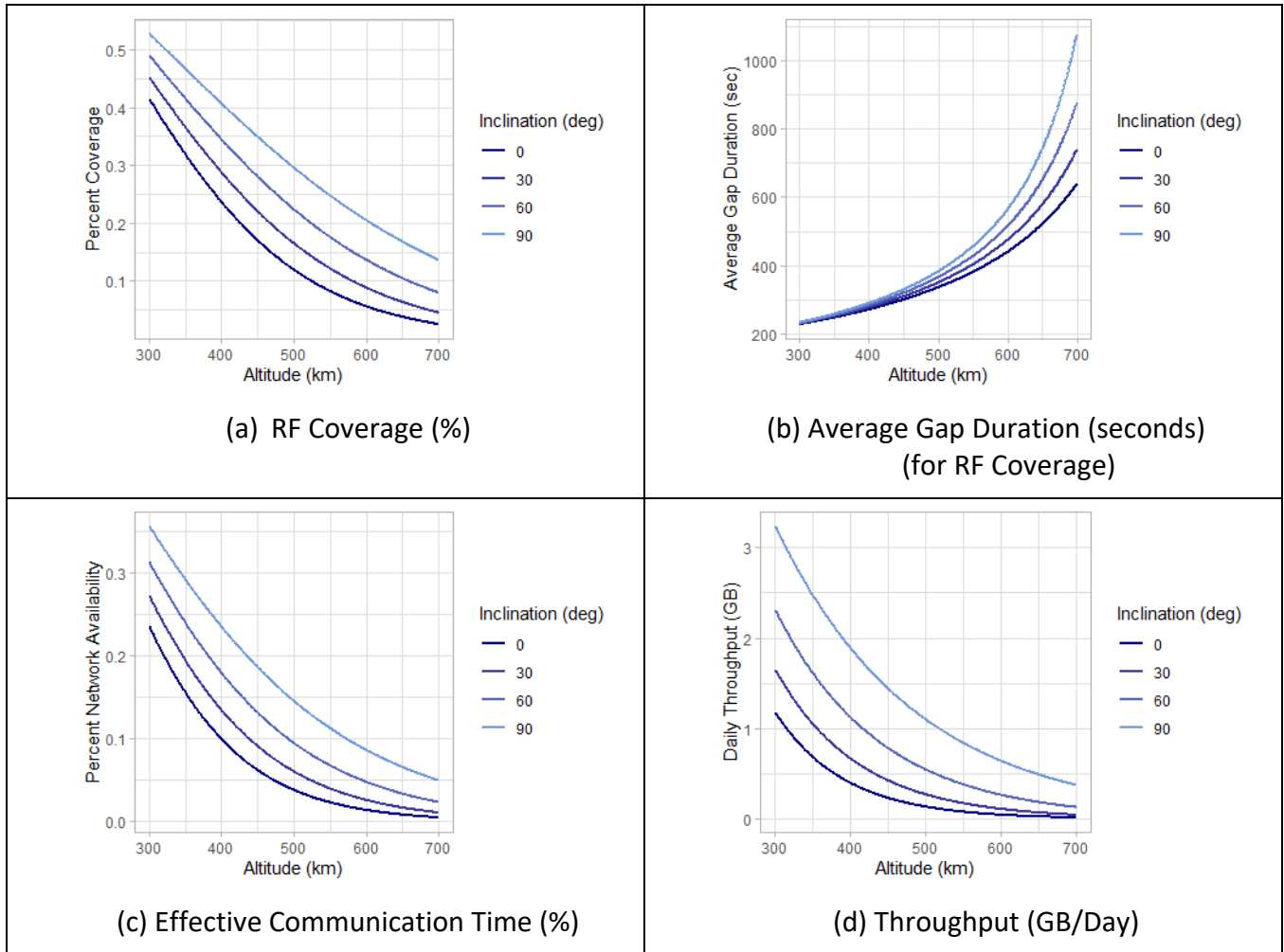
Longer simulation times will also improve regression predictions by reducing the variance in the model results. Because the regression models only take orbit altitude and inclination as input parameters, it only makes sense to use them to describe the steady-state behavior of the orbit, as the transient behavior also depends on other orbital parameters. Nevertheless, the modeling results are obtained over a finite simulation period and hence are only an approximation to steady-state values, and this approximation improves as the simulation period is lengthened.

D.3 Model Verification

First, we show that the regression models' qualitative behavior matches the patterns of physical and network modeling results. The initial proof-of-concept for the regression model approach is based on simulation data for the Iridium system only. All regression models used in CART will follow the approach outlined here, and updates to the document will include corresponding results.

Example model predictions for four of the evaluation criteria are summarized in Figure D - 1. The results are consistent with expectations; overall performance worsens with increasing altitude, as coverage, throughput, and availability all decrease, and the average gap duration increases. These metrics also improve with increasing inclination apart from gap duration, which varies little at low altitudes and worsens with increasing inclination at high altitudes. Additionally, the effective communication time model closely tracks the RF coverage model (Pearson correlation 0.989), and the predicted effective communication time values are always smaller than the corresponding RF coverage values as expected.

Next, we describe a technique both for evaluating the *prediction* accuracy of the regression models on novel data and for selecting between competing models of the same performance measure: Leave-One-Out Cross-Validation, or LOOCV, a standard model selection technique widely used in machine learning [28]. Although this technique will be more useful for distinguishing model types with access to more training data, we demonstrate it here with the currently available training set by comparing our chosen models against a simple least-squares regression baseline with the same predictor variables.

**Figure D - 1. (a) – (d) Predicted Iridium Modeling Results by Altitude and Inclination**

LOOCV proceeds by training each model on a copy of the training set with one data point removed and then using the trained models to predict the value of that held-out data point. This prediction is then compared to the actual value of that point using some metric (we use absolute difference). This process is repeated for each point in the data set, and the resulting prediction errors are averaged to produce an estimate of the model's overall ability to predict unseen data. These average errors for the GLMs specified in Table D - 1 are compared to those for the corresponding linear regression baselines in Table D - 2.

Table D - 2. Average Leave-One-Out Cross-Validation Error

	RF Coverage (%)	Average Gap Duration (in RF Coverage) (sec)	Effective Communication Time (%)	Throughput (GB/day)
GLM	5.31%	159.39	3.75%	0.188
Linear baseline	7.66%	162.78	6.49%	0.361
Difference				

In each case, the corresponding (non-linear) GLM outperforms the baseline linear model (or close to matches it, in the case of average gap duration). From this we expect the GLMs to be better at predicting the modeled quantities for new users on average than a simple least-squares regression.

Furthermore, we can use this analysis to estimate how a model's prediction error will depend on the choice of user by looking at the individual leave-one-out prediction errors *before* averaging. For example, the individual LOOCV errors for the beta regression RF coverage model are shown in Figure D - 2. Each point in this plot is a single user annotated with the model's prediction error after being trained on all other users. According to this, we expect the coverage model to perform quite well on new users with low altitude and inclination (the lower left-hand corner of the plot), and we expect it might make larger errors on new users with inclinations above 75 degrees or so (the upper quarter of the plot). This kind of analysis can both provide clues on how to improve the model—in this example, coverage at high inclinations merits further investigation—and establish expectations for how trustworthy the model's predictions will be when used in practice. A test case was completed for a user at an altitude of 400km and 20-deg inclination; a combination in which we would expect the RF coverage model to perform well. The results did indeed perform as expected – the RF coverage result directly from the physical model (in STK) was 23.8%, and the predicted coverage from the Beta RF Coverage model was 27%.

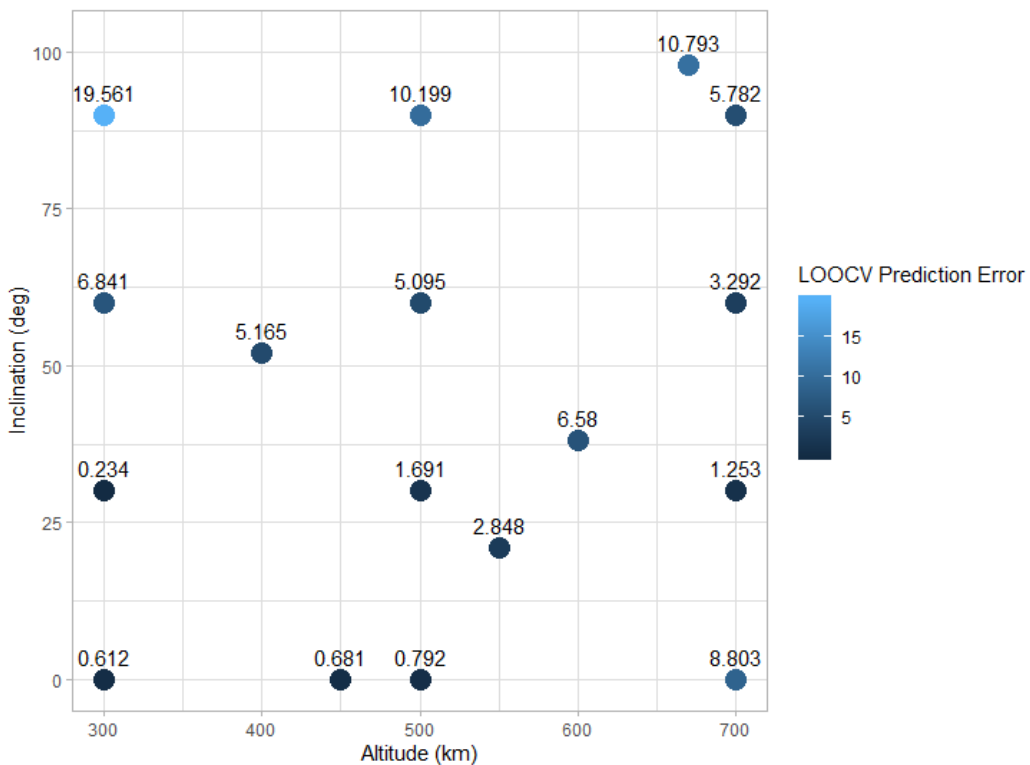


Figure D - 2. Beta RF Coverage Model Leave-One-Out Errors

APPENDIX E: LIST OF ACRONYMS

Acronym	Definition
ADD	Algorithm Description Document
AGC	Automatic Gain Control
AWGN	Additive White Gaussian Noise
CART	Commercial Asset Recommender Tool
CONOPS	Concept of Operation
COTS	Commercial-Off-The-Shelf
DDP	Datagram Delivery Protocol
DTE	Direct to Earth
EIRP	Effective Isotropic Radiated Power
FCC	Federal Communications Commission
FFT	Fast Fourier Transform
FIR	Finite Impulse Response
FSS	Fixed Service Satellite
FTP	File Transfer Protocol
GLMs	Generalized Linear Models
GNSS	Global Navigation Satellite System
GSFC	Goddard Space Flight Center
GSM	Global System for Mobile
HTS	High Throughput Satellite
HTTP	HyperText Transfer Protocol
IOC	Initial Operating Capability
IP	Internet Protocol
IPX	Internetwork Packet Exchange
LLC	Logical Link Control
LOOCV	Leave-One-Out Cross-Validation
LTE	Long Term Evolution
ML	Maximum Likelihood
MSS	Mobile Satellite Service
NASA	National Aeronautics and Space Administration
NCO	Numerically Controlled Oscillator
NFFT	Number Fast Fourier Transform
NFS	Network File System
NS3	Network Simulator
NSD	Network Services Division
PA	Power Amplifier
PDMA	Program Data Management Analyst
PDP	Packet Data Protocol
PLL	Phase Lock Loop
PSE	Program and Systems Engineering
QAM	Quadrature Amplitude Modulation
QPSK	Quadrature Phase Shift Keying
RAAN	Right Ascension of the Ascending Node

CART Algorithm Design Document

Acronym	Definition
RF	Radio Frequency
RPC	Remote Procedure Call
RRC	Root Raised Cosine
SCaN	Space Communications and Navigation Program
SCPC	Single Carrier Per Frequency
SN	Space Network
SNMP	Simple Network Management Protocol
SQL	Structured/standardized query language
SSL	Space to Space Links
SSV	Server-Side Validation
STK	Systems Tool Kit
SWaP	Size Weight and Power
TBD	To Be Determined
TBR	To Be Reviewed
TED	Time Error Detection, Time Error Detector
TIFF	Tagged Image File Format
TT&C	Telemetry, Tracking & Command
UI	User Interface
VCO	Voltage Controlled Oscillator
WRC	World Radiocommunication Conference
WWW	World Wide Web